ΕΛΛΗΝΙΚΗ
ΕΠΙΣΤΗΜΟΝΙΚΗ
ΕΤΑΙΡΕΙΑ
ΕΔΑΦΟΜΗΧΑΝΙΚΗΣ
& ΓΕΩΤΕΧΝΙΚΗΣ
ΜΗΧΑΝΙΚΗΣ

Τα Νέα της Ε Ε Ε Ε Γ Μ

90

Αρ. 90 – ΜΑΙΟΣ 2016

[What] to teach or not to teach - That is the question

The first century of modern geotechnology is coming to an end. There has been an explosion of knowledge in our field, and we have gained great insight into soil and rock behavior through exceptional experimental and numerical capabilities. Today, our field is broader than any single person can master, and we publish in more journals than we can follow (probably more than 30 journals, complemented by a similar number of trade magazines). There is unlimited access to information, and effective measurement systems and powerful analysis/design tools are readily available.

The first century has also highlighted difficulties in geotechnical design, to the point that we have extensively accepted that our field is a combination of both art and science. Could this be the reason for consistently disappointing blind prediction exercises? We need to reassess the role of empiricism, question often invisible biases and incorrect concepts or approaches that have crept into teaching and practice, and bring back an emphasis on deep understanding coupled with multi-disciplinary fluency.

Research and education are warranted by the practice of geotechnical engineering. Our students today will reach the prime of their professional careers at the time when geotechnical engineering challenges that are sprouting today will dominate their professional lives, for instance, issues related to climate change, sea level rise, energy needs and sustainability. Confronting those needs will require a sound

(συνέχεια στην σελίδα 3)

Π Ε Ρ Ι Ε Χ Ο Μ Ε Ν Α

(συνέχεια από την πρώτη σελίδα)

and resourceful scientific foundation. In this context, let's pause to reflect on our educational programs.

Bare Core: The Fundamentals

While knowledge has expanded, teaching time remains limited and only a very small subset of concepts can be covered in the curriculum. I often wonder about the key fundamental concepts our students should deeply understand if we were forced to reduce the contents of our courses to a bare minimum, say, a few pages, while satisfying multidisciplinary fluency. The underlying assumption is that young engineers will be able to readily add pragmatic procedures to a well-funded knowledge structure while still preserving the engineering versatility fundamentals provide.

Clearly, they will need mechanics (e.g., equilibrium and plasticity), physics (e.g., conservation), chemistry (e.g., water and minerals), biology (e.g., limiting factors to life and bio-mediated processes), earth science / geology (e.g., formation history), and materials (e.g., particulate matter).

For the sake of this letter, let me address the latter. I like to start the course on soils with the fundamental realization that *soils are particulate materials.* Then, all observations summarized in the table below are true and causally related.

The particulate nature of soils was recognized in the early stages of soil mechanics, yet it is seldom emphasized in our classes. Observations in the table apply to all soils and fractured rocks.

Soils are particulate geo-materials, therefore

Soils are inherently non-linear (Hertz and electrical contacts), non-elastic (Mindlin contact), porous and pervious (i.e., porosity between grains is interconnected).

Particle-level characteristics and processes integrate to make the macroscale response

- size: determines the balance between particle-level forces (capillary and electrical forces gain relevance when particles are smaller than 10μm-to-50μm in size);
- shape: reflects formation history and it affects grain packing, anisotropy, stiffness, strength and permeability - among others;
- spatial arrangement: is determined by electrical forces in fine grained sediments (pore fluid pH and ionic concentration), and by grain shape and relative grain size in coarse grained soils;
- porosity: varies widely and it is stress-dependent in [unstructured] fine grained soils, but it varies in a narrow range and it is mostly defined at the time of packing in coarse grained soils.

The particulate skeleton (frictional) coexists with the pore fluids (viscous)

- both are very different: the key is to anticipate their distinct responses to imposed boundary changes
- the skeleton and the fluid interact: this gives rise to coupled fluid pressure, effective stress, volumetric strains and shear response;
- mixed fluids: add capillary effects onto the particulate skeleton;
- generalization: all hydro-chemo-bio-thermo-mechanical processes are coupled.

The mechanical behavior of the particulate skeleton is effective stress-dependent:

- includes: stiffness (Hertz), frictional strength (Coulomb), and dilation upon shear (Taylor)
- frictional strength limits the maximum stress anisotropy a soil can experience
- other properties may depend on effective stress as well (e.g., thermal conductivity of dry soils)

Particle-level deformation mechanisms change with strain level

- small-strain deformation: it takes place at constant-fabric and grain deformations concentrate at inter-particle contacts; in this strain regime, volume change, pore pressure generation and frictional losses are minimal;
- large-strain deformation: it involves fabric changes (the role of contact-level grain deformation vanishes);
- threshold strain between the two regimes: it is higher for smaller particles and at higher confinement.

Soils are not inert, and often change within the time scale of engineering projects

- corollary: natural soils may behave differently than freshly remolded clay or recently packed sand

Not to Teach (Pruning)

There are enduring misnomers, superseded practices and restraining recipes in our field. We all share responsibility for pruning them out; in particular, we-educators, journal editors and conference organizers can play an effective role to this end. Examples follow.

- Terms with multiple semantics: the term "clay"' is used to indicate size, mineral (crystal or amorphous), or any soil that plots above the A-line on the plasticity chart. Let's use the term '"clay" to indicate "clay minerals", and classify fine grained soils according to their sensitivity to changes in pore fluid chemistry.
- Misnomers: the salient example is "cohesive soil" - this is a dangerous oxymoron indeed. Let's abandon the qualifier cohesion (to the extent that it results from curve fitting improper strength data), and related expressions such as "cohesive soil" and "cohesionless soil".
- Incorrect concepts: We often misuse the term "lubrication" in discussions of friction and to explain the dry-branch of the compaction curve. We imagine primary and secondary consolidation as sequential rather than concurrent processes. We infer peak strength and critical state void ratio even when specimens experienced progressive failure and shear localization. We invoke tensile strength to explain desiccation crack formation. And, we make indiscriminate use of the term thixotropy in relation to time-dependent changes in fine-grained sediments.
- Superseded: We teach graphical approaches that have become detached from their physical-mathematical underpinning (e.g., the determination of coefficient of consolidation using sqrt-t or log-t methods: a simple spreadsheet calculation can readily fit the diffusion equation to the data). We keep concepts developed for hand plotting

and hand calculations (e.g., meaning of preconsolidation pressure and its determination), and preserve the use of parameters that add limited information (e.g., plastic limit is highly correlated to LL, then, we need to reassess its value and the adequacy of PI-based correlations).

- Restrictive/simplistic ''tricks" that are not sound: from "buoyant unit weight" and UU tests ... to total stress analyses - Are we not ready for a clean parting from total stress yet?

- Fragile correlations and equations with local validity: diagnostic symptoms include dimensionally inhomogeneous expressions and equations that violate asymptotic trends for extreme values of the variables

To Tweak and Refocus

In an attempt to bring clarity, we have polarized soil conditions and have developed a curriculum around extremes. Consider two cases. First, we teach as if soils are either dry or water saturated, while reality involves these two extremes and all unsaturated conditions in between. Second, we cover drained and undrained analyses, yet, these are two extremes when the rate of pore pressure dissipation is either much faster (drained) or much slower (undrained) than the rate of loading.

There are some old-sounding but most elegant concepts that I like to cover in class, but with renewed emphasis on understanding rather than on devoting full focus to the development of engineering solutions. Examples include "feeling" equilibrium with Mohr circle, combining equilibrium and failure conditions in a Mohr-Coulomb analysis to show limiting stress anisotropy in soils, the beauty of elastic solutions, the "essentially engineering" upper and lower bounds (i.e., we do not need the exact solution, but reliable and narrow bounds), and even flownets (i.e., to highlight the identification of boundary conditions and to "experience" flow patterns and seepage forces).

To Teach (Evolving Emphasis)

Gradually, my lectures are evolving by shifting emphasis and incorporating other topics that -in my mind- students will need to remain up-to-date and intellectually agile in a changing world:

- Place continued emphasis on the particulate nature of soils and fractured rocks, and the critical relevance of effective stress! Extend the coverage of other needed scientific foundations (Note: early reviewers of this note suggested a dual track: one that emphasizes skills that will be immediately useful in practice -with exposure to the scientific foundations-, and another that emphasizes the scientific foundations and provides less of the practice-oriented skills).

- Present an updated discussion of formation history and diagenesis, bonding and structured soils (i.e., salient deviations from observations made in the table), natural and manufactured soils (e.g., mine tailings and fly ash), stratigraphy and spatial variability (at all scales).

- Increase emphasis on well-designed field tests to measure properties for engineering design. Principally, the laboratory-measured stiffness/compressibility is critically affected by sampling effects and aggravated by seating effects: in particular, oedometer tests should be limited to situations where the anticipated vertical shortening is a significant fraction of the specimen initial height.

- Extend teaching examples to a wide range of fluids, pressure, effective stress and temperature conditions that upcoming geotechnical problems will impose (including grain crushing effects).

- Emphasize both short- and long-term performance monitoring with a focus on making *a priori* predictions and assessing interpretations (noting that there are innate monitoring limitations such as accelerating bifurcations).

- Increase awareness of the pervasive tendency to localizations of all kinds which break down the common assumption of homogeneity (from shear bands and compaction bands, to dissolution pipes, flow localization, fingering, and a wide range of opening mode discontinuities or fractures).

- Introduce repetitive loads (mechanical, thermal, chemical, moisture): they may determine long-term performance.

- Continue reflecting on the role of the engineer in society, within an ever changing world as the driver for innovation.

Closing - Your Thoughts?

Geotechnical engineering has evolved and continues to develop as a result of the synergistic interaction between education, research and practice. This synergism is needed today more than ever before as our field gains preeminent roles in the most challenging problems humanity has ever faced. I would like to see our students embrace these challenges and thrive in the new opportunities our field presents, and hope that this excitement permeates into the classroom.

Geotechnical education has underplayed the importance of first principles while trying to focus on prescriptive solutions needed by practitioners to solve today's problems. If we let the pendulum swing further towards the "practice" end, we will delay advances needed to enhance the solution of today's problems and future generations of students will be ill-prepared to tackle the challenges that our profession will face.

But, choices are difficult, and I must admit that I struggle with the decision of what to teach and not to teach... I look forward to hearing your thoughts! I will compile your feedback -sent to me or directly to this blog- and synthesize it in the closure.

J. Carlos Santamarina

Georgia Institute of Technology, Atlanta-jcs@gatech.edu

This letter benefited from the writings, conversations and feedback from many colleagues, in particular: J. Atkinson, E. Alonso, *C.* Arson, R Bachus, R. Bonaparte, S. Chong, M. Dusseault, D. Frost, A. Garcia, A. Gens, G. Gudehus, J. Jang, P. Mayne, J. Mitchell, M. Pantazidou, S. Roshankhah, A. Schofield, and R. Sullivan

ΑΡΘΡΑ

Major Projects

Utilisation of deep groundwater barrier walls using soil bentonite and biopolymer slurries in geotechnical and environmental applications

Jonathan Hale, Alexandre Hubaut, Philippe Vincent

Menard Bachy, 13-15 Lyon Park Road 2113 Macquarie Park NSW

jhale@menardbachy.com.au, hubaut@menardbachy.com.au
pvincent@menardbachy.com.au

1. Introduction

Menard Bachy has carried out over the last 15 years a large number of groundwater containment structures utilising a wide range of techniques. One particular technique is the Soil Bentonite (SB) wall which is one of the most efficient, cost effective and environmentally friendly solutions to implement in-situ cut off (low permeability) walls. SB walls have been utilised historically for a wide range of applications including confinement of contaminated ground water around landfills, toxic tailing ponds but also for the improvement of performance of dams and other types of water retaining structures. In the delivery of complex projects SB walls have also been utilised in combination with other mechanical and hydraulic structures such as PVC membranes, hydraulic gates, leachate collection trenches, and sumps but also sheet piles and other retention systems.

For the particular case of sites presenting environmental challenges, involving soil and groundwater pollution, a strategy requiring both removal and treatment of the source of the contamination as well as control of the contaminated groundwater plume acting as the pollution carrier is required. In the case of urban excavations where treatment is complicated by access and impact on community contamination confinement is often preferred. In any case, the adopted strategy needs to take into account the future use of the site, combined solutions involving both the reduction of the source of pollution and control of the pollution carrier generally offer the most sustainable outcome.

This paper presents a range of projects performed in Australia and overseas utilising different forms of SB walls. A particular focus is given on project methodology, site validation and trial testing but also production and quality control. The paper also provides a comparison of the environmental impact that different cut off wall techniques have and how they compare with SB type walls.

2. Technical options for constructions of a groundwater barrier

2.1 Slurry cut-off wall

Slurry Walls are a trenching technique that utilises the thixotropic properties of a fluid to provide excavation support. The slurry prevents the trench from collapsing by providing outward pressure, hence balancing the inward hydraulic forces and preventing water flow into the trench. Slurry design vary based on the in-situ soil and groundwater composition, however typical properties are highly viscous (flow cone <40seconds), a density slightly higher than water (>1025kg/m^3) and filtrate loss <25ml.

The method is a continuous process where excavation and backfilling operations are undertaken through the slurry.

(Stage 1) The leading face of the excavation is progressed using a long reach excavator, typically capable of 18m - 20m deep reach. Deeper excavation (up to +50m depth) is then progressed in panel sections using a crane rig equipped with a clam shell excavation tool. Excavation is then verified by physical observation of key material (aquitard) and depth measurements.

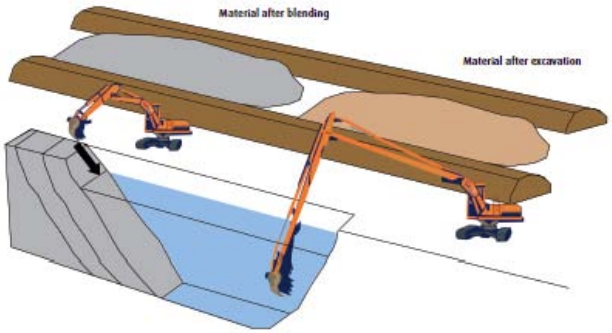

Figure 1: Schematic of slurry wall excavation under bentonite slurry

(Stage 2) The leading face is then followed with a backfilling operation that progressively displaces the slurry to balance out the excavated volume, in this way a balance in slurry height is targeted. Slurry height is maintained at a minimum of 1m-2m higher than the in-situ groundwater to ensure the outward pressure is maintained. Typically the backfilling process firstly utilises a tremie pipe that allows initial backfilling of the trench from the base of the excavation to the top. The secondary phase utilises a batter to maintain the progressive filling operation of the trench.

(Stage 3) The back fill material is specific to each application of the slurry cut-off wall and is designed prior to installation. Example backfill material comprises Soil Bentonite, Cement Bentonite, Soil Cement Bentonite or a combination of permeable and reactive material (implemented in Drainage and Permeable Reactive Barriers). Mixing operations utilising in-situ material is carried out concurrently to the excavation process. Backfill material primarily engineered from imported material may be mixed off-site or in a centralised mixing area. Verification of mixing is undertaken by regular testing for backfill slump and slurry viscosity as well as periodic permeability testing as appropriate.

Picture 1: Slump Testing

Picture 2: Viscosity

Table 1: Advantages of different types of slurry cut off wall

Groundwater Barrier	*Advantages*
Soil Bentonite	• Lowest cost of all underground barriers • High productivity • Verifiable continuity and depth • Low permeability (10^{-9} m/sec) • Positive connection with aquitard (key inspection possible) • Excellent resistance to contaminated groundwater • Accommodates large strains and is ideal where large ground movements are to be expected • The slurry remains fluid, allowing time for penetrating difficult layers or obstacles • Can be combined with HDPE membrane to provide air tightness • Re-use of most of the excavated materials
Soil Cement	• Most of the advantages of SB slurry walls apply to SCB walls • Higher strength than SB or CB walls • Greater trench stability is possible because the SCB backfill creates a shorter backfill slope • More resistant to erosion and burrowing animals - essential in levee applications
Cement Bentonite	• Useful on smaller project with limited access or narrow work zones because of the smaller equipment footprint • Low Permeability (10^{-8} m/sec) • No excavated soils are used in the final barrier wall, which is beneficial in areas with contaminated backfill soils • Since CB slurry is heavier than bentonite slurry and self-hardens, this method can provide improved trench stability and more easily overcome weaker ground conditions • Since the slurry sets after ~1 day, overlapping segments can be constructed in any direction or order to form a continuous barrier • Segments can be used to traverse up or down moderate slopes (5-15%) with minimal earthwork construction • Construction of walls through porous ground conditions is possible • Can be used to remove unsuitable materials below the groundwater without shoring or dewatering • CB backfill, once set, has a higher strength than SB backfill
Composite Slurry Walls	• Use of the slurry method allows for the economical insertion of vertical panels or elements into the ground in a narrow self-supporting trench, even below the groundwater table • Use of plastic panels may be necessary in extremely aggressive groundwater environments or in cases where methane or other gas migration needs to be prevented • The use of the slurry trench technique provides a way to install steel sheeting in difficult driving conditions
Combination Slurry Wall Systems	• Minimum cost for maximum benefit using two or more slurry wall technologies • Capability to solve isolated constructability issues with minimum cost and risk • Capability to modify groundwater patterns by diverting, extracting or containing groundwater with one continuous system

This continuous process is one key defining aspect of the method resulting in one element without multiple joints often required with most forms of alternative cut-off wall techniques.

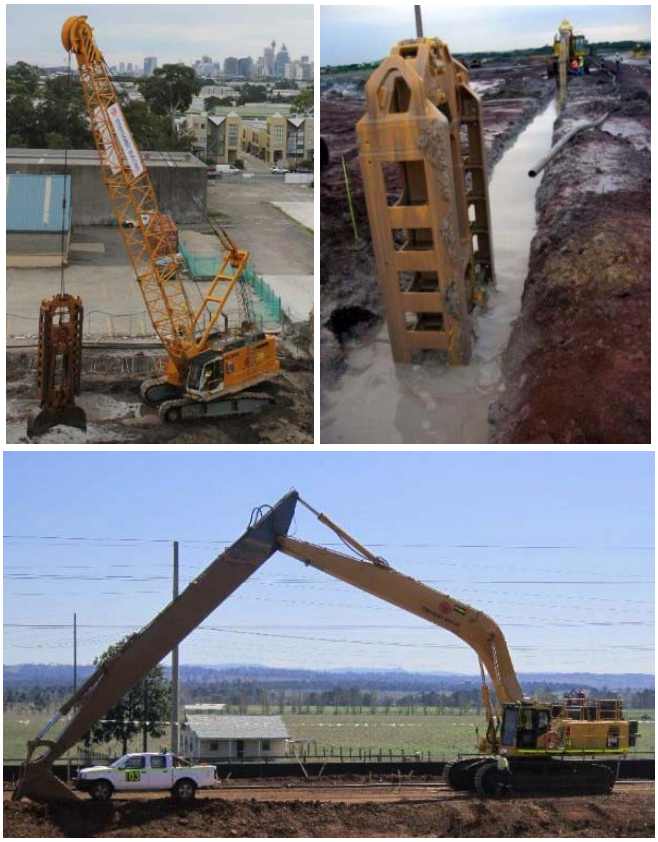

Picture 3: Clam Shell – Mascot (top left), Mayfield (top right) and Long Reach Excavator (low) Mt Arthur Coal

2.2 Bio-polymer drains

Bio-polymer trenches are constructed for draining, diverting or collecting groundwater or leachate or underground gas. They offer a cost effective way to construct deep collection drain trenches by eliminating the difficulties and costs associated with temporary shoring and dewatering associated with conventional construction.

Bio-Polymer trenches utilise the continuous trenching method as described in Section 2.1, however the slurry composition consists of polymer chains within the fluid that is highly viscous, entrain suspended soil particles and engage the trench surface to promote trench stability. Similar to the bentonite slurry technique the excavation and backfilling operations are undertaken through the Bio-Polymer slurry for trench stability. However following trench installation the polymer chains are readily broken down through a chemical reaction leaving the permeable backfill material in place.

The ability to support continuous trenches within complex groundwater and contaminated environments for the backfill of a wide range of media provides an opportunity that is both cost effective and low risk. The applications are somewhat limited to the imagination of the engineers tasked with solving the groundwater and contaminated land issues. Some examples of applications consist of:

- Drainage lines combined with HDPE liners allow the capture of leachate and gas and avoid draw down of neighbouring groundwater environments
- Rapid installations of air sparging systems for treatment of contaminated plumes
- Subsurface drain to lower groundwater level or encapsulated sites

2.3 Permeable reactive barriers

Permeable reactive barriers (PRB) are an in-situ method of remediating contaminated ground water plumes. The bio-polymer trenching method is utilised for the installation of an engineered back fill material to target and treat ground water as it flows through the barrier wall.

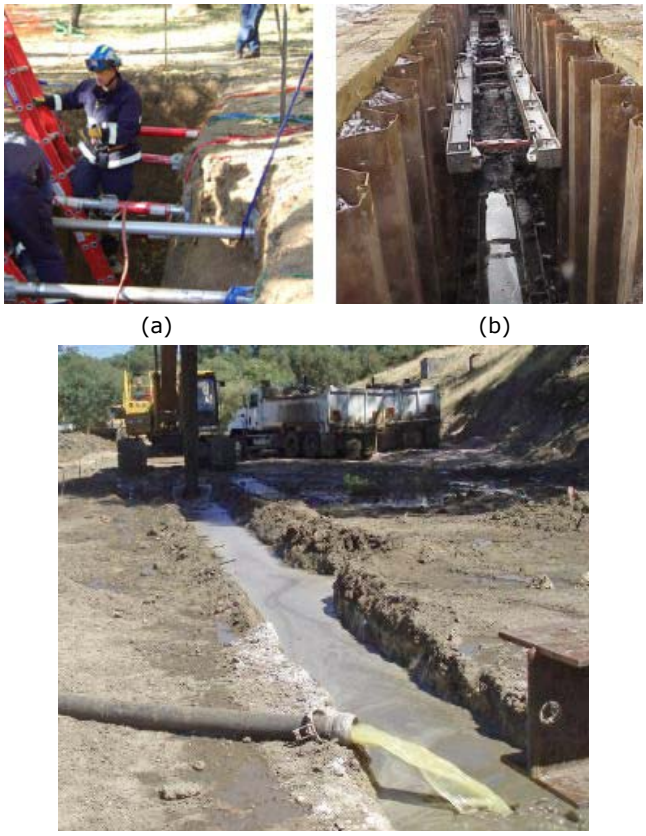

(a) (b)

(c)

Picture 4: Conventional Trenching Methods (left & center) compared to Slurry Trench (right), (a) propping, (b) sheet piling, (c) bio-polymer

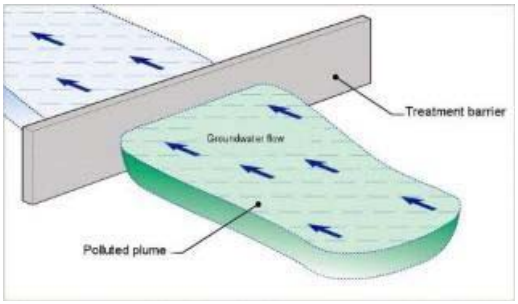

Figure 2: Active Barrier Polluted plumed treated when passing

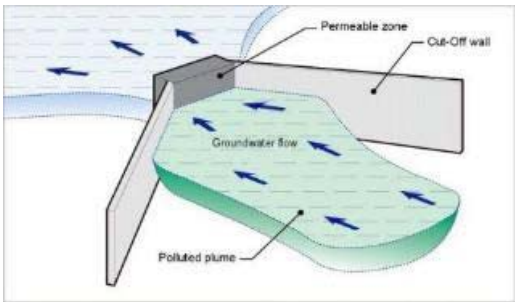

Figure 3: Funnel Gate Polluted plumed forced to a high capacity

The bio-polymer trenching method allows rapid installation without over excavation of contaminated soils and unnecessary exposure to construction personnel.

PRB walls address a wide range of contaminants such as chlorinated solvents, organics, metals, inorganics and radionucleides. Several processes are used within PRBs to treat contaminants which include:

- Adsorption (e.g., using activated coal and zeolite for organics)
- Precipitating for non-organics (e.g., lead precipitation using lime)
- Degradation (e.g., PCE, TCE can be degraded by iron filings)

Often the primary cost for PRB installations is the reactive material installed within the barriers. Hence there is pressure to optimise the barrier dimensions to achieve the ideal residence time and concentration for the intended design life. Reactive material is often blended with a clean sand to reduce the density of a reactive material across the barrier. Funnel and gate systems offer opportunities to utilise low cost soil bentonite cut-off walls to funnel ground water into a treatment zone. This zone can further be designed with a cell arrangement that allows maintenance of the reagent material. This concept allows a controlled response to the investment in reactive material as well as facilitates long term monitoring of the treatment process.

3. Case studies

3.1 Slurry cut-off wall

3.1.1 Soil bentonite slurry: Mayfield, NSW

The Mayfield site is approximately 155 ha within the former Newcastle Steelworks site on the south bank of the Hunter River at Mayfield. Over a period of 130 years this site has housed copper smelters, steelworks and ancillary operations. Steelworks wastes (slag) have been used to fill much of the site. The site was previously occupied by coke ovens, gas holders and other processes associated with steel making. Contaminants of concern identified on site include petroleum hydrocarbons (including benzene, toluene, ethyl benzene and xylenes), metals, ammonia, cyanide, phenols and polycyclic aromatic hydrocarbons.

Following the in-depth review of 32 options and alternatives, Menard Bachy was engaged to design and construct the barrier wall to reduce the migration of contaminated groundwater to the adjacent Hunter River, as part of a remediation strategy for the site.

The strategy finally adopted for the steelworks site initially relied on containment and comprised the following key elements as shown in Fig. 4:

- Construction of an upgradient groundwater barrier wall diverting flows away from the most contaminated area of the site (Area 1)
- Sealing the site surface area with an inert capping layer, which both prevents the infiltration of surface water, and provides a physical barrier between contaminated soils and humans on the site.
- Improved drainage infrastructure and contouring of the site, which will contribute to both the reduction of surface water infiltration and the management of possible contaminated surface water run-off from the site.

The soil bentonite wall is 1,510m long, 0.8m wide and has depths ranging from 25m to 49m, keyed into the basal confining layer of clay or weathered rock. Given the range of depths of excavation, two pieces of equipment working in sequence were used: a backhoe modified to dig to 25 metres to complete the first phase of the trench, and a mechanical clamshell to excavate the deeper material.

The success of the ground barrier was demonstrated through a thorough quality control program implemented during each phase of the project and which satisfied the design criteria:

- Maximum required permeability of 10-8m/s
- Surface completion to be trafficable: long term settlement of the wall less than 50 mm total settlement, and 1:50 differential distortion

The long term performance of the wall is being closely monitored via a system of groundwater monitoring wells fitted with automatic water level loggers located both inside and outside of the barrier wall.

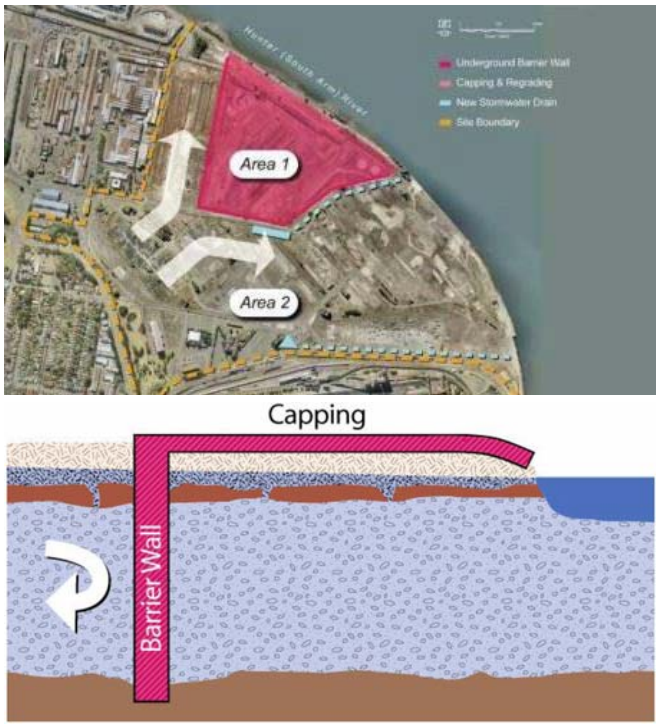

Figure 4: Schematic of Mayfield Site Remediation concept

3.1.2 Soil bentonite slurry: Mt Arthur MINE, NSW

The Mt Arthur alluvial cut-off wall project comprised the construction of a dam wall style bund along the western boundary of BHP Billiton's Mt Arthur Coal site, near Denman Road, Muswellbrook. The structure was required to protect the mine from a 1000yr flood event. Due to the presence of alluvial gravel deposits above the bedrock, the cut-off wall was required beneath the flood levee to block off subsurface flow given the increase in water pressure in association to the proposed flood.

The cut-off wall was 1340m in length and was socketed into the underlying bedrock at depths ranging between 4m and 13m below existing ground level. The Slurry Bentonite cut-off wall was constructed prior to the bund wall with a target permeability of 1 x 10^{-9}m/s, with a thickness of 0.8m.

One of the main challenges on the project was to allow for utilisation of water from the mine into the slurry design. Water quality testing of the source water showed results up to 5 times the recommended limit for slurry design, recording Total Dissolved Solids at 2500mg/L and Hardness at 1000mg/L. Resulting mix design found an additional 30% additional bentonite was required to achieve the target slurry properties.

Assessment of the actual depth to rock compared with the assumed rock depth from geotechnical investigations, found a close relationship. Variation is likely explained by varying soil/rock strength and possible variation due to the constructed working platform. This assessment for the client

and contractor is crucial to provide accurate budget estimates, however variation is always likely based on the actual encountered aquitard interface.

Picture 5: Bentonite slurry supported trench

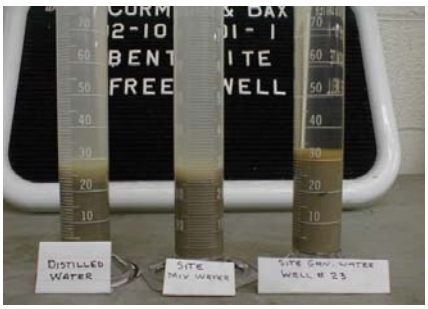

Picture 6: Slurry sedimentation assessment mine water compared with local tap water

3.1.3 Soil bentonite slurry: Liddell Coal MINE, NSW

Operational requirements at Liddell Coal Operations (Glencore) required an increase in water storage within one of the water storage dams. In order to achieve the design capacity of 2GL Menard Bachy was engaged by Glencore to install a bentonite slurry cut off wall in the mining spoil around the perimeter of the new water storage dam. This cut off wall was designed to prevent the flow of water through the mining spoil anticipated when the water level was increased in the water storage dam above 1GL. The design permeability was set at 1 x 10^{-8}m/s.

Over this 5 week period in 2014, 5,200m^2 of bentonite slurry cut off wall was installed over 600 linear metres. The ground conditions consisted of up to 7m of replaced overburden overlying shale bands and clay over bedrock. The max depth excavated using the longreach excavator was 14m.

The existing dam had been constructed within the area of an old dragline spoil area. As a result the subsurface material consisted a wide range of material including boulders up to 1m in diameter. This provided a unique constructability challenge to implement a barrier with large obstructions. To handle the obstructions the risk was assessed as a possible increase in trench width at localised obstruction locations and a reduced productivity. Considering the project was a remote site the risk of an enlarged trench was observed as acceptable. A Komatsu PC850 was paired with a long arm boom to meet the challenge of clearing the obstructions, however during the project a typical 0.8m trench width was maintained for the full length of the wall.

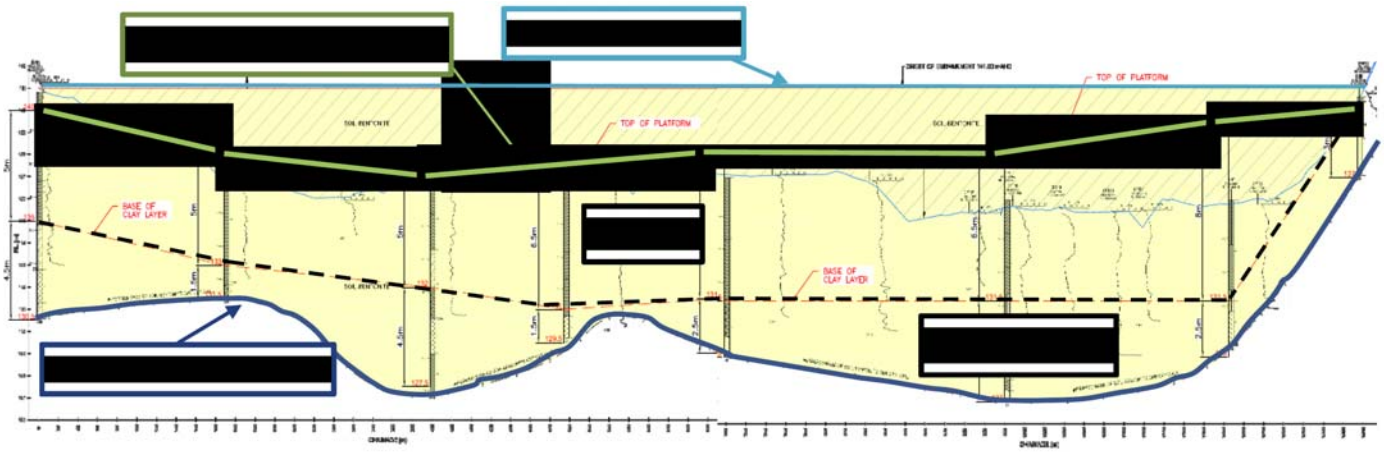

Figure 5: Geological section compared with barrier wall toe

Picture 7: Barrier wall being excavated through dragline spoil

Picture 8: Subsurface material – up to 1m diameter

3.1.4 Cement bentonite slurry: Port Bonython, NSW

The Santos Port Bonython Hydrocarbon Fractionation Plant is located on Weeroona Bay, approximately 35km from Whyalla in the Northern Spencer Golf. Soil and groundwater beneath the site appeared to be primarily impacted by crude oil leaking from adjacent storage tanks. The groundwater impacts were in the form of light non-aqueous phase liquids (LNAPL) typically floating on the groundwater or locked up in the formation and dissolved phase hydrocarbons in the groundwater. The presence of both off-site impacts and the potential for discharge to the marine environment necessitated a rapid evaluation of long-term mitigation and remediation options. In a collaborative evaluation of options a cement bentonite barrier wall was selected by Santos as the preferred remedial alternative, as it provides the highest level of confidence that off-site migration would be controlled and the long-term impacts mitigated.

The barrier wall is aligned adjacent to and sub-parallel to the ocean shoreline over a length of about 450m and is required to extend to a typical depth of 6-7m below initial surface level. The scope of works included the pre-excavation along the wall alignment through extremely high strength, abrasive sandstone, progressive backfilling and re-excavation under cement bentonite slurry, installation of a capping beam spanning the trench, the tracking and burial of contaminated soil and finally reinstating the site to natural contour levels.

After the initial rock breaking excavation, the wall was re-excavated under the cement bentonite slurry in panels which replaced the excavated material with the final cement bentonite mix to form the low permeability barrier. The mix design adopted produced a final wall with a permeability in the order of 5 x 10^{-9}m/sec and unconfined compressive strength of approximately 80kPa.

Picture 9: Depth sounding

3.2 Permeable reactive barriers

3.2.1 Continuous PRB walls: Bellevue, WA, Australia

A waste storage site operated a chemical/oil recycling and treatment facility in Bellevue, WA until a fire destroyed the facility in February 2001. Following the fire a series of investigations and risk assessments were undertaken at and in the vicinity of the property. Groundwater investigations confirmed the presence of a plume of hydrocarbons and halogenated organics originating from the former waste storage site. Subsequent groundwater monitoring indicated the presence of a separate off-site plume from a local source containing trichloroethene (TCE). Monitoring of data indicated that the two plumes converged beneath the escarpment prior to entering the Damplands.

A zero valent iron (ZVI) permeable reactive barrier (PRB) was proposed. As elevated concentrations of nitrate in the groundwater were confirmed during the delineation investigation, calculations showed that most of the ZVI material thickness would be consumed through nitrate passivity. Thus, a second PRB for denitrification was also designed upstream and in front of the ZVI wall.

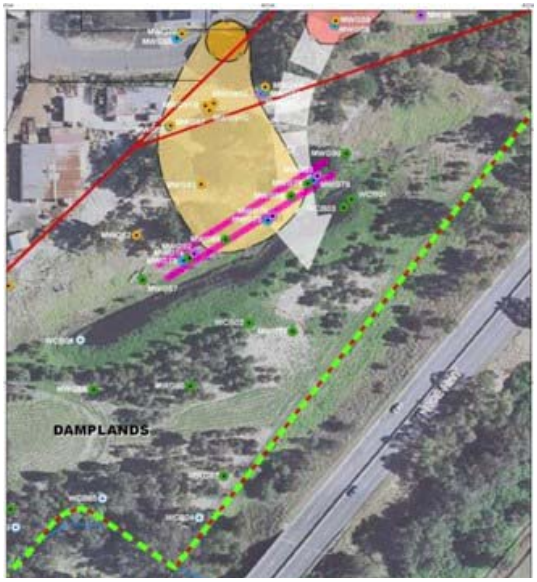

Picture 10: Operation Diagram

Picture 11: One of two parallel trenches dug to install permeable reactive barriers in Bellevue

Each PRB was designed to be 76 m long and extending down to the Leederville Formation clay layer at depth of approximately 11 m. The ZVI PRB was a mixture of ZVI and

sand. The denitrification PRB was a mixture of saw dust, chips and sand.

Menard Bachy was awarded the contract for the construction of the pair of PRBs based on an alternative proposal using deep trenching technology with a biopolymer slurry in lieu of execution of caissons and secant piles using a large diameter steel casing pushed into the ground and excavating the soil from within the casing. This alternative had a number of advantages including lesser cost and reduction of total and on site construction time, controlled width and continuity, control of key in depth, simplification of the environmental management plan, and lesser consumption of PRB material.

This project is the first application of a ZVI wall of industrial scale in Australia utilising the technique of PRB trenching.

3.2.2 Funnel & Gate PRB: Solva Chemie Plant, Berbe, Switzerland

The solvent reprocessing plant belonging to Solva Chemie is located at Bätterkinden, between Soleure and Berne. Until 1992, without a protective concrete slab, plant subsoil was polluted by chlorinated solvent infiltrations. The source of contamination having run dry, ground water was still polluted by a mixture of chlorinated solvents that canton authorities requested to be eliminated in accordance with the Swiss Federal order on contaminated sites.

The Engineering Consultant (Geotechnisches Institute) studied several solutions and proposed treatment of the natural ground water to the authorities, via an active wall through which solvents would be eliminated. The characteristic feature of this site is a ground water table with a low flow rate (about 10 l/min for the whole site) flowing towards Mühlibach, a subsoil with average perviousness and watertight substratum. After agreement from the authorities, the Geotechnisches Institute chose the solution proposed by Sif Groutbor (Soletanche Bachy subsidiary), associated with ATE, of installing a filtering gate.

This system includes the following:

- A water-collecting drainage system: horizontal drilling and draining wall,
- A soil bentonite slurry wall,
- A filtering gate built according to the patented panel-drain technology, containing a filter with a volume of 1 m3 and weighing about 5 tons, through which water can filter. They also patented a treating product "Iron" with an added set of catalysts, enabling lower pollutant levels to canton administration-permitted thresholds. The whole unit is gravity operated, is always accessible via the top and requires minimal maintenance.
- A discharge system including an observation well and gravity flow towards Mühlibach.

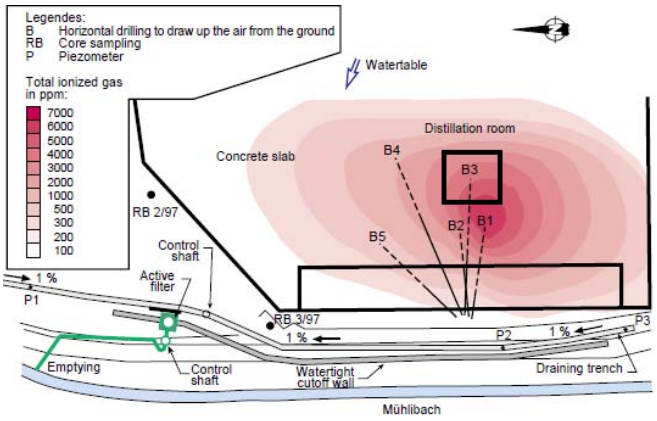

Figure 6: Operation Diagram

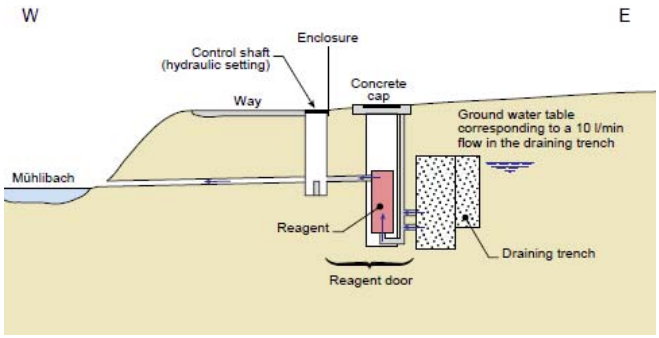

Figure 7: Schematic section

Ground Water samples were analysed both upstream and downstream. The following table presents the results obtained and demonstrate the effectiveness in reducing concentration of key contaminants immediately following the installation of the Funnel and gate system.

Table 2: Analysis results after 15 days of operations

Dissolved elements (µg/l percentage)	Upsteam	Downstream
Vinyl chloride	3	0.23
Trichlorethylene	94	0.46
Cis 1-2 dichlorethylene	199	2
Perchlorethylne	25	0.16
1.1.1. trichlorethane	9	0.22
1.1 dichlorethane	0.67	0.5

4. Sustainability considerations

The key contribution of slurry wall technologies to the sustainable development aspect is the ability to install underground structure whilst both involving limited quantities of excavation and minimal amount of imported materials such as cement or steel both high contributors in CO2 emissions for instance.

Another key benefit of the slurry wall techniques over other traditional methods is associated with the very high production rates. This translates into overhead cost savings and benefit projects with tight construction schedules. In particular, the performance of civil works in urban contaminated environment can often lead to negative impact on the local community. Production of excessive noise, increased traffic and potential for air contamination represent a few of such adverse impacts. As a result, a reduction in overall program of works results in decreased impact over the local communities.

Further, excavation works are carried out under slurry limiting both risk of generating dust but also providing increased certainty in construction schedules through improved ability to control geotechnical risks such as subterranean voids and presence of localised weaker strata. Experience indeed shows that many conventional shoring techniques suffer extended delays due to unforeseen ground conditions of either geotechnical or hydrogeological nature.

The ability to install cut off walls in a controlled fashion, with minimal exposure of contaminated material and in an unmatched of time provides unrivalled construction benefits for modern urban civil works.

When scoring sustainability for geotechnical works, the estimated carbon footprint can often be an important indicator. Carbon footprint is the sum of all emissions of CO_2 in a year, induced by site activities and by the production of materials used in construction.

Today's access to new tools for assessing and benchmarking several environmental indicators for various competing solutions allows for accurate comparison of ground im-

provement techniques and assist both contractors and clients in retaining the "best for project" schemes. Figure 9 illustrates a comparison being performed on a range of solutions in accordance with the European Norm En 15804.

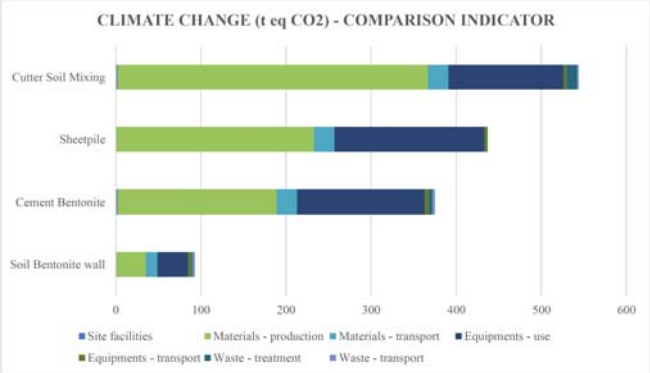

Figure 8: Climate Change (t eq CO_2) – Comparison of various Cut off wall schemes (Prism solution – Menard Bachy)

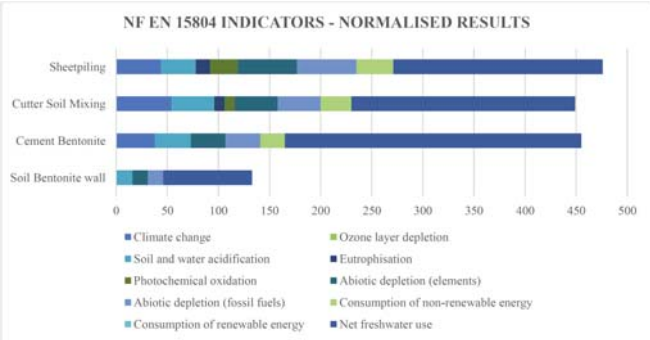

Figure 9: NF EN 15804 Indicators – Comparison of various Cut off wall schemes (Prism solution – Menard Bachy)

Going forward, it is anticipated that regulation to limit carbon emmissions with the view to limit the impact on climate change will become tougher. Further, increasing constraints on urban development to meet stringent environmental regulation as well as stakeholders requirements to limit impact on local communities are strong incentives to develop more environmentally friendly techniques.

5. Conclusions and Recommendations

Low permeability barriers can be succesfully implemented to control groundwater in a diverse range of applications such as open cut excavation in urban environement, control of horizontal seepage and channeling of contaminated water to prevent discharge in watercourses but also control of groundwater inflow in open cut mines, upgrades of dam and landfills capacity.

The methods utilised to install such walls are readily adaptable through use of a range of alternative stabilising agents to also install permeable barriers. These can then be utilised to install deep collection drains, or even reactive agents to breakdown or capture groundwater contamination.

Whilst enabling to perform tasks that could not be achieved before, the methods of slurry bentonite and bio-polymer installation of underground barriers also grant significant benefits in advancing the construction performance on criteria such as cost, program and environmental impact.

The slurry wall concept is a highly flexible construction technique that is proven to be the most effective method for developing in ground installations. Therefore the future of slurry type wall is somewhat limited to the imagination of the engineer/environmentalist assessing individual projects over a wide range of industries.

6. References

Bouzalakos S, Crane R, Liu H, Timms W, *Geotechnical and modelling studies of low permeability barriers to limit mine water seepage*. Water in Mining congress, Chile, 28-30 May 2014

BRGM/RP – 25609 – FR, *Quelles techniques pour quels traitements – Analyse couts – bénéfices,* May 2010

Jones. S, Spaulding, C & Smyth. P. *Design and construction of a deep soil-bentonite groundwater barrier wall at Newcastle, Australia.* Proceedings of the 10th Australia New Zealand Conference on Geomechanics 2007, Brisbane

Liausu, P & Spaulding, C. C*onstruction d'une paroi etanche en sol-bentonite sur le site de l'ancienne acierie de Newcastle.* Revue Travaux 2007, no. 836, pp. 75-79

NEPM (2003). *Impact Statement for the National Environment Protection (Air Toxics) Measure* 2003, National Environment Protection Council, NSW Australia

Ryan, C & Spaulding, C. *Vertical groundwater barriers for contaminated site reclamation.* Proceedings of the 10th Australia New Zealand Conference on Geomechanics 2007, Brisbane

Spaulding, C. *Soil Bentonite Cut-off Walls for Confinement of Existing Landfills: Tempe Tip - A Case Study.* XVIth SEAsian Geotech Conference 2007

US EPA (1998), *'Evaluation of Subsurface Engineered Barriers at Waste Sites'* EPA-542-R-98-005, July 1998

Παρουσίαση άρθρων, στην συγγραφή των οποίων μετείχαν Έλληνες, στο XVI European Conference on Soil Mechanics and Geotechnical Engineering, Edinburgh, 13-17 September 2015 (κατ' αλφαβητική σειρά, στα ελληνικά, του ονόματος του πρώτου συγγραφέα).

The effect of cracking on the response and design of diaphragm walls and adjacent buildings

L'effet de fissuration à la réponse et le dimensionnement de parois moulées et aux bâtiments adjacents

E.M. Comodromos and M.C. Papadopoulou

ABSTRACT The development of the bending moment corresponding to the maximum tensile stress the concrete accommodated (relatively low with reference to the capacity of the wall) produces cracking initiation. Despite the fact that concrete cracking significantly affects the diaphragm wall response by provoking substantial decrease in its stiffness, it is often disregarded or is introduced by empirically reducing the bending stiffness. A very interesting approach for estimating the bending stiffness of concrete sections and the bending moment of cracked sections as a function of the curvature is provided by the moment–curvature relationship derived from the beam theory. This model has been implemented in many structural software codes that can calculate and use the nonlinear moment-curvature response for a given reinforced concrete section. The proposed approach has been applied in the case of a deep excavation supported by diaphragm wall, where a nonlinear mutli-stage simulation process has been implemented. Comparative analyses disregarding the cracking onset have been carried out as well and interesting conclusions were drawn relating the effect of cracking and reduction in the bending stiffness to the response of the diaphragm wall, the bending moment distribution along the wall and the displacement field in the surrounding soil and adjacent buildings.

1 INTRODUCTION

In many cases the criterion for the design of diaphragm walls to resist lateral loads is not the ultimate capacity but the lateral deflection of the diaphragm as well as the settlements induced to adjacent structures. Even a few centimeters of displacement could cause significant stress development on these structures. As a result, in such cases, a displacement based design concept is considered more appropriate than the capacity based design, which limits the soil-structure interaction mechanism to the determination of the bearing capacity of the diaphragm wall.

The estimation of the response of diaphragm walls does not always allow for concrete cracking which substantially reduces the bending stiffness, leading to underestimation of diaphragm lateral displacements and settlements of adjacent buildings. In order to predict the displacement field, several approaches have been developed, ranging from application of empirical relationships to sophisticated nonlinear numerical procedures. In many cases, where the response of an adjacent building is crucial for the design process and high precision is required, a profound multi-stage numerical analysis, including the adjacent building and allowing for all material nonlinearities (soil and concrete), provides reliable results which can be used in the design.

With the aim of investigating the effect of cracking, a nonlinear multi-stage simulation process has been implemented. The bending stiffness of the diaphragm and the bending moment of cracked sections were estimated by the moment–curvature relationship derived from the beam theory as a function of the curvature. Comparative analyses disregarding the cracking onset have been carried out as well and interesting conclusions were drawn relating the effect of cracking and reduction in the bending stiffness to the response of the diaphragm wall, the bending moment distribution along the wall and the displacement field in the surrounding soil and adjacent buildings.

2 EFFECT OF CRACKING

2.1 Formulation

According to the Euler's beam theory the bending moment M of a beam can easily be obtained using the following equation:

$$M(z) = E_{\mathrm{DW}} I_{\mathrm{DW}} \phi = E_{\mathrm{DW}} I_{\mathrm{DW}} \frac{d^2 y(z)}{dz^2} \qquad (1)$$

where M is the bending moment; E_p the effective DW elastic modulus, I_p the effective DW moment of inertia and y is the horizontal DW displacement. In the case of linear elasticity (no cracking occurrence), M is estimated straightforwardly from Eq. (1). The value of the bending stiffness can be estimated from Eqs. (2) and (3).

$$E_{\mathrm{DW}} = \left[1 + (n-1)\frac{A_{\mathrm{s}}}{A_{\mathrm{c}}}\right] E_{\mathrm{c}} \qquad (2)$$

$$I_{\mathrm{DW}} = \frac{t_{\mathrm{DW}}^{\ 3}}{12} + \frac{1}{2}(n-1) A_{\mathrm{s}} h_{\mathrm{s}}^2 \qquad (3)$$

where E_c is the elastic modulus of concrete, E_s the elastic modulus of steel, $n=E_s/E_c$, Ac the area of the concrete, As the total area of steel reinforcement, t_{DW} the DW thickness, and h_s the distance from the centroidal axis of the cross-section to the centroidal axis of the steel bars.

Despite the fact that the above formulae are valid in the case of uncracked behavior, for simplification, it is widely used in field measurements and back analysis process even when partial cracking occurs (Smethurst & Powrie, 2007). The effect of cracking is then introduced by empirically reducing the bending stiffness.

A more accurate procedure in estimating the bending moment is given by Eq. (4):

$$M = E_{\mathrm{DW}} I_{\mathrm{DW}} \phi = \left(E_c I_c + E_s I_s\right)\phi \qquad (4)$$

Concrete and steel Young's moduli, E_c and E_s, remain unchanged, while moments of inertia change as cracking develops. The moment of inertia of the concrete can be estimated taking into account the shape of the uncracked section, and the moment of inertia of the steel reinforcement is given by Eq. (5):

$$I = \sum_{i=1}^{n} \left(\frac{A_{\mathrm{si}}^2}{16\pi} + A_{\mathrm{si}} h_{si}^2 \right) \cong \sum_{j=1}^{n} A_{\mathrm{si}} h_{\mathrm{si}}^2 \qquad (5)$$

where A_{si} is the section of a reinforcing steel bar i and h_{si} is the distance from the centroidal axis of steel bar i to the centroidal axis of the cross-section, as shown in Fig. 1.

When cracking occurs, the cendroidal axis of the DW section differs from the neutral axis, and therefore a better estimation of the curvature is given by Eq. (6) rather than by the second derivative of the displacement field at the center of the DW.

$$\phi = \frac{|\varepsilon_t| + |\varepsilon_c|}{h} \qquad (6)$$

A very interesting approach for estimating the bending stiffness of the DW and the bending moment of cracked sections as a function of the curvature is provided by the moment–curvature relationship derived from the beam theory (Park & Paulay 1975).

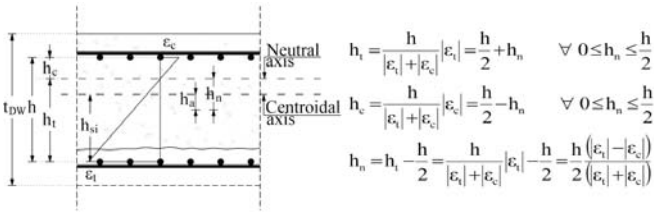

Figure 1. Formulation and definition for a rectangular reinforced concrete section under flexural deformation.

This model has been implemented in many structural software codes that can calculate and use the nonlinear moment-curvature response for a given reinforced concrete section. Comparative results of the application of the aforementioned approaches are given by Comodromos et al. (2009). Figure 2 and illustrate the variation of bending moment M with curvature φ numerically established by applying the method of Park & Paulay (1975), while Fig. 3 shows the variation of bending stiffness as cracking effect increases.

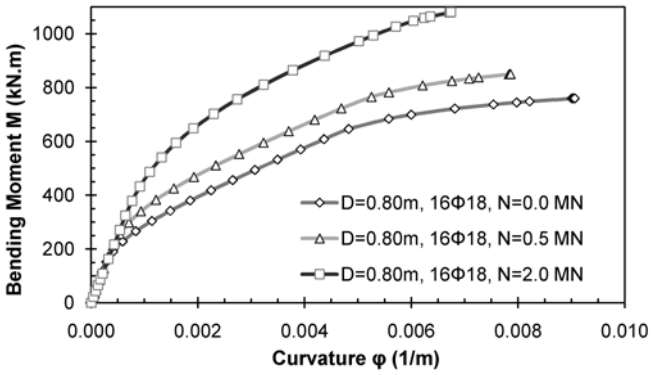

Figure 2. Moment-curvature curves for a pile (D=0.80 m with 16Φ18 steel bars) under axial load 0, 0.5 and 2.0 MN provided by the program code SOFISTIK (after Comodromos et al. 2009).

The effect of DW cracking is mentioned in the special CIRIA report C580 (Gaba et al. 2003) where it is emphasized that the flexural stiffness should be calculated and taken into account at each construction stage. When no numerical codes accounting for the flexural variation are available it is proposed as a rule of thumb to reduce the initial value of $E_{DW}I_{DW}$ to 70% and 50% during construction and long-term stages respectively.

It is evident that the application of the above rule of thumb instead of carrying out an iterative analysis accounting for flexural stiffness variation is quite helpful in reducing the required calculation time. However, as underlined in the CIRIA C580 Report, this simplified approach should be considered carefully. Therefore, prior to any application the above empirical recommendations are validated through a simplified analysis of a reinforced concrete beam presented in the next paragraph.

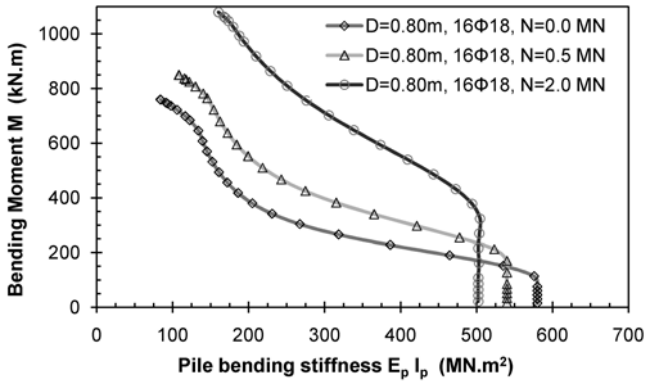

Figure 3. Variation of bending stiffness as applied moment increases for a pile (D=0.80 m with 16Φ18 steel bars) under axial load 0, 0.5 and 2.0 MN provided by the program code SOFISTIK (after Comodromos et al. 2009).

2.2 Validation

A primary evaluation of the nonlinear behavior of due to stiffness reduction of the reinforced concrete section is carried out through a simplified analysis of a reinforced concrete beam. More specifically, a 10.0 m length cantilever with a 0.80 m × 1.00 m rectangular section reinforced with 10 steel bars Φ20 mm at each side of 20 mm, was considered. A point load of 100 kN at the free edge of the beam leads to a 1000 kN·m bending moment at the base, while the yielding moment of the section is 1033 kN·m. The results of the numerical analysis are given in Fig. 4. More specifically, the continuous line corresponds to linear elastic analysis with E_c = 32000 MPa. The deflection at the edge of the beam equals to 23.8 mm, whereas in the case of linear analysis with a 50% reduction of the stiffness (bold continuous line) is approximately double. A nonlinear analysis with zero tensile concrete strength and a value of f_{ctD} = 2.9 MPa is also conducted and the deflection is presented with dashed normal and bold lines respectively. Ignoring concrete tensile strength, consideration which is often adopted in reinforced concrete analyses, leads to excessive deflection, while allowing for concrete tensile strength leads to a deflection of the same order with the 50% stiffness reduction guidance. However, it should be emphasized that the aforementioned rule of thumb, which is widely adopted internationally, is to be used only when the developed bending moment is of the order the cross section strength, and for lower levels of loading it leads to conservative results. The same analyses have been carried out for different constraint conditions. The results for a cantilever beam with a slider at the other edge loaded up to its maximum capacity are presented in Fig. 5 and lead to similar conclusions. For the same constraints (cantilever – slider) and for a load that leads to 50% of the yielding moment, linear analysis without any stiffness reduction is more appropriate than adopting a 50% reduced value of elasticity modulus, as shown in Fig. 6.

The simplified analysis presented above demonstrates that in order to conduct a linear analysis the application of stiffness reduction is indispensable, provided that actions lead to depletion of the cross section capacity. This case is applied thereafter together with a nonlinear analysis to allow for nonlinear behavior of a reinforced concrete diaphragm wall.

3 APPLICATION TO AN UNDERGROUND STATION

3.1 Project - site description

The effect of cracking is examined hereafter in the case of an underground station with adjacent building very close to

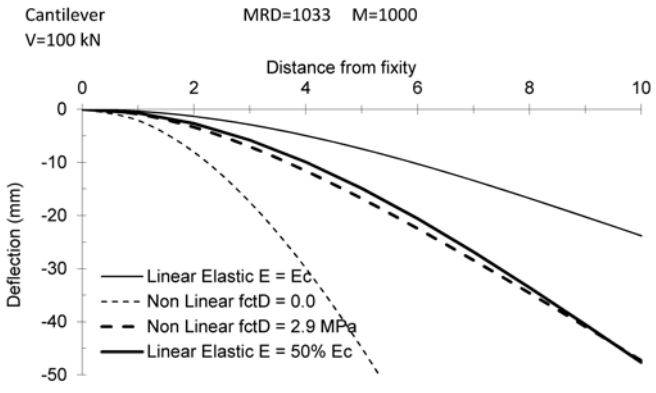

Figure 4. Deflection comparison of a cantilever beam provided by a linear analysis and the analysis accounting for cracking, loaded up to its maximum capacity.

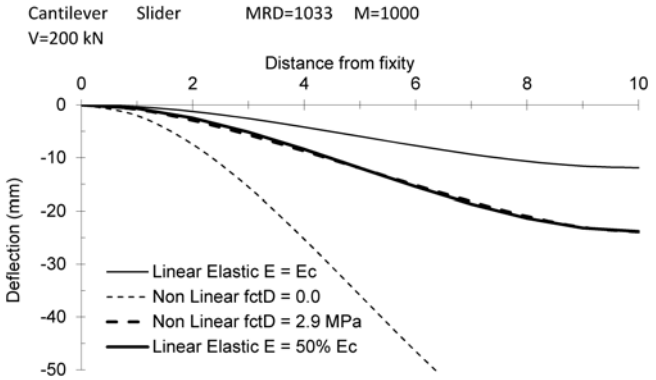

Figure 5. Deflection comparison of a cantilever beam with a slider at the other edge provided by a linear analysis and the analysis accounting for cracking, loaded up to its maximum capacity.

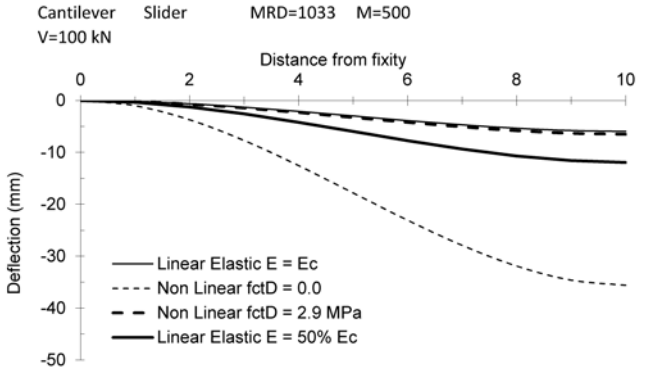

Figure 6. Deflection comparison of a cantilever beam with a slider at the other edge provided by a linear analysis and the analysis accounting for cracking, loaded at the 50% of its maximum capacity.

the diaphragm wall. The station, named as Analipsis station, is part the underground of Thessaloniki, it is 210 m long and 16.4 m wide. The thickness of the panels is t = 1.20 m, the depth of the diaphragm wall is H = 44.0 m and the basement of the station is 28.0 m below the ground surface. The DW cross section of concrete grade C30/37 was reinforced with 15 steel bars of 32 mm in diameter on each side.

The ground conditions at the site comprise about 2.0 m of fill material overlying a formation of sandy clay consisting of two main layers. Soil strength and deformation modulus are increasing with depth and therefore the soil profile has been subdivided in 5 sub-layers, namely 1, 2, 3, 4 and 5 as shown in Fig. 7. The groundwater level was encountered at 5.0 m below the ground level. Pressuremeter tests were carried out at the area to assess the in situ horizontal stresses and, according to the evaluation of the results, a constant value of K_0 = 0.54 has been adopted. The main soil properties of each soil layer, derived from the carried out geotechnical investigation and the evaluation of in-situ and laboratory tests are summarised in Table 1 while detailed information is given by Comodromos et al. (2013).

Table 1. Geotechnical properties of soil layers.

Layer	1	2	3	4	5
Depth (m)	0 -3	3-10	10-35	35-40	40-60
Eff. cohesion c' (kPa)	3	3	5	40	50
Eff. angle of friction φ' (deg)	30	25	25	25	25
Poisson's ratio	0.3	0.3	0.3	0.3	0.3
Bulk mod. in loading K (kPa)	5.0	6.0	10.0	12.0	12.0
Bulk mod. in unload. reload. (MPa)	25.0	39.0	105.0	144.0	144.0

3.2 Numerical analysis - results evaluation

The finite element analysis code SOFiSTiK was used to evaluate the effects of cracking on the response of the diaphragm wall and the adjacent building. The finite element mesh is illustrated in Fig. 7 where soil layers, excavation stages, the diaphragm wall and the adjacent building are included. The ground is simulated by shell elements with properties as shown in Table 1. Bearing in mind the crucial effect and the necessity for settlements predictions to the adjacent buildings, a constitutive law with double hardening has been applied. The model accounts for the stress dependent stiffness in primary loading and unloading/reloading stress paths. Three assumptions were made for the concrete diaphragm wall behavior. More specifically, it was considered as i) linear elastic with a modulus of elasticity E_c = 32 GPa, ii) linear elastic with a 50% reduction in stiffness and iii) nonlinear using the moment-curvature section relationship and assuming tensile concrete strength f_{ctD} = 2.9 MPa. Linear elastic behaviour was attributed to the adjacent building with properties corresponding to reinforced concrete of grade C20/25. The stiffness of the columns and the beams were appropriately adjusted to take into account the 2D numerical simulation. On each floor a loading equal to functional loads was applied.

The whole procedure and sequence of simulating corresponds to actual construction sequence. More specifically, the first step consists of the in situ state of stress establishment, which was followed by 6 excavation stages.

The results of the three analyses for the final excavation stage are presented in Figures 8 and 9 where the bold continuous lines correspond to the elastic analysis with no stiffness reduction, the normal continuous lines stand for the linear elastic analysis with a 50% reduction in stiffness and the dashed lines represent the results of the nonlinear analysis. The application of 50% stiffness reduction when conducting a linear analysis is validated, as the results are in close agreement with those of the nonlinear analysis. On the contrary, ignoring post-cracking behavior and adopting the initial stiffness in a linear analysis underestimates the resulting displacements. It is obvious that, for the final excavation stage, in the analyses with post-cracking behavior, the maximum bending moments developed are lower than the moment derived by the elastic analysis, since they are limited by the yielding value (M_y = 4534 kN·m). With regard to the horizontal displacements of the diaphragm wall, the effect of cracking is significant as the increase in maximum values reaches 30%. The same impact is also obvious on the settlements of the adjacent building, Fig. 9.

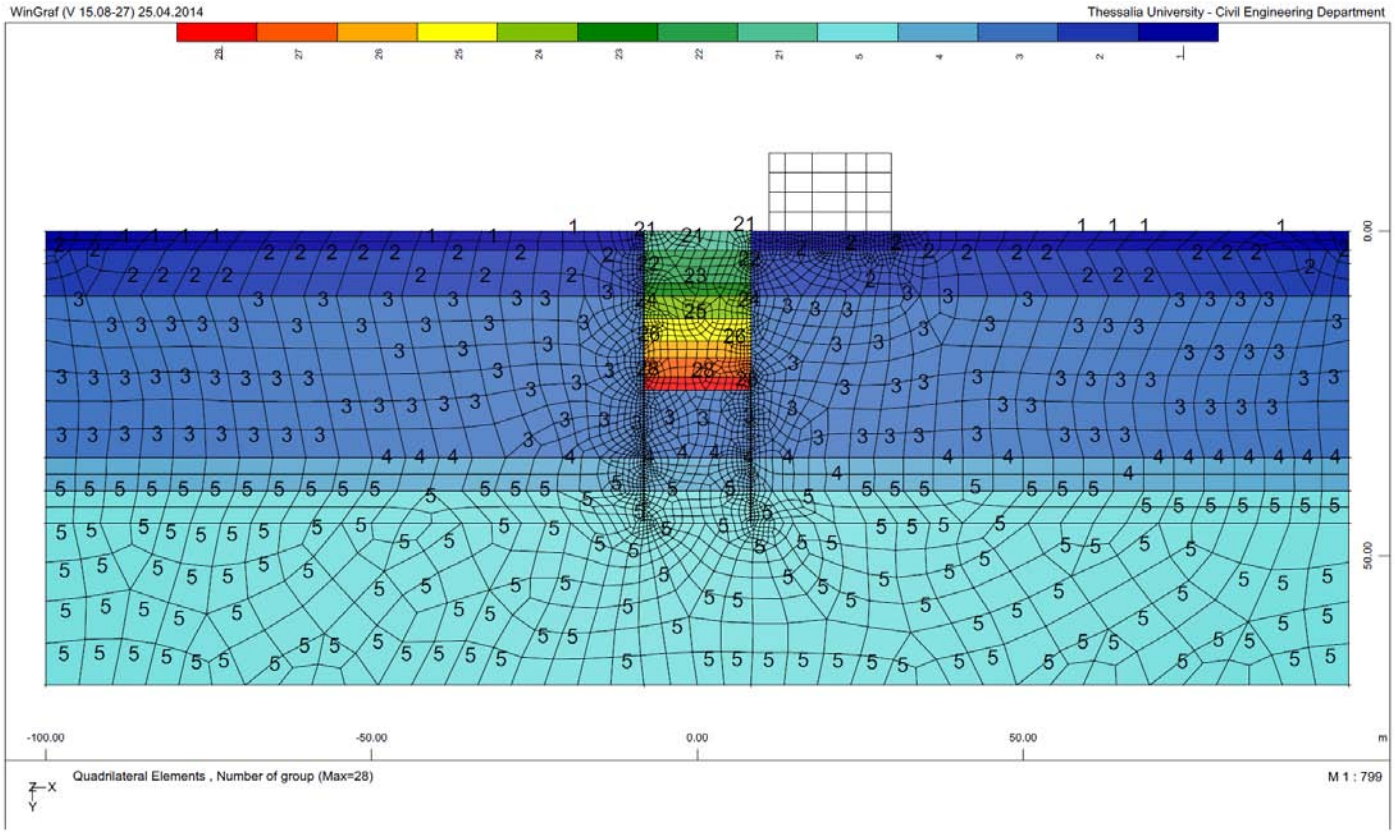

Figure 7. Finite element mesh presenting soil layers, excavation stages and an adjacent building.

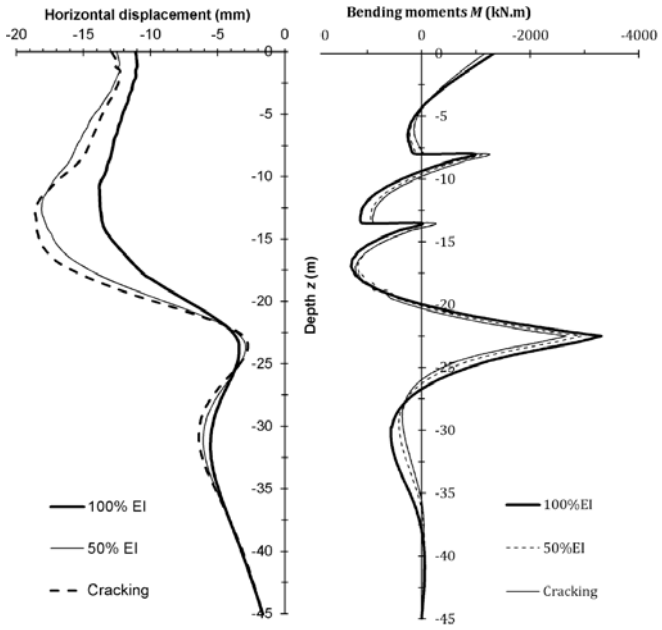

Figure 8.

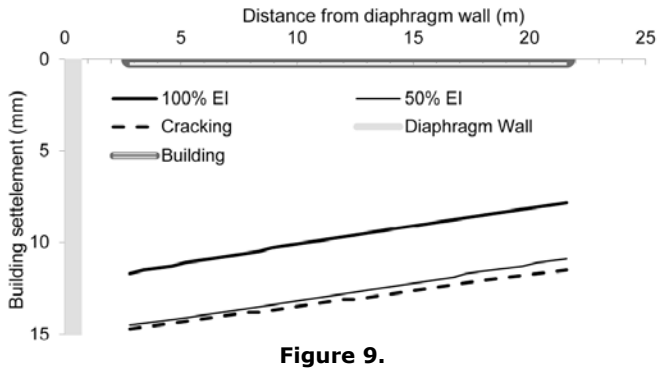

Figure 9.

Given that displacement control is crucial during the construction of diaphragm walls, allowing for cracking effect is indispensable and can be accomplished either by means of nonlinear analysis or by conducting linear analysis and appropriately reducing the initial value of $E_{DW}I_{DW}$. However, it should be emphasized that the latter simplified approach leads to reasonable results in the case of high bending moment values, close to the cross section bending capacity. This is typically the case of the final excavation stage which is usually the most crucial for the diaphragm wall design.

4 CONCLUSIONS

A methodology accounting for cracking effects of concrete on the response of diaphragm walls has been presented. It was found that initial bending stiffness of the wall can be used to estimate bending moment provided that the calculated value is less than the cracking moment. Further loading increment initiates cracking in concrete and, as a result, bending stiffness of the diaphragm must be reduced, otherwise bending moments are overestimated. Furthermore, the effect on the displacement field is also significant, as disregarding cracking and stiffness reduction lead to underestimated values of diaphragm horizontal displacements and adjacent buildings' settlements. The proposed method makes use of nonlinear moment-curvature relationships of concrete sections that are incorporated in structural software codes and is able to accurately predict the response of a concrete diaphragm wall undergoing cracking.

ACKNOWLEDGEMENT

The information provided by Attiko Metro S.A is gratefully acknowledged.

5 REFERENCES

Comodromos, E.M. Papadopoulou M.C. & Rentzeperis I.K. 2009. The effect of cracking on the response of pile test

under horizontal loading, *J Geotech Geoenv Engrg, ASCE*, **135**(9), 1275-1284.

Comodromos, E.M. Papadopoulou M.C. & Konstantinidis G.K. 2013. Effects from diaphragm wall installation to surrounding soil and adjacent buildings, *Computers & Geotechnics* **53**, 106- 121.

Gaba, A,R, Simpson, B. Powrie, W. & Beadman, D.R. 2003. *Embedded retaining walls: guidance for economic design*, CIRIA Report C580. London.

Park, R. & Paulay, T. 1975. *Reinforced concrete structures*, Wiley, New York.

Smethurst, J. A. and Powrie, W. 2007. Monitoring and analysis of the bending behaviour of discrete piles used to stabilise a railway embankment, *Géotechnique* **57**(8), 663–677.

Numerical interpretation of the coupled hydromechanical behaviour of expansive clays in constant volume column tests

Interprétation numérique du comportement hydromécanique d'argiles expansibles lors de test en colonnes à volume constant

V. Mantikos, A. Tsiampousi, D.M.G. Taborda and D.M. Potts

ABSTRACT Experimental and numerical studies of the behaviour of expansive clays have been attracting increasing interest, due to their good sealing properties, which render them ideal to be used as engineered barriers (buffers) in both active (e.g. nuclear) and non-active waste disposal facilities. Both large scale and laboratory scaled experiments indicate that the sealing capabilities of the buffer are fundamentally governed by its volumetric behaviour when wetted. In this paper, a constant volume column infiltration test, performed under isothermal conditions on compacted MX80 bentonite, is modelled numerically using the Imperial College Finite Element Program (ICFEP). A modified version of the Barcelona Basic Model is used to simulate the behaviour of the buffer, which is inherently partly saturated. The numerical results agree well with the observed experimental data, especially with regard to the advancement of the wetting front. A detailed interpretation of the computed evolutions with time of stress state, suction and void ratio at different elevations along the sample's axis is carried out, providing insight into the complex hydro-mechanical response of the buffer during the experiment. Indeed, even though the overall volume of the sample was kept constant, a region of localised dilation, which induced the contraction of other zones of the material, was observed to advance simultaneously with the wetting front along the height of the soil column.

1 INTRODUCTION

Deep geological disposal is a permanent method of disposing of high level nuclear waste and it gains support from researchers for being the safest option. The function of a buffer in the sealing arrangement is to isolate the waste canister from erosion, mechanical loading and radionuclide transfer. In-depth investigation of the fundamental behaviour of expansive clays is in progress in all nuclear power generating countries to model and assess their performance as a buffer material.

Of particular research interest is the re-saturation of the buffer under constrained swelling conditions. Different theoretical approaches have addressed the mechanical aspect of this phenomenon through a suction dependent stress state surface (Gens & Alonso, 1992), often incorporating a double structure (Alonso et al. 1999) or a generalised plasticity model (Sanchez et al. 2005). Moreover, vapour diffusion (Kröhn 2005) or liquid water flow (Hoffmann et al. 2007) theories may be used to explain the hydration process. The thermal and chemical effects that add to the complexity of the problem are not discussed here.

To increase confidence in modelling the coupled behaviour, full scale field and laboratory tests were carried out (Schanz et al. 2013). Laboratory tests include constant suction or constant stress conditions, free swell tests or constant volume hydration tests. Schanz et al. (2008) propose a sensitivity analysis procedure to identify the important modelling parameters using swell test data.

The unsaturated hydraulic permeability of clays is most suitably measured by unsteady methods (Benson et al. 1997; Cui et al. 2008). One common test for bentonite buffers is the column infiltration technique (swell test), where a cylindrical specimen is wetted at one end. This test simulates the confined hydration conditions in the buffer, enabling the study of the evolution in density and permeability as hydration progresses along the column (Delage et al. 2010).

In this paper, a constant volume column infiltration test (Marcial et al. 2008), performed under isothermal conditions on compacted MX80 bentonite, is modelled numerically using the Imperial College Finite Element Program (ICFEP) (Potts & Zdravkovic 1999). A modified version of the Barcelona Basic Model (BBM) (Georgiadis et al. 2005, Tsiampousi et al. 2013) is used to simulate the behaviour of the buffer, which is inherently partly saturated.

2 SIMULATED INFILTRATION TEST

The hydration test described by Marcial et al. (2008) was selected for the purpose of acting as a reference model for the numerical analysis results. The test was conducted under iso-thermal conditions, at T=20°C. The soil material was subjected to a 39MPa static compaction stress to achieve a density of 1.7 Mg/m^3 after rebound, so that it would have a high swelling potential and a double porosity structure. The water content was measured at 8.2%, which corresponds to 103MPa suction. The specimen was prepared with a diameter slightly smaller than the apparatus cylinder to avoid friction developing during placement. Figure 1 presents the arrangement of the apparatus.

The sample was placed inside a 50mm diameter x 250mm long rigid cylinder in the form of compacted bricks and the system was sealed and thermally isolated. The radial stress was interpreted by Marcial et al. (2008) from the deformation of thin semi-rigid zones of the cylinder, calibrated so that 60MPa of pressure gave 5μm deflection. Relative Humidity (RH) probes where placed at distances of 4.5cm, 9.5cm, 14.5cm, 19.5cm and 25cm from the base of the sample.

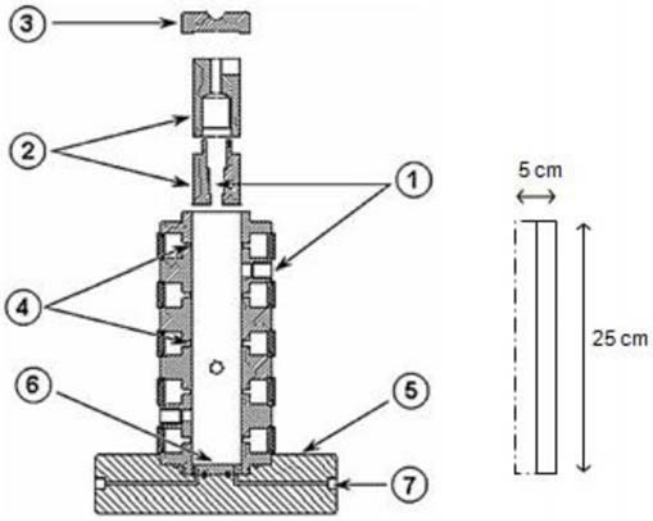

Figure 1. Infiltration column: (1) holes for RH sensors location (2) split head piston (3) piston cap (4) 2mm thick zones for lateral stress monitoring (5) column base (6) porous stone (7) water intake circuit. (Marcial et al. 2008).

3 NUMERICAL MODEL

3.1 Finite element mesh

Quadrilateral 8-noded isoparametric elements were used for the discretisation of the sample. Displacement degrees of freedom were assigned to all nodes, whereas pore water pressure (PWP) degrees of freedom were assigned only to corner nodes.

3.2 Boundary conditions

In order to force constant volume conditions, no radial dis-

placements were allowed along the left and right vertical boundaries of the finite element mesh and no vertical displacements along the horizontal top and bottom boundaries.

All boundaries have been considered impermeable, with the exception of the bottom boundary where a constant water pressure of 10kPa was prescribed to simulate water infiltration.

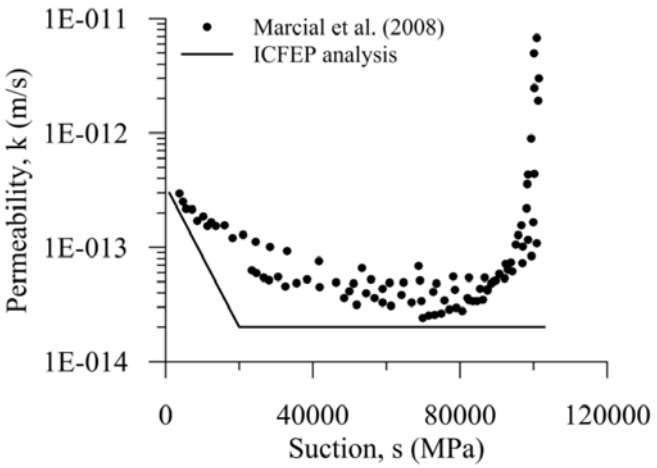

Figure 2. Variability of permeability with suction (data from Marcial et al., 2008).

3.3 Constitutive, water retention and permeability models

The material used for the experiment was MX 80, a commercial bentonite from Wyoming, USA. It is a Na-smectite with some Ca (Delage et al. 2010), high montmorillonite content (80%), high liquid limit and specific surface, making it a highly expansive clay.

The Barcelona Basic model (Alonso et al. 1990) was used as the constitutive model for the analysis, with the modifications proposed by Georgiadis et al. (2005) and Tsiampousi et al. (2013), in conjunction with a Van Genuchten (1980)-type soil-water retention curve (SWRC). The respective model parameters are summarised in Table 1 and were calibrated based on laboratory data reported by Tang et al. (2008) and Dueck (2008).

The variation of permeability, k, with suction, s, adopted in the analysis is shown in Figure 2, in comparison with experimental data from Marcial et al. (2008). In the analysis, the logarithm of permeability varies linearly with suction, from its saturated value k_{sat} corresponding to suction p1 to a minimum value k_{min} at suction p2 (values in Table 1).

3.4 Initial conditions/stress state

The compaction-induced suction was 103 MPa, corresponding to an initial degree of saturation of 32.3%. No load was initially applied ($\sigma_r = \sigma_v = 0$) resulting in a compressive initial mean effective stress which is equal to the induced suction. The initial void ratio was set to 0.66.

3.5 Type of analysis

The infiltration test described above was simulated in a hydro-mechanical (HM) coupled consolidation, partly saturated, axi-symmetric analysis. The Imperial Finite Element Program (ICFEP) (Potts & Zdravkovic 1999) was used, which employs a modified Newton-Raphson solution technique with an error controlled sub-stepping stress-point algorithm. ICFEP uses a sign convention for the stresses where tension is considered positive. This applies also for the pore water pressures, i.e. suction has a positive sign. The same convention is used herein. As consolidation is a time-dependent process, time steps were assigned to each increment. Each of the first 60 increments corresponds to one minute of simulated time, each of the next 23 increments correspond to one hour and after increment 84 the time step was set to one day. The duration of the test was 208 days, modelled in 290 increments.

Table 1. Values of parameters used in model

Parameter	Value	Unit	Description
Seepage properties			
k_{sat}	3e-13	m/s	Saturated permeability
k_{min}	0.2e-13	m/s	Minimum permeability
p_1	1000	kPa	Pore pressures at which permeability starts changing
p_2	20000	kPa	Pore pressures at which permeability ceases changing
Mechanical parameters			
$\alpha_g = \alpha_f$	0.4		Model parameter controlling YS an PP shape
$\mu_g = \mu_f$	0.9		Model parameter controlling YS an PP shape
$M_g = M_f$	0.35		Generalised normalised stress ratio in critical state
p_c	24.6	kPa	Characteristic pressure
v_1	2.54		Specific volume at mean net stress p = 1kPa
$\lambda(0)$	0.25		Fully saturated compressibility coefficient
κ	0.01		Elastic compressibility coefficient
r	0.33		Maximum soil stiffness parameter
B	3.8E-5	1/kPa	Soil stiffness increase parameter
κ_s	0.231		Elastic compressibility coefficient for changes in suction
χ	1.0		Parameters controlling the variation of elastic compressibility coefficient with degree of saturation
ω	0.0		
μ	0.4		Poison ratio
s_0	400000	kPa	Yield value of suction
λ_s	0.3		Plastic compressibility coefficient for changes in suction
SWRC			
s_{air}	1000	kPa	Air entry suction
α	2.8E-5		Fitting parameter
n	1.3		Fitting parameter
m	1		Fitting parameter
S_{r0}	0.15		Residual degree of saturation

4 COMPARISON WITH EXPERIMENTAL DATA

The numerical results are compared to the experimental data given by Marcial et al. (2008) in figures 3 and 4. Figure 3 presents the evolution of suction with time along the height of the sample. The numerical predictions are in good agreement with the measured data. Furthermore, the hydraulic gradient at different heights derived from the numerical analysis evolves with time in a manner qualitatively similar to that observed in the laboratory test (Figure 4).

5 INTERPRETATION OF PREDICTED BEHAVIOUR

Figures 5 and 6 illustrate the stress path at a Gauss point

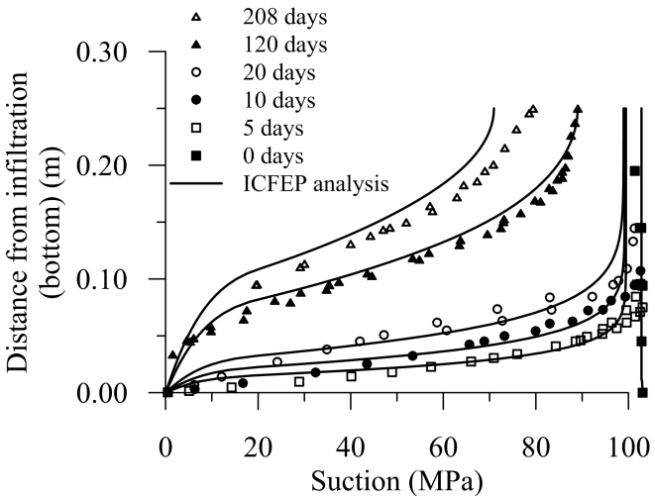

Figure 3. Comparison of suction profile at different time steps with laboratory data from Marcial et. al (2008).

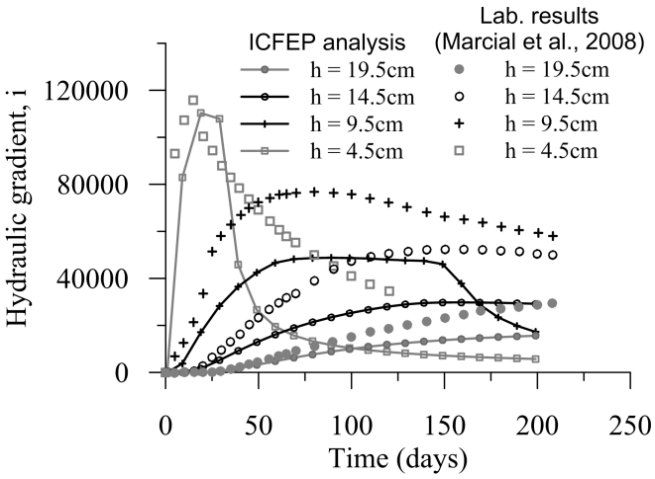

Figure 4. Comparison of hydraulic gradient at different height increments with laboratory data from Marcial et. al (2008).

located at a distance of 14.75mm from the bottom boundary of the mesh (infiltration boundary), on the mean net stress-suction (p-s) and mean net stress-deviatoric stress (p-q) planes, respectively. Figure 7 illustrates the evolution of void ratio with time at various distances from the infiltration boundary. Examination of the three figures provides a better insight into the mechanisms controlling the behaviour of the column of soil and contributes to a more comprehensive explanation of the observed results.

The initial stress state of the particular Gauss point studied is represented by point (a). As water infiltrates the base of the sample, the saturation front gradually advances upwards. The soil below the saturation front swells, causing local compression above the saturation front. Therefore, the soil at a given cross-section initially compresses slightly and starts swelling only when the saturation front has reached this section. The initial small decrease in void ratio is associated with the sample being initially sheared in compression, as indicated by the path from (a) to (b) in Figure 6. This is followed by shearing in extension ((b) to (c)) when the wetting front has advanced enough for the current cross-section to swell. Concurrently, suction reduces due to infiltration of water and therefore the yield surface (Y.S.) in the p-q plane shrinks. This is indicated by the reduction in the preconsolidation mean stress, p_0, at the current value of suction, as shown in Figures 5 and 6. As shearing in extension continues, the stress path yields on the Y.S. at point (c). At this particular instance, yielding has occurred only on the p-q plane (Figure 6) and not on the s-p plane (Figure 5). Although the stress path yields on the wet side of critical state, the Y.S. keeps on shrinking due to further reduction in suction, which dominates the behaviour, and the stress path reverses in direction but always remains on the Y.S. in the p-q plane. At point (d) where q=0, the soil collapses, the void ratio reduces dramatically (Figure 7) and the stress path is simultaneously on the loading collapse (L.C.) curve on the s-p plane (Figure 6) and the Y.S. on the p-q plane (Figure 5).

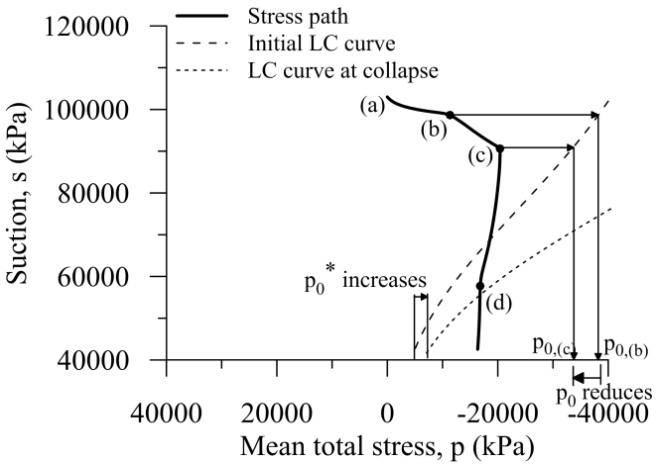

Figure 5. Stress paths in s-p space for h = 14.75mm.

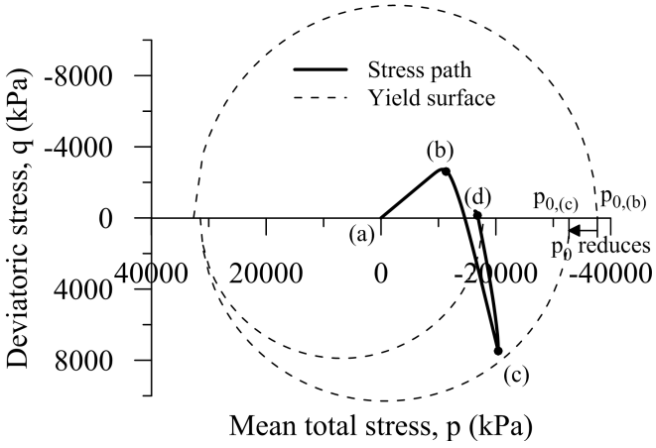

Figure 6. Stress paths in p-q space at h = 14.75mm.

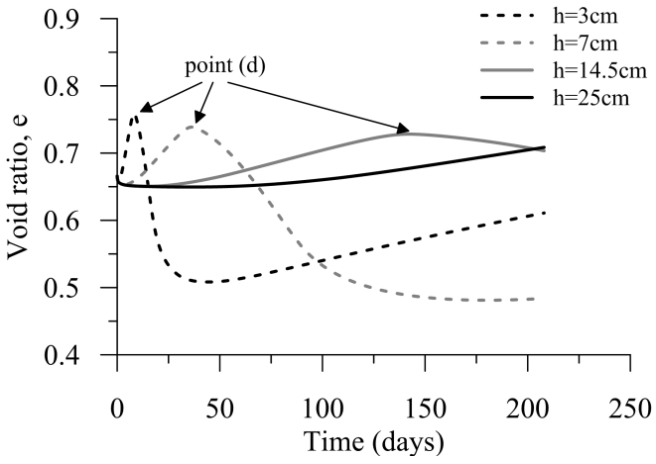

Figure 7. Evolution of void ratio at different heights.

From (c) to (d) the L.C. has moved as a result of plasticity having been induced in the p-q plane. As discussed above, p0 has decreased. Nonetheless, because of yielding on the wet side, p_0^*, which is the preconsolidation mean stress defined at zero suction, has increased, meaning that the

new L.C. at the instance of first wetting-induced collapse plots to the right of the initial one in Figure 5. Note that the hardening parameter of the model is p_0* and not p_0.

In Figure 7 it can be seen that the void ratio keeps increasing until the cross-section collapses upon reaching the L.C. curve. As saturation continues, the front of wetting-induced collapse advances upwards with the saturation front, allowing sections beneath it (i.e. h=3cm) to swell again. This results in a wavelike evolution of void ratio within the sample.

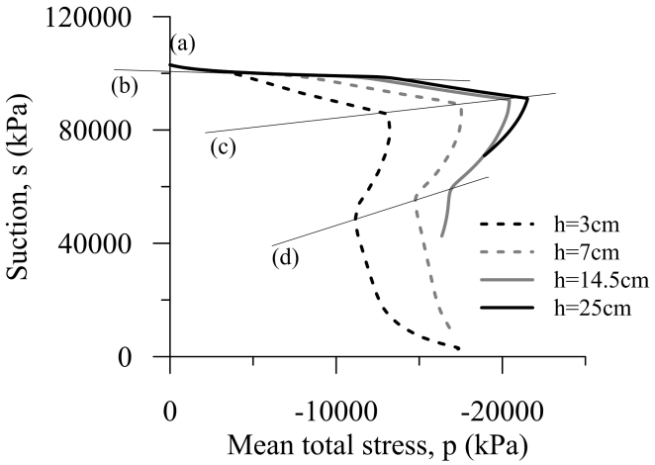

Figure 8. Stress paths in s-p space at different heights (height increasing from left to right).

Figure 8 illustrates the stress paths on the s-p plane at different heights along the soil column. They all exhibit a similar shape, which further supports the above discussion. In Figure 8, the initial stress point (a), the point where the direction of shearing changes from compression to extension (b), the yielding point on the q-p plane (c) and the point of collapse (d) are all shown.

6 CONCLUSIONS

Many processes happen simultaneously within the buffer, even if thermal phenomena are ignored. An attempt is made to identify and interpret them. Despite neglecting the effect of a double porosity structure, the analysis successfully provided insight into the complex response of bentonite when hydrated, helping identify mechanisms within the buffer which would otherwise be concealed.

The results show that the propagation of the water front is a time-dependent process, leading to alternate compression/swelling. As a result, it has been demonstrated that soil along the axis of the buffer exists at different void ratios and stress states. Moreover, as compacted bentonite is highly expansive, swelling-induced stresses were shown to be high enough to cause yielding in terms of deviatoric stress, while collapse occurs under reducing suction.

REFERENCES

Alonso, E. E., Gens, A. & Josa, A. 1990, A constitutive model for partially saturated soils, *Géotechnique* **40** (3), 405-430.

Alonso, E. E., Vaunat, J. & Gens, A. 1999. Modelling the mechanical behaviour of expansive clays, *Engineering Geology* **54** (1-2), 173-183.

Benson, C. H. & Gribb, M. M. 1997. Measuring unsaturated hydraulic conductivity in the laboratory and field, *Proceedings of the 1997 1st Geo-Institute Conference,* 113-168. ASCE, Logan, UT, USA.

Cui, Y. J., Tang, A. M., Loiseau, C. & Delage, P. 2008. Determining the unsaturated hydraulic conductivity of a compacted sand-bentonite mixture under constant-volume and free-swell conditions, *Physics and Chemistry of the Earth* **33**, S462-S471.

Delage, P., Cui, Y. & Tang, A. 2010. Clays in radioactive waste disposal, *Journal of Rock Mechanics and Geotechnical Engineering* **2** (2), 111-123.

Dueck, A. 2008. Laboratory results from hydro-mechanical tests on a water unsaturated bentonite, *Engineering Geology* **97** (1–2), 15-24.

Gens, A. & Alonso, E. E. 1992. A framework for the behaviour of unsaturated expansive clays, *Canadian Geotechnical Journal* **29** (6), 1013-1032.

Georgiadis, K., Potts, D. M. & Zdravkovic, L. 2005. Three-dimensional constitutive model for partially and fully saturated soils, *International Journal of Geomechanics* **5** (3), 244-255

Hoffmann, C., Alonso, E. E. & Romero, E. 2007. Hydro-mechanical behaviour of bentonite pellet mixtures, *Physics and Chemistry of the Earth, Parts A/B/C* **32** (8–14), 832-849.

Kröhn, K. 2005. New evidence for the dominance of vapour diffusion during the re-saturation of compacted bentonite, *Engineering Geology* **82** (2), 127-132.

Lagioia, R., Puzrin, A. M. & Potts, D. M. 1996. A new versatile expression for yield and plastic potential surfaces, *Computers and Geotechnics* **19** (3), 171-191.

Marcial, D., Delage, P. & Cui, Y. J. 2008. Hydromechanical couplings in confined MX80 bentonite during hydration. *1st European Conference on Unsaturated Soils, E-UNSAT 2008*, 249-255. CRC Press, Durham, United kingdom.

Potts, D. M. & Zdravkovic, L. 1999. *Finite element analysis in geotechnical engineering. theory.* London, Thomas Telford.

Sanchez, M., Gens, A., do, N. G. & Olivella, S. 2005. A double structure generalized plasticity model for expansive materials, *International Journal for Numerical and Analytical Methods in Geomechanics* **29** (8), 751-787.

Schanz, T., Datcheva, M. & Zimmerer, M. 2008. Identification of coupled hydro-mechanical parameters with application to engineered barrier systems, *1st European Conference on Unsaturated Soils, E-UNSAT 2008,* 797-803. CRC Press, Durham, United Kingdom.

Schanz, T., Long Nguyen-Tuan & Datcheva, M. 2013. A Column Experiment to Study the Thermo-Hydro-Mechanical Behaviour of Expansive Soils, *Rock Mechanics and Rock Engineering* **46** (6), 1287-301.

Tang, A. M., Cui, Y. J. & Barnel, N. 2008. Compression-induced suction change in a compacted expansive clay. *1st European Conference on Unsaturated Soils, E-UNSAT 2008,* 369-374. CRC Press, Durham, United kingdom.

Tsiampousi, A., Zdravkovic, L. & Potts, D. M. 2013. A threedimensional hysteretic soil-water retention curve, *Geotechnique.* **63** (2), 155-164.

Van Genuchten, M. T. 1980. A closed-form equation for predicting the hydarulic conductivity of unsaturated soils. *Soil Sci. Soc. Am. J.* **44**, 892-898.

Analysis of the mechanical behaviour of a partially saturated lime-treated clay

Analyse du comportement mécanique d'une argile partiellement saturée, traitée à la chaux

M. Mavroulidou, X. Zhang, M.J. Gunn

ABSTRACT The paper studies the mechanical behaviour of lime treated London Clay based on suction-controlled triaxial testing. The experimental results showed that lime reduced the compressibility and considerably improved the shear strength of the soil (despite the observed strain softening behaviour at large strains). The results are represented graphically using different stress state variable expressions and three different failure criteria. The three failure criteria are subsequently evaluated based on the quality of the fitting of the results.

1 INTRODUCTION

Soil improvement with lime is a technique used extensively in construction, in particular for pavement engineering. For such practical applications simple tests e.g. CBR or unconfined compression tests are sufficient. Therefore most literature on the subject reports results on these tests. With an increasing use of the technique in a wider range of applications, the need has emerged for more thorough experimental evidence. This can provide the basis for constitutive models able to describe the behaviour of lime-treated soils for a variety of problems under saturated and partially saturated conditions. The latter aspect is particularly relevant, as lime-treated soils are typically compacted after treatment, and hence, by definition partially saturated. In addition during its service life the lime-treated soil will be exposed to environmental conditions that could induce partial saturation.

This paper analyses results of an experimental study on a lime treated high plasticity clay soil. This included suction-controlled triaxial testing data, using the axis translation technique. When analyzing the shearing testing results for a partially saturated soil the form of the failure criterion can vary according to the selected stress state variable(s). In order to select the most useful criterion for practicing engineers (in terms of ease of fit) the results will be analysed using three different approaches:

- considering separately the contributions of the mean net stress and suction used as independent stress variables (e.g. Basic Barcelona Model in Alonso et al. 1990 and sequels, or Toll 1990), namely the mean net stress ($p-u_a$) and the matric suction $s=u_a-u_w$, where p is the mean stress, and u_a, u_w the air and water pressures respectively. The particular shear failure criterion used in this study is that by Toll (1990), extending the concept of critical state to unsaturated soils; this is written as:

  $$Q = M_a (p - u_a) + M_b (u_a - u_w) \quad (1)$$

  where q is the deviator stress, M_a the critical state stress ratio with respect to the mean net stress ($p-u_a$) and M_b the critical state stress ratio with respect to the matric suction.

- representing the results using a Bishop's type stress where χ in Bishop's (1959) expression is replaced by the degree of saturation S_r (e.g. Jommi 2000):

  $$p'' = (p - u_a) + S_r*(u_a-u_w) \quad (2a)$$

  The shear failure criterion following the concepts of critical state and using this stress variable will then be written as:

  $$q = M [(p - u_a) + S_r* (u_a - u_w)] \quad (2b)$$

- using a mean coupling stress as in Murray & Sivakumar (2010) defined as:

  $$p'_{coup} = (p - u_a) + (u_a-u_w)\, v_w/v \quad (3a)$$

  where v is the specific volume given by (1+e), v_w the specific water volume given by (1+e S_r), and e the void ratio. The corresponding shear failure criterion was expressed as:

  $$q = M_a (p - u_a) + M_b (u_a - u_w) \quad (3b)$$

  The above expression was obtained by normalising the q : p'_{coup} axes by s; M_a would then be the slope of the partially saturated soil critical state line, claimed to be unique, and $M_b=M_a(v_w/v-1)+\Omega$, where Ω is the intercept of the q/s axis at $p'_{coup}/s = 1$. Substituting M_b in Equation (3b) and multiplying by s:

  $$q = M_a (p - u_a) + [M_a (v_w/v - 1) + \Omega]s \quad (3c)$$

2 MATERIALS AND PROCEDURES

The soil used in this study was statically compacted London Clay obtained from a deep excavation near Westminster Bridge in London. After air-drying the soil for one month and pulverising it, the portion passing through a BS 425 μm sieve was retained for testing. The required hydrated lime percentage to treat this soil was determined as 4% (per dry soil mass) through the initial consumption of lime (ICL) testing, as well as the lime fixation point (LFP) obtained from plasticity tests. For the sake of comparison, some additional testing was also carried on (fewer) untreated London Clay specimens compacted at the same dry densities as the lime-treated ones (i.e. 1.43 g/cm^3, corresponding to the maximum standard Proctor dry density of the clay soil). The lime treated specimens were left to cure for a week wrapped in several layers of cling film and stored in controlled environmental conditions. The necessary curing time was determined based on prior Unconsolidated Undrained (UU) triaxial testing for six different curing periods between one and 166 days, which showed that for this amount of lime and curing method, there would be no further gain in strength during testing, beyond that already achieved after 7 days of curing.

All specimens were isotropically consolidated to the required stress level and then subject to constant suction shearing (using axis translation) following a $q/(p-u_a)=3$ path. Some duplicate specimens were also subjected to isotropic compression only up to higher stress levels, in order to observe the compressibility of the material after yielding (the stress levels of the consolidation stage prior to shearing were not high enough to lead to yielding in isotropic compression).

3 RESULTS

3.1 Isotropic compression

Figure 1(a)-(c) presents isotropic compression results for the lime-treated soil at different suction levels, plotted in terms of the three different stress variables. Regardless of the representation used, the results do not give a clear indication that suction allows the Normal Compression Line (NCL) to cross into metastable states above the zero suction NCL (as is the case for uncemented partially saturated soils). This could indicate that the behaviour of the lime-treated soil in isotropic compression was largely controlled by the chemical reactions due to lime rather than suction. However for this statement to be conclusive the data needs to be extrapolated to higher pressures.

Comparing the sets of different plots it can be seen that the results plotted in terms of Bishop's and coupling stress respectively show very little differences, which is also reflected in the variation of the parameter *λ(s)* with suction (i.e. the slope of the normal compression line) (see Figure 2).

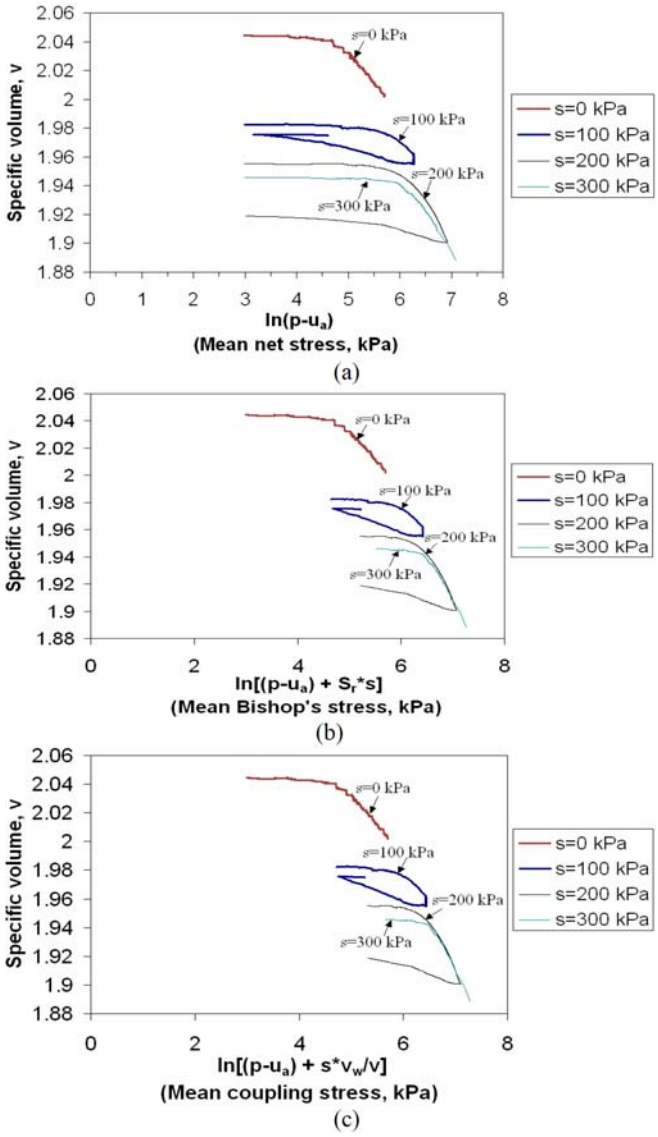

Figure 1. Isotropic compression results for the lime-treated soil, in terms of: (a) net stress; (b) Bishop's stress; (c) Coupling stress

This is non-monotonic (as observed also elsewhere, e.g. Wheeler & Sivakumar 1995) although it can be argued that, due to the very small compressibility of the soil, the differences are somewhat exaggerated by the scale used in the graphs; it should also be noted that the normal compression curves were not straight lines, which led to a certain ambiguity in the determination of a constant *λ(s)*. A non-linear shape of the curves is however realistic because, if extrapolated to higher stresses (that the available equipment for this study could not match), the gradient *λ(s)* during the debonding processing would be expected to continually increase with gradual bond breakage, until the cemented soil curve coincides with that of the uncemented soil upon complete breakage of bonds.

On the other hand, a monotonic increase of the yield points in isotropic compression (determined using Casagrande's approach) is shown in Figure 3.

To demonstrate the effect of the lime on the compressibility of the clay soil, two additional figures were included (both in terms of net stresses only, for illustrative purposes). Figure 4 presents comparative isotropic compression results of the untreated vs. lime-treated soil for two different levels of suction. These showed that, overall, lime treatment had a favourable effect on the compressibility of the material, which was drastically reduced both before and after yield; thus whereas the NCL of the untreated clay at suctions s=0 kPa and s=300 kPa was determined as λ=0.144 and 0.079 respectively (based on this graph), those of the lime treated clay at the same suction levels were 0.043 and 0.051 respectively. The improvement is particularly considerable in the s=0 kPa case and clearly shows the role of the lime in the reduction in compressibility. The yield stresses of the lime-treated soil were also higher than those of the untreated soil, which is consistent with the behaviour of cemented geomaterials. This is depicted graphically in Figure 5 (complemented by additional results not presented here) in terms of the Loading Collapse (LC) curve the two soils (untreated and lime treated). Whereas the figure shows an expansion in the LC for both soils, reflecting the suction hardening behaviour, the LC curve of the lime treated soil moved to the right-hand side of the untreated soil LC curve, reflecting the considerable increase in the yield stress of the treated soil. This indicates that the elastic range of the lime-treated soil is enlarged, which can be attributed to cementation bonding.

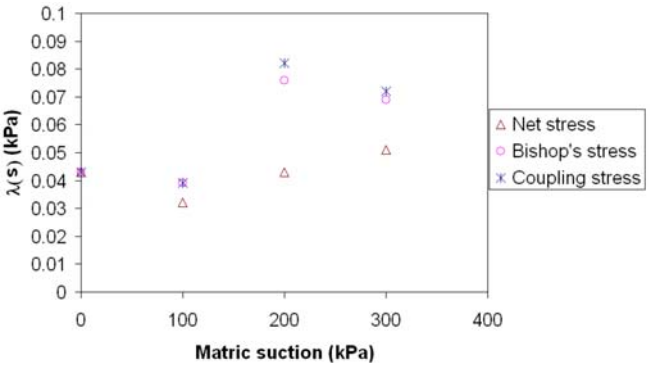

Figure 2. Variation of the NCL gradient λ(s) with suction

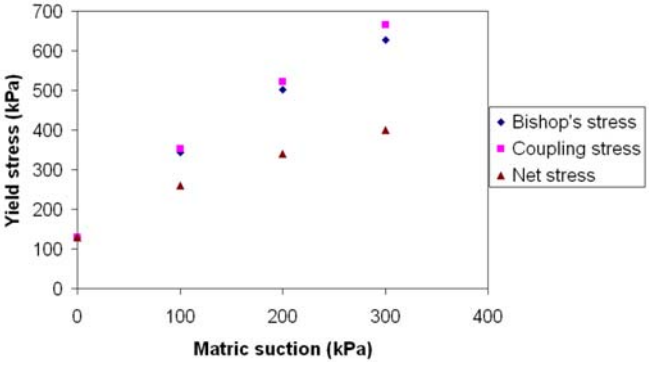

Figure 3. Variation of the yield stress with suction

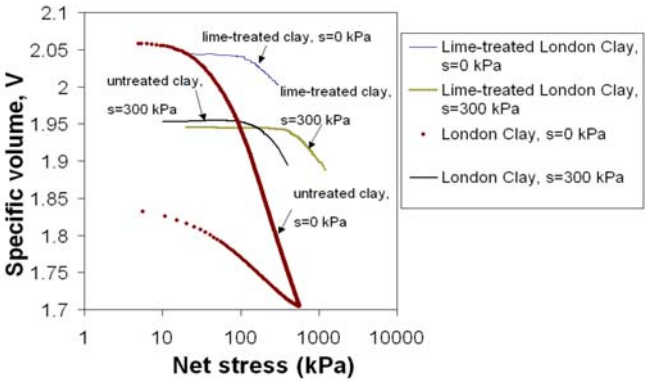

Figure 4. Indicative comparative isotropic compression plots for the lime-treated vs. the untreated clay

As mentioned earlier, the curves of the treated and untreated soil shown in Figure 4 did not eventually converge as is the expected behaviour; this is because the range of pressures applied only captured perhaps some initial yield linked

to the start of breakage of the cementation bonds but not that corresponding to their full breakage.

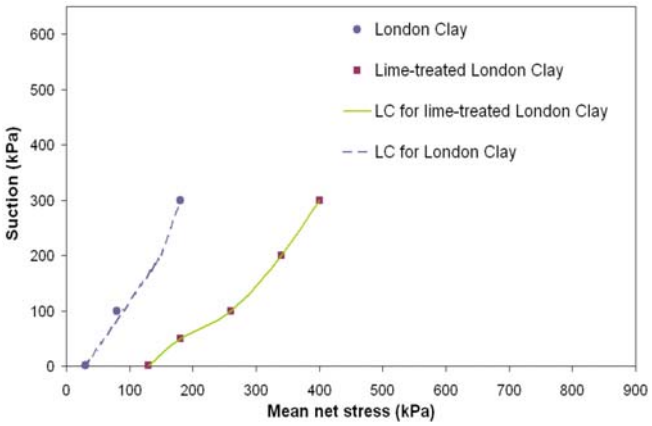

Figure 5. Loading Collapse (LC) yield curves for the lime-treated vs the untreated clay

Note that although the two soils were initially compacted at the same dry densities, the London Clay underwent swelling during saturation, so that the void ratio of the soil before isotropic compression had increased compared to that of the lime-treated soil. Conversely, very little swelling was noted for the lime-treated specimens. This shows the beneficial effect of lime on the volumetric stability of the London Clay when subject to water content variations.

3.2 Constant suction shearing result analysis

Due to space limitations the analysis of the shearing testing results in terms of failure criteria will be shown without prior presentation of the stress-strain curves of the soil. Thus, Figure 6 (a)-(c) plots the peak strength and post-rupture strengths (as defined in Burland 1990) together with the critical state line of the untreated London Clay. For the saturated lime-treated soil the peak angle of friction was found to be $\varphi'_p=26.5^\circ$; the results for both saturated soils (treated and untreated) were reasonably well represented by a unique Critical State line in the q : p' plane, with a slope of M=0.88 corresponding to an angle of internal friction of $\varphi'_c=22.5^\circ$. This implies that lime did not affect the frictional characteristics of the clay soil. Although consistent with observations made for cement treated soils (Mitchell & Soga 2005) this was somewhat unexpected, as lime does not only produce cementation between particles but also modifies the mineralogy of the soil; hence a change in the frictional characteristics would have been expected. The post-rupture strength envelopes for the partially saturated lime-treated soil appear to also form lines of the same gradient, i.e. the lines for all suctions used (including the zero suction line) tend to be essentially parallel but the intercepts with the q axis are increasing with suction. This is in line with the assumptions made in the BBM model (Alonso et al. 1990) although other researchers' results have challenged this. It should be noted that due to the brittleness of the material there could be an ambiguity as to the selection of the 'critical state'. Indeed, if the end of test results were selected there would have been some slight variation in the slopes of the lines of the different suctions (with M gradients slightly increasing with suction) but the average would again be around the value of the zero suction CSL line i.e. 0.88-0.89. Thus, based the above observations, for the failure criterion according to Toll (1990) (Eqn 1), M_a coefficient was considered to be a constant and equal to the saturated soil critical state gradient M. With the value of M_a=M=0.88 the values of M_b were then calculated to fit the presented data. The M_b values were not constant and although in most cases they decreased with suction and/or S_r, there were no clear trends in the variation of Mb with suction or S_r (see Fig 8). From a modelling point of view this is inconvenient, as it appears that M_b is not a material constant. Excluding the two irregular, encircled points in Figure 8 it is however possible that a linear trend is implied. This is unlike results for Kiunyu gravel plotted in Toll (1990) which showed a non-linear but clear pattern of reduction of M_b with S_r; however Toll's M_a value also varied with S_r (whereas in our analysis it was kept constant); also the range of S_r involved in this study were very narrow (as opposed to Toll 1990).

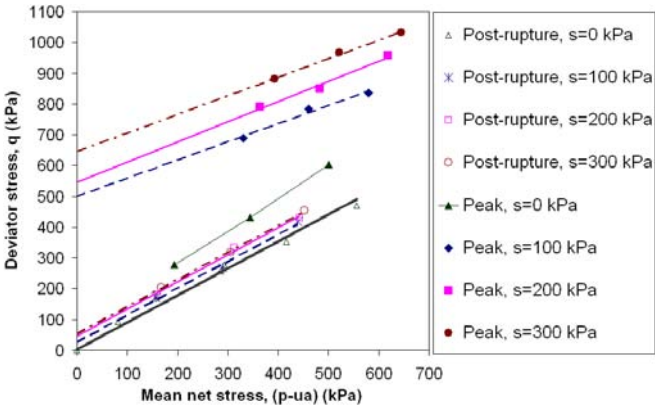

(a)

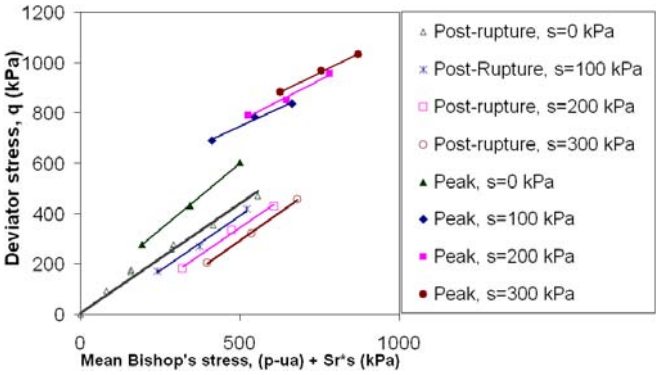

(b)

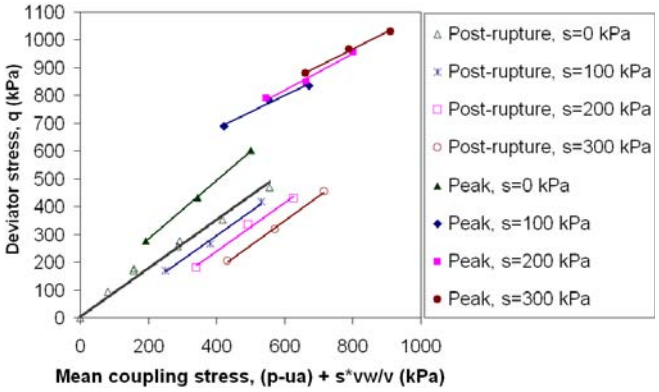

(c)

Figure 6. Peak and post-rupture strength envelopes plotted for different failure criteria; (a) Eqn (1); (b) Eqn (2b); (c) Eqn (3b).

Using a Bishop type stress or a coupling stress (Fig 6(b)-(c)), the post-rupture lines are again parallel, with gradients around the saturated soil critical state M of 0.88; if normalised dividing by the matric suction s, they form straight lines of gradients of 0.88 and 0.89 respectively (which are consistent with the untreated saturated soil critical state values) with a very good coefficient of determination R^2 (see Fig 7). This is consistent with the assumptions of the second failure criterion expressed in (Eqn 2b) considering a unique q - p'' critical state gradient M, equal to that of the saturated soil; however an intercept must also be added,

for this criterion to give a good fit to the data. On the other hand Murray & Sivakumar's (2010) criterion in the form of (Eqn 3c), which provides an intercept, fits the data appropriately for the normalized plots. Figure 7 supports Murray & Sivakumar's (2010) observations based on different soils, that unique failure lines can be obtained by normalizing the coupling stress and the deviator stress by the suction, s. Overall, the assumption of a constant 'critical state' line of a gradient M equal to that of the saturated soil appears to be legitimate based on the presented results (Murray & Sivakumar suggest that M_a>M).

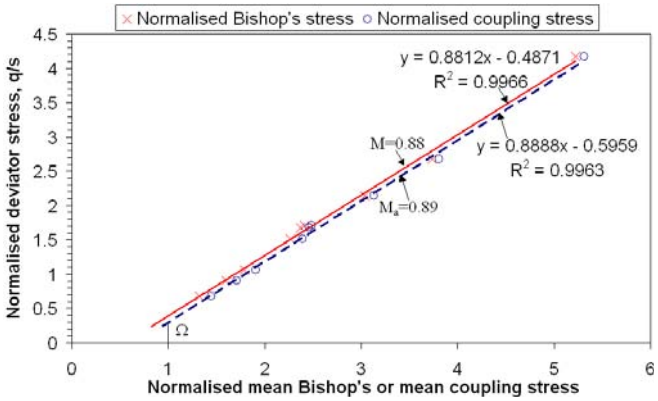

Figure 7. Normalised q/s vs. normalised p´´/s or p´$_{coup}$/s plots.

Having obtained the value of Ma from the normalised plot in Figure 7 as M_a =0.89, the value of the coefficient M_b = M_a (v_w/v – 1) + Ω for the third failure criterion (Eqn 3b) can be found. Murray & Sivakumar (2010) made the observation that this value appeared to be universally Ω=0.6 (approximately) for all soil types and kept it as such for the analysis of all data from the literature, performed in their book. This observation was made for soils including kaolin, gravel, an intermediate plasticity residual Jurong soil and a silt. The only soil that did not show a value of Ω=0.6 was a bentonite enriched sand soil; the authors attributed the discrepancy to the fissured nature of the soil but still analysed the results for an assumed value of Ω=0.6. In the case of the lime treated soil shown in Figure 7 it can be seen that Ω=0.3. This value was therefore used to fit the present data (and not Ω=0.6). This gave a clearly linear correlation of the coefficient M_b with v_w/v (consistent with Murray & Sivakumar 2010) unlike the coefficient M_b of Eqn (1), whose variation with S_r did not show any clear trends (see Fig 8). Overall, based on the results, Eqn (3c) appears to provide the most useful criterion to fit the data, as it appears to be based on two material constants (M_a and Ω). Alternatively, Eqn (2b) can be used if similarly modified with an intercept Ω', thus also involving two material constants (M and Ω').

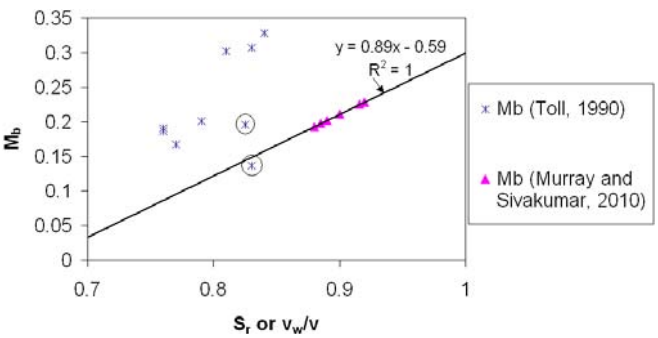

Figure 8. Variation of M_b for Eqn (1) and (3b) respectively.

An interesting observation based on the results of Figure 6(a)-(c) is that, whereas the post-rupture envelopes for the partially saturated soil expressed in terms of mean net stress, plot higher than the saturated soil post-rupture point envelope/critical state line and that the higher the suction, the higher the location of the respective envelope on the plot, the opposite is true when the results are plotted in terms of mean Bishop's stress or mean coupling stress. Murray & Sivakumar (2010) attribute this to preferential shearing between the more highly stressed aggregates which their choice of stress variable reflects. A final observation can be made on the peak stress point envelopes; these all plot higher that the saturated lime-treated soil peak strength envelope and are continually increasing with suction (the untreated soil did not show any peak as it was strain hardening up to the critical state value). The peak envelopes were much higher than the post-rupture ones for each individual suction level, suggesting that the additional peak strength is largely dependent on the cementation bonding. With the exception of the s=0 kPa peak strength envelope, the other suction level envelopes appear to be reasonably parallel with a gradient of about 0.6 but increasing intercepts. The discrepancy for the s=0 kPa envelope could be due to the different curing conditions adopted for the saturated soil study.

4 CONCLUSIONS

The research studied a lime-treated clay based on suction-controlled triaxial testing. The beneficial effect of the lime on the soil properties was shown. The results were interpreted and quantified using different stress variable expressions and resulting failure criteria. Suggestions were made regarding the appropriateness of the criteria based on the data fitting.

ACKNOWLEDGEMENT

The research was carried out by Dr X. Zhang at London South Bank University. It was funded by the UK Engineering and Physical Sciences Research Council (EPSRC) through grant EP/E037305/1.

REFERENCES

Alonso, E.E., Gens, A., & Josa, A. 1990. A constitutive model for partially saturated soils, *Géotechnique* **40** (3), 405-430.

Burland, J.B. 1990. On the compressibility and strength of natural clays. *Géotechnique* **40**, 329-378.

Jommi, C. 2000. Remarks on the constitutive modelling of unsaturated soils. *Experimental Evidence and Theoretical Approaches in Unsaturated Soils* (Eds: Tarantino & Mancuso) Balkema Rotterdam

Mitchell, J.K.& Soga, K. 2005. *Fundamentals of Soil Behavior*, 3rd Ed, Wiley, Hoboken NJ

Murray, E.J. & Sivakumar, V. 2010. *Unsaturated Soils*, Wiley-Blackwell, Chichester.

Toll, D.G. 1990. A framework for unsaturated soil behaviour, *Géotechnique* **40** (1), 31-44.

Wheeler, S.J. & Sivakumar, V., 1995. An elasto-plastic critical state framework for unsaturated soil. *Géotechnique* **45**(1), 35-53.

ΔΙΑΚΡΙΣΕΙΣ ΕΛΛΗΝΩΝ ΓΕΩΜΗΧΑΝΙΚΩΝ

Διαλέξεις Ηλία Μιχάλη στα Ηνωμένα Αραβικά Εμιράτα

Το μέλος της ΕΕΕΕΓΜ προσεκλήθη από το παράρτημα του Institution of Civil Engineers του Ηνωμένου Βασιλείου στα Ηνωμένα Αραβικά Εμιράτα και παρουσίασε διάλεξη με θέμα τις εσωτερικές επενδύσεις σηράγγων, στο Abu Dhabi, στις 24 Μαΐου 2016 και στο Dubai, στις 25 Μαΐου 2016. Στη συνέχεια παρατίθεται η σχετική πρόσκληση που απέστειλε το ICE.

Tunnel lining designs and application, Abu Dhabi

Unreinforced concrete tunnel lining. Maliakos - Kleidi Motorway Tunnel.

About this event

In this ICE UAE Learned Event, speaker Ilias Michalis, Associate Technical Director at Arcadis, will evaluate the application limits of Unreinforced & Steel Fibre Reinforced Concrete (SFRC) for tunnel final linings.

Key areas of focus will include:

- Recent tunnel cases with unreinforced and Steel Fibre Reinforced Concrete tunnel linings
- Existing Design Codes and Design Recommendations
- Numerical analyses of unreinforced concrete tunnel linings under static and seismic loading conditions. T1 & T2 tunnels of Maliakos – Kleidi Motorway and T 26 tunnel of Athens – Patras Motorway in Greece
- Numerical analyses of SFRC tunnel linings under static loading conditions. Doha Metro Project
- Critical thoughts about the geostatic loads on to the tunnel final linings
- Critical thoughts about the ground elastic modulus for designing tunnel final linings
- Conclusions

Επίσης, ο Ηλίας Μιχάλης παρουσίασε προσκεκλημένη διάλεξη στο

2016 DFI Middle East Conference
May 11- May 12, 2016
American University in Dubai, UAE

(http://www.dfi.org/dfieventlp.asp?13266) με θέμα «The Case of "Hard Soils –Weak Rocks" Challenges of Geotechnical Evaluation» [Ilias current position (since December 2015) is Associate Technical Director / Geotechnical and Tunnelling of Arcadis. He is leading technically the Geotechnical and Tunnelling design group of Dubai office. He has 22 years of experience, working as tunnelling and geotechnical expert in major infrastructure projects, including among others: (a) Athens and Thessaloniki Metros in Greece, (b) the 700km Egnatia Motorway in North Greece and (c) three major concession motorways in Greece of a total length 700km approximately.]

ΠΡΟΣΦΟΡΑ ΕΡΓΑΣΙΑΣ

Civil Engineer – Tunnelling / Rock Engineering (m/f) GW3 (525e)

Job Description

Your new work environment is the Hydropower and Water Resources Division, Department of Geotechnical Engineering, Geology and Dams with the following tasks:

- Long term assignments as resident for site supervision
- Assistance in project management in the fields of Tunnelling and Rock Engineering
- Short-term assignments and fieldwork to validate the rock mechanical / geological site conditions will be necessary.
- Evaluating geotechnical investigation and testing results, interpreting and characterizing subsurface conditions, and preparing reports and memorandums. Adopt the design according to the investigation results.
- Feasibility Study, Tender and Construction design. Especially preparation of Technical Specifications, Method Statements etc.
- Claim Management.

Required Skills

- Degree in Civil Engineering from a University (PhD/Dr.-Ing. or MSc/Dipl.-Ing.) with focus on geotechnical engineering / rock mechanics.
- At least 10 years of professional experience in the respective fields, including rock engineering, cavern, dam construction and tunnelling.
- Professional experience in site supervision, especially in drill&blast and TBM tunnelling.
- Good verbal and written English communication skills. Additional communication skills such as Spanish, French, or Russian are beneficial.
- Professional experiences in oversea projects are beneficial.
- Willingness to travel domestically and internationally to support project needs. Assignments may include travel to remote locations and outside work in various climates. Willingness to work as Expatriate.
- Motivation and flexibility, independent, structured and responsible work skills and willingness to grow personally and professionally.
- Ability to work with a multicultural team or with contractors and clients.

We offer:

- International environment and challenging tasks
- Performance related salary
- Attractive continued education and advanced training offerings
- Intensive training in your area of responsibility
- A supportive team and a working atmosphere to enjoy

Job Location

Bad Vilbel, Hessen, Germany

Branch of study/apprenticeship

Degree in Civil Engineering from a University (PhD/Dr.-Ing. or MSc/Dipl.-Ing.) with focus on geotechnical engineering / rock mechanics

Nationality

N/A

http://www.lahmeyer.de/en/home.html

Grand Ethiopian Renaissance Dam Project (GERDP)

Project and Job opportunity description

Assignment:

Engineering Geologist with at least 15 years of experience.

Scope of the works of the project:

Main Works comprise the following:

- Construction of an RCC dam on the Blue Nile River 15 km upstream of the South-Sudan border with a foundation at elevation 500 m a.s.l.. The dam will be approximately 1780 m long and 160 m high and will have a concrete volume of 10.5 Mm^3, creating a reservoir of about 75 billion m3. The dam has left and right banks with a central low block housing an ungated spillway.

- The Saddle Dam raises the watershed from el. 600 m a.s.l. up to 646 m a.s.l. The dam follows the morphology of the watershed with a crest length of approximately 5.2 km and an ungated emergency spillway on the right bank. The maximum dam height is 50 m.

- The two powerhouses of the open air type are situated immediately downstream of the dam on the left and right banks of the river. They are separated by a low block on the middle and linked by a road passing through a tunnel under the transformer bays. The right and left powerhouses contain ten and six turbines, respectively.

Location/climate

The proposed project is located in the western part of Ethiopia and is part of Blue Nile (Abbay) River Basin which covers about 172,000 km2 of the Ethiopian territory. The pro-

ject area is located near Bameza town near the South Sudan border.

The site is at 9-10 hours by car to Addis Ababa, 30 minutes to Guba (town of 6.000 inhabitants).

The project area is a dry steppe-type climate with annual rainfall of 850 mm. Mean monthly temperatures ranging between 23° C and 33° C.

Accommodation:

The Geologist will get an accommodation on temporary camp and one vehicle (possibly shared).

The camp is located at elevation 1420 m a.s.l..

Site Staff:

On site, the resident team in charge of supervision of the works comprises up to 20 expatriate engineers that manage engineers and technicians provided by the Client.

The following positions are foreseen on site:

- Chief Resident Engineer
- Deputy Chief Resident Engineer
- Design Review – Team Leader – Technical Office Engineer
- Concrete Manufacturing & Laboratory Testing Supervisor
- Engineering Geologist
- Diversion Works & Cofferdam Supervisor
- RCC Dam Supervisor
- Foundation Treatment Supervisor
- Gated Spillway Supervisor
- Quality Assurance / Safety Supervisor
- Hydro-mechanical Equipment Supervisor

The Engineering Geologist will work under the technical direction of the Chief Resident Engineer which, in turn, reports to the JV Management.

Rotation:

6 working days per week with annual leave of 30 days.

The assignment is an assignment for 12 months on site (with possible extensions).

One international return economy air ticket is paid every four months for the residents.

Mobilisation date: Start asap.

Detailed tasks assigned:

Main tasks of the Engineering Geologist include:

- Cooperation with the Geology Experts in verifying the geotechnical parameters to be used for civil works design.
- Verification, with the assistance of Client's Geologists, of geological conditions of all Project areas.
- Supervision of the works relevant to foundations types and treatment, excavation methods and supports, construction material.
- Supervision of the grouting program for dam works and other Project areas.
- Verification of the "adverse physical conditions" which may have impact on the contractual issues.
- Determination of the work progress for interim payments, as a function of the Bill of Principal Quantities of the Permanent Works.
- Monthly activity report to be included in the ER Monthly Report.

http://www.gpcsa.com/en/job-board

«Προκειμένου να στελεχωθεί ομάδα παρακολούθησης έργου για την κατασκευή φράγματος CFRD, ζητείται πολιτικός μηχανικός με εμπειρία σε αντίστοιχο έργο. Το έργο βρίσκεται στην Ινδία και η εργασία αφορά επισκέψεις και παρακολούθηση του έργου για προκαθορισμένα χρονικά διαστήματα.

Πληροφορίες: Ιωάννης Σίσκος, Πολιτικός Μηχανικός, email: ioannis.siskos@gmail.com

ΠΡΟΣΕΧΕΙΣ ΓΕΩΤΕΧΝΙΚΕΣ ΕΚΔΗΛΩΣΕΙΣ

Για τις παλαιότερες καταχωρήσεις περισσότερες πληροφορίες μπορούν να αναζητηθούν στα προηγούμενα τεύχη του «περιοδικού» και στις παρατιθέμενες ιστοσελίδες.

3rd International Course on Geotechnical and Structural Monitoring, 7-9 June 2016, Poppi, Tuscany, Italy www.geotechnicalmonitoring.com/en

ISL 2016 12th International Symposium on Landslides Experience, Theory, Practice, Napoli, June 12th-19th, 2016, www.isl2016.it

2ο Πανελλήνιο Συνέδριο Εξόρυξης και Εναλλακτικών Μεθόδων Διαχείρισης Αποβλήτων, 15-16 Ιουνίου 2016, Αθήνα, www.erasmus.gr/microsites/1091

8éme Edition des Journées Africaines de la Géotechnique (JAG-2016) - Géotechnique et emergence socio-économique des pays d'Afrique intertropicale, 20-24 June 2016, Douala, Cameroun, www.8jag-cngc.org/8jag/en

BCRRA 2017 Tenth International Conference on the Bearing Capacity of Roads, Railways and Airfields, 28 –30 June 2017, Athens, Greece, www.bcrra2017.com

ICONHIC 2016 1st International Conference on Natural Hazards and Infrastructure: Protection, Design, Rehabilitation, 28-30 June 2016, Chania, Greece, http://iconhic2016.com

ICONHIC 2016 Performance-based soil-structure interaction of lifelines and infrastructure, gerolymos@gmail.com, asextos@civil.auth.gr & a.sextos@bristol.ac.uk

Conference in Honour of Michele Maugeri, 01 July 2016, Catania, Italy, www.associazionegeotecnica.it

4th GeoChina International Conference Sustainable Civil Infrastructures: Innovative Technologies for Severe Weathers and Climate Changes, July 25-27, 2016, Shandong, China, http://geochina2016.geoconf.org

S3: Slopes, Slides and Stabilization, August 1-3, 2016, Denver, USA, events@dfi.org

6th International Conference on Recent Advances in Geotechnical Earthquake Engineering and Soil Dynamics August 1-6, 2016, Greater Noida (NCR), India, www.6icragee.com

EUROC 2016 - ISRM European Regional Symposium Rock Mechanics & Rock Engineering: From Past to the Future, 29-31 August 2016, Ürgüp-Nevşehir, Cappadocia, Turkey http://eurock2016.org

ICEGE 2016 1st International Conference on Energy Geotechnics, 29-31 August 2016, Kiel, Germany, www.iceg-2016.de

3rd ICTG – 3rd International Conference on Transportation Geotechnics 4 - 7 September 2016, Guimaraes, Portugal, www.civil.uminho.pt/3rd-ICTG2016

IAS'5 5th International Conference on Geotechnical and Geophysical Site Characterisation, 5-9 September 2016, Gold Coast, Queensland, Australia, http://www.isc5.com.au

The World Multidisciplinary Earth Sciences Symposium– WMESS 2016, 5-9 September 2016, Prague, Czech Republic www.mess-earth.org

3rd European Conference on Unsaturated Soils E-UNSAT 2016, 12-14 September 2016, Paris, France, http://eunsat2016.sciencesconf.org

ACCUUS 2016 15th World Conference Underground Urbanisation as a Prerequisite for Sustainable Development, September 12-15, 2016, http://acuus2016.com

SAHC 2016 - 10th international Conference on Structural Analysis of Historical Constructions 13-15 September 2016, Leuven, Belgium, www.sahc2016.be

Hydropower Development Europe 2016 - Flexible hydropower and pump storage generation for a safe renewable electricity system, 14 – 15 September 2016, Lyon, France, http://www.wplgroup.com/aci/event/hydropower-development-europe-2016

13 Baltic States Geotechnical Conference Historical Experiences and Challenges of Geotechnical Problems in Baltic Sea Region, 15 - 17 September 2016, Vilnius, Lithuania, http://www.13bsgc.lt

Dam Surveillance Practice - 3rd Experts Seminar, 18 - 23 Sep 2016, Landeck, Tyrol, Austria, www.atcold.at/de/home-1/41-2016-veranstaltungen/155-dam-surveillance-practice-2016

ACE 2016 12th International Congress on Advances in Civil Engineering, 21-23 September 2016, Istanbul, Turkey, http://www.ace2016.org

International Geotechnical Engineering Conference on Sustainability in Geotechnical Engineering - Practices and Related Urban Issues, 23-24 September 2016, Powai, Mumbai, India, www.igsmumbaichapter.in

EuroGeo 6 – European Regional Conference on Geosynthetics, 25 – 29 Sep 2016, Istanbul, Turkey, www.eurogeo6.org

8th Nordic Grouting Symposium State of the art – Future Development, 26-27 September 2016, Oslo, Norway, http://nordicgrouting.com

5th International Scientific Conference on Industrial and Hazardous Waste Management, 27 - 30 September 2016, Chania, Crete, Greece, http://hwm-conferences.tuc.gr

Basements and Underground Structures 2016, 5-6 October 2016, London, United Kingdom, https://basements.geplus.co.uk

2nd International Specialized Conference on Soft Rocks – ISRM 2016 Understanding and interpreting the engineering behavior of Soft Rocks, 6-7 October 2016, Cartagena, Colombia, www.scg.org.co/?p=1634

The British Tunnelling Society
Conference and Exhibition 2016
October 11 – 12, 2016, London, United Kingdom
www.btsconference.com

The BTS Conference 2016 will take place on Tuesday 11th and Wednesday 12th October at the Queen Elizabeth II Conference Centre, Broad Sanctuary, Westminster, SW1P 3EE.

Two days of focused presentations from both the UK and overseas that address the challenges faced by today's tunnelling industry will be given by experts of international standing. A speaker programme of this quality is a must for all tunnelling professionals and we are confident that those who attend will not leave disappointed.

Exclusive presentations on Hong Kong and Australian projects…

More details of the 2016 conference programme will be shared with you over the coming weeks, but just as a taster we can announce we've secured some exclusive presentations from various International Projects of Technical Significance from Hong Kong, Australia and a very special report from the US that promises to tell all about one of the most challenging tunnelling projects ever undertaken.

HS2 and Crossrail Keynote

Keynotes will be delivered from the Major Projects coming up in the UK, including HS2 and Crossrail 2, whilst a special session has been set aside for a raft of 'lessons learned' from Crossrail including: Temporary SCL Works finding; TBM Advance Rates and Parameters in focus; and a Monitoring and Instrumentation review.

Future of TBM technology debate

We will also be holding an exclusive 'Future of TBM technology' debate with a panel that already features Lok Home, President of The Robbins Company, and Werner Burger, Chief Engineer at Herrenknecht.

For more information about the 2016 event please contact:

Speaking opportunities: Tris Thomas
tris@tunnellingjournal.com

Delegate registration & sponsorship: Daniel Lee-Billinghurst
daniel@tunnellingjournal.com

ARMS 9, 9th Asian Rock Mechanics Symposium, ISRM Regional Symposium, 18-20 October 2016, Bali, Indonesia, http://arms9.com

SFGE 2016 Shaping the Future of Geotechnical Education International Conference on Geo-Engineering Education 20 - 22 October 2016, Minascentro, Belo Horizonte, MG, Brazil, http://cobramseg2016.com.br/index.php/sfge-sobre/?lang=en

10th ICOLD European Club Symposium & Exhibition, 25-30 October 2016, Antalya, Turkey, http://trcold.com

1st International Symposium on Seismic Rehabilitation of Heritage Structures 30-31 October 2016, Tehran, Iran, www.srhs.ir

NEMO International Conference Probing the Santorini volcano for 150 years / Διεθνές συνέδριο NEMO 150 χρόνια μελέτης ηφαιστείου της Σαντορίνης, 3-5 November 2016, Santorini, Greece, http://nemo.conferences.gr

GeoAsia 6 - 6th Asian Regional Conference on Geosynthetics 8-11 November 2016, New Delhi, India, http://seags.ait.asia/news-announcements/11704

5th International Conference on Geotechnical Engineering and Soil Mechanics, 15-17 November 2016, Tehran, Iran, www.icgesm2016.ir

RARE 2016 Recent Advances in Rock Engineering 16-18 November 2016, Bangalore, India, www.rare2016.in

TBM DiGs Istanbul 2016 2nd International conference on "TBM DiGs in difficult grounds", 16-18 November 2016, Istanbul, Turkey, www.tbmdigsturkey.org

GEOTEC HANOI 2016, The 3rd International Conference on Geotechnics for Sustainable Infrastructure Development, 24-25 November, Hanoi, Vietnam, www.geotechn.vn

5th International Conference on Forensic Geotechnical Engineering, 8-10 December 2016, Bangalore, Karnataka, India, http://5icfge.com

International Symposium on Submerged Floating Tunnels and Underwater Tunnel Structures (SUFTUS-2016), 16—18 December 2016, Chongqing, China, www.cmct.cn/suftus

International Workshop on "Advances in Multiphysical Testing of Soils and Shales", 18-20 January 2017, Villars, Switzerland, http://atmss.epfl.ch

ICNCGE-2017 International Conference on New Challenges in Geotechncial Engineering, 23 January 2017, Lahore, Pakistan, www.pges-pak.org/home/icncge-2017

AfriRock 2017, 1st African Regional Rock Mechanics Symposium, 12 – 17 February 2017, Cape Town, South Africa, www.saimm.co.za/saimm-events/upcoming-events

AFRICA 2017 - Water Storage and Hydropower Development for Africa, 14-16 March 2017, Marrakech, Morocco, www.hydropower-dams.com/AFRICA-2017.php?c_id=89

EPS'17 5th International Conference on the Use of EPS Geofoam Blocks in Construction Applications, 22-24 May 2017, Istanbul, Turkey, www.geofoam2017.org

World Tunnel Congress 2017 Surface challenges – Underground solutions, 9 to 16 June 2017, Bergen, Norway, www.wtc2017.no

EUROCK 2017 Human Activity in Rock Masses, 13-15 June 2017, Ostrava, Czech Republic, www.eurock2017.com

BCRRA 2017 Tenth International Conference on the Bearing Capacity of Roads, Railways and Airfields, 28th to 30th June 2017, Athens, Greece, www.bcrra2017.com

GeoMEast2017, 15 - 19 July 2017, Sharm El-Sheik, Egypt, www.geomeast2017.org

3rd International Conference on Performance-based Design in Earthquake Geotechnical Engineering (PBD-III), July 16 - 19, 2017, Vancouver, Canada, http://pbdiiivancouver.com

19th International Conference on Soil Mechanics and Geotechnical Engineering, 17 - 22 September 2017, Seoul, Korea, www.icsmge2017.org

GeoAfrica 2017
3rd African Regional Conference on Geosynthetics
9 – 13 October 2017, Morocco

11th International Conference on Geosynthetics (11ICG)
16 - 20 Sep 2018, Seoul South Korea
csyoo@skku.edu

http://people-x.com/webmail/11ICG/m-e01.htm

AFTES International Congress
"The value is Underground"
13-16 November 2017, Paris, France

World Tunnel Congress 2018
20-26 April 2018, Dubai, United Arab Emirates

EUROCK 2018
22-26 May 2018, Saint Petersburg, Russia

Contact Person: Prof. Vladimir Trushko
Address: 21-st line V.O., 2
199106 St. Petersburg
Russia
Telephone: +7 (812) 328 86 71
Fax: +7 (812) 328 86 76
E-mail: trushko@spmi.ru

16th European Conference on Earthquake Engineering (16thECEE), 18-21 June 2018, Thessaloniki, Greece, www.16ecee.org

CPT'18 4th International Symposium on Cone Penetration Testing, 21-22 June 2018, Delft, Netherlands, www.cpt18.org

UNSAT2018 The 7th International Conference on Unsaturated Soils, 3 - 5 August 2018, Hong Kong, China, www.unsat2018.org

11th International Conference on Geosynthetics (11ICG)
16 - 20 Sep 2018, Seoul, South Korea
csyoo@skku.edu

ARMS10
10th Asian Rock Mechanics Symposium
ISRM Regional Symposium
October 2018, Singapore

Contact Person: Prof. Yingxin Zhou
Address: 1 Liang Seah Street
#02-11 Liang Seah Place
SINGAPORE 189022
Telephone: (+65) 637 65363
Fax: (+65) 627 35754
E-mail: zyingxin@dsta.gov.sg

14th ISRM International Congress
2019, Foz de Iguaçu, Brazil

Contact Person: Prof. Sergio A. B. da Fontoura
E-mail: fontoura@puc-rio.b

ISDCG 2019
7th International Symposium on
Deformation Characteristics of Geomaterials
26-28 June 2019, Strathclyde, Scotland, UK,

Organizer: TC101

The 17th European Conference on
Soil Mechanics and Geotechnical Engineering
1st - 6th September 2019, Reykjavik Iceland
www.ecsmge-2019.com

The theme of the conference embraces all aspects of geotechnical engineering. Geotechnical engineering is the foundation of current as well as future societies, which both rely on complex civil engineering infrastructures, and call for mitigation of potential geodangers posing threat to these. Geotechnical means and solutions are required to ensure infrastructure safety and sustainable development. Those means are rooted in past experiences enhanced by research and technology of today.

At great events such as the European Geotechnical Conference we should: Spread our knowledge and experience to our colleagues; Introduce innovations, research and development of techniques and equipment; Report on successful geotechnical constructions and application of geotechnical design methods, as well as, on mitigation and assessment of geohazards and more.

Such events also provide an opportunity to draw the attention of others outside the field of geotechnical engineering to the importance of what we are doing, particularly to those who, directly or indirectly, rely on our services, knowledge and experience. Investment in quality geotechnical work is required for successful and safe design, construction and operation of any infrastructure. Geotechnical engineering is the key to a safe and sustainable infrastructure and of importance for the society, economy and the environment. This must be emphasized and reported upon.

ΕΝΔΙΑΦΕΡΟΝΤΑ ΓΕΩΤΕΧΝΙΚΑ ΝΕΑ

Από τη ζέστη στο κρύο
Πυρήνας πάγου διηγείται τη μεταμόρφωση μιας τροπικής Ανταρκτικής

Μια πολύτιμη στήλη πάγου που ανασύρθηκε από το βυθό της Ανταρκτικής αποκαλύπτει πώς η απομονωμένη ήπειρος μεταμορφώθηκε από τροπικός παράδεισος στην παγωμένη έρημο που βλέπουμε σήμερα.

Η Ανταρκτική παραμένει στην κατάψυξη εδώ και εκατομμύρια χρόνια, δεν βρισκόταν όμως πάντα στο νότιο πόλο του πλανήτη: μέχρι πριν από 160 εκατομμύρια χρόνια ήταν μέρος της υπερηπείρου Γκοντβάνα, ενωμένη με την Αφρική και την Αυστραλία. Αρκετές φορές στη μακρά ζωή της, η Αυστραλία βρισκόταν πολύ βορειότερα και απολάμβανε τροπικό ή εύκρατο κλίμα.

Οι πάγοι θυμούνται την ιστορία της Ανταρκτικής

Ο πυρήνας πάγου που ανασύρθηκε από το βυθό έξω από το Ουίλκις Λαντ της Ανατολικής Ανταρκτικής καλύπτει τεράστιο χρονικό διάστημα, από τις αρχές της Ηώκαινου Εποχής πριν από 54 εκατομμύρια χρόνια μέχρι τα μέσα του Μειόκαινου πριν από 12 εκατομμύρια χρόνια.

«Ο πυρήνας πάγου από το Ουίλκις Λαντ είναι ο πρώτος που δίνει ολόκληρη την ιστορία μετά το Ηώκαινο» λέει στο περιοδικό New Scientist ο Ούλριχ Σάλτζμαν του Πανεπιστημίου του Νορθούμπρια στη Βρετανία.

Όπως ανέφερε ο Σάλτζμαν στο συνέδριο της Ευρωπαϊκής Ένωσης Γεωεπιστημών που πραγματοποιήθηκε τον Απρίλιο στη Βιέννη, ο πάγος περιείχε κόκκους γύρης που δίνουν στοιχεία για τις κλιματικές συνθήκες κάθε εποχής.

Πριν από περίπου 54 χρόνια, όταν η μέση θερμοκρασία της περιοχής έφτανε τους 16 βαθμούς Κελσίου, το κλίμα ήταν υποτροπικό και η Ανταρτική καλυπτόταν από δάση φοινικόδεντρων.

Στις αρχές του Ολιγόκαινου, πριν από 33 εκατομμύρια χρόνια, οι φοίνικες είχαν δώσει τη θέση του σε εύκρατα είδη όπως «πρωτόγονα» κωνοφόρα που επιβιώνουν μέχρι και σήμερα στη Νέα Ζηλανδία και την Τασμανία.

Στα μέσα του Μειόκαινου, πριν από 23 εκατομμύρια χρόνια, η εποχή των δασών είχε τελειώσει. Με τη μέση θερμοκρασία να έχει πέσει στους 6 βαθμούς, τα δέντρα έδωσαν τη θέση τους στα βρύα και άλλα είδη που χαρακτηρίζουν την τούνδρα.

Ακόμα και η τούνδρα όμως δεν κράτησε πολύ. Πριν από 12,5 εκατομμύρια χρόνια, «οι παγετώνες κυριάρχησαν και μετέτρεψαν την Ανταρκτική σε λευκή έρημο» αναφέρει ο Σάλτζμαν.

«Το Ουίλκις Λαντ πρέπει να ήταν το τελευταίο καταφύγιο για την ξυλώδη βλάστηση» εκτιμά.

Η ιστορία όμως δεν τελειώνει εδώ: η ανθρωπογενής κλιματική αλλαγή φέρνει αστάθεια στο κάλυμμα πάγου της Ανταρκτικής, ενώ οι ολοένα αυξανόμενες ροές ερευνητών και επισκεπτών φέρνουν άθελά τους ξένα είδη φυτών.

Ποιος ξέρει; Ίσως μια μέρα η λευκή ήπειρος θα ξανανιώσει τη ζεστασιά του τροπικού της παρελθόντος.

(Βαγγέλης Πρατικάκης / Newsroom ΔΟΛ, 9 Μαΐου 2016, http://news.in.gr/science-technology/article/?aid=1500075829&ref=newsletter)

Gottardo 2016

Στην Ελβετία η μεγαλύτερη σιδηροδρομική σήραγγα του κόσμου

Η μεγαλύτερη στον κόσμο σιδηροδρομική σήραγγα θα εγκαινιαστεί επισήμως την 1η Ιουνίου.

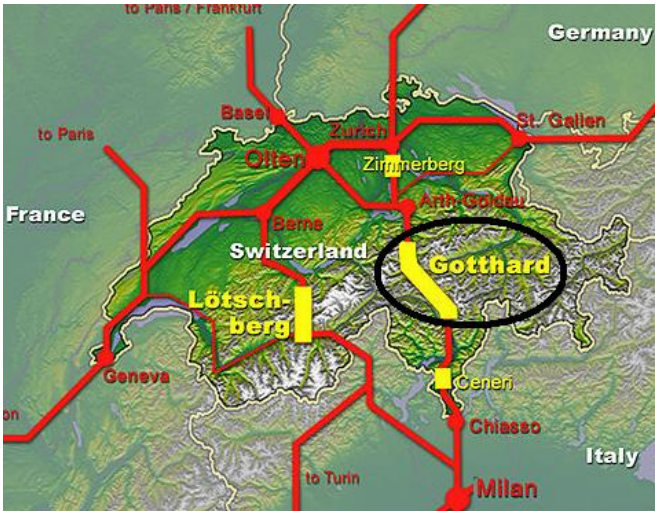

Η σήραγγα Gotthard Base θα συνδέσει σιδηροδρομικά με γραμμή υψηλής ταχύτητας τη βόρεια και τη νότια Ευρώπη και θα αποτελέσει μια από τις βασικές σιδηροδρομικές συνδέσεις στις Άλπεις και η μεγαλύτερη παγκοσμίως, με μήκος περίπου 57,1 χιλιομέτρων.

Στα επίσημα εγκαίνια της σήραγγας αναμένεται να παρευρεθούν αρχηγοί κρατών και κυβερνήσεων από τις γειτονικές χώρες της Ελβετίας, οι υπουργοί Μεταφορών των κρατών κατά μήκος του διαδρόμου εμπορευματικών μεταφορών Ρότερνταμ-Γένοβα καθώς και 1.100 επισκέπτες και εκπρόσωποι μέσων ενημέρωσης.

Το Σαββατοκύριακο στις 4 και 5 Ιουνίου, οι επισκέπτες θα μπορούν να διασχίσουν με ειδικούς συρμούς τη μακρύτερη σιδηροδρομική σήραγγα του κόσμου, σύμφωνα με την πηγή της ελβετικής κυβέρνησης.

Η μεταφορά εμπορευμάτων έχει προγραμματιστεί να ξεκινήσει τον Δεκέμβριο του 2016. Η κατασκευή της σήραγγας ξεκίνησε το 1996, με το συνολικό κόστος να διαμορφώνεται στα 9,8 δισ. ελβετικά φράγκα ή 10,3 δισ. αμερικανικά δολάρια.

(Κέρδος online, 11.05.2016, http://www.kerdos.gr)

Switzerland is Opening the World's Longest-Ever Rail Tunnel

It will ultimately become part of a faster network streamlining rail travel across Europe.

A test train entering the Gotthard Base Tunnel's Northern section (Arnd Wiegmann/Reuters Pictures)

They may look stunning, but for Europeans, the Alps can be a real pain in the neck. Reaching to just under 16,000 feet, the mountain range forms a thick wall across the continent's West and center, dividing countries and making much European long-distance travel laborious and slow. Nowadays, the mountains are of course breached by several major tunnels and highways, a network that has brought hitherto remote valleys within several hours' journey of major cities. The Alps, nonetheless, still form a speed-slowing barrier between Southern and Northern Europe even today. Starting June 1st, however, that barrier should be considerably less impenetrable.

That's because next month, Switzerland is opening the longest railway tunnel ever constructed. At a length of 35.5 miles, the new Gotthard Base Tunnelburrows deep beneath the mountains to connect Switzerland's German- and Italian-speaking regions, ultimately linking the Swiss lowlands with the North Italian plain. It exceeds the length of its longest predecessor, Japan's Seikan Tunnel, by a little over three kilometers (1.9 miles). Running at up to 8,000 feet below mountain peaks at times, it also runs deeper below ground level than any other tunnel yet built. So great is the amount of rock and rubble created by the excavation—over 28 million tons—that steep artificial hills have been created in the valleys at the tunnel's mouth.

While the tunnel's opening is a triumph, the sheer length of its gestation time shows the degree of commitment—and money—that major infrastructure works require. The tunnel was first approved in 1992 in a national referendum, a product of Switzerland's system of direct democracy, which sees national votes held on many issues. Work began in 1996, and the actual drilling of the tunnels was only completed in 2011. The total cost to date: roughly $10.3 billion.

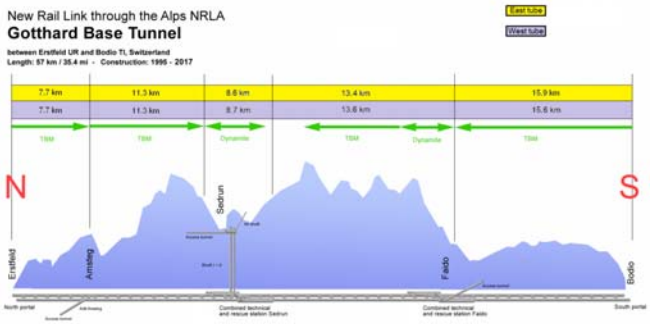

The benefits of this huge outlay, however, will be numerous. Now that trains will run on a specially constructed, almost entirely flat track, trains through the tunnel will be able to reach speeds of 150 miles per hour. This will slash the journey time between Zurich and Milan to just two hours and 30 minutes, considerably faster than the current four hours and 40 minutes. While that's impressive, shorter hops between sub-Alpine cities aren't really the new tunnels main raison d'etre, and wouldn't alone necessarily be worth an injection of over $10 billion.

The tunnel's real role is as part of something much grander, an installment of a massive railway development plan designed to streamline cargo transit across Europe. When complete, this faster network will slash journey times and haulage costs and lure cargo companies off of the continent's highways and onto the rails. If all goes to plan, this will mean that highways are less congested and the air is markedly less polluted. With less traffic, the death toll on roads should also be reduced.

This matters a lot to the alpine regions, where the limited number of road crossings across the mountains creates bottlenecks that spike pollution and congestion in formerly peaceful, remote spots. But it's not only in the tunnel's immediate vicinity where the change should be felt.

The St. Gotthard Massif, under which the new tunnel passes. (Airviews Photography/Flickr Creative Commons)

The first of these streamlined rail corridors, running through the Gotthard Base Tunnel, will be a line that stretches all the way from Rotterdam in the Netherlands south to Genoa

on the Mediterranean Coast. The termini are well-chosen—they essentially form the two furthest points of the mainland section of Europe's Blue Banana, a heavily urbanized corridor housing more than 110 million inhabitants. While Genoa is Italy's busiest port by tonnage, Rotterdam remains the busiest port in Europe bar none. A speedier link to both these ports, where much container traffic from Asia offloads, will make European cargo transit faster, and thus more competitive. It may also have the effect of shifting some cargo destined for Switzerland and Southern Germany south to Genoa, Now that the port has a swifter onward rail connection.

The Gotthard Base Tunnel is still just the longest of the tunnels on several upcoming routes that will radically streamline trans-alpine transit. In Austria, two new tunnels, the Semmering Base Tunnel and the Koralm Tunnel, should be ready by 2024. These will slash journey times between the country's two main cities, Vienna and Graz, but their main achievement will be to provide a far faster rail corridor ultimately reaching from the Baltic port of Gdansk to Bologna (and thus on to Rome). Meanwhile, in Austria, work has already begun on a major new tunnel under the Brenner Pass that, at 34 miles, will be almost as long as the Gotthard Base Tunnel. Running under the Alps due south of Innsbruck, this will provide a faster route between Italy and the German cities of Munich and Berlin—and possibly on to Scandinavia.

Meanwhile a new East-West alpine link has been given the green light, one that will link Lyon in France with Turin via high-speed rail (a project that has so far proved highly controversial). It should be in service by 2028, ultimately creating a fast rail corridor as far east as Budapest.

All these routes' alpine sections are of course already served by existing tunnels, many of which were considered great feats in their era. Current infrastructure still often requires trains to undertake slow climbs, or to ring the sides of valleys in order to make a smoother ascent, and isn't suitable for high-speed trains. This makes journeys along these lines scenically spectacular, but slow. The new tunnels might not be as appealing to tourists (except those in a hurry), but their speed should make the old era of alpine transit seem sclerotic and woefully inefficient.

So far, so good. But while the Gotthard tunnel may point toward a faster, cleaner future for European transit, it's not quite on the way to realizing its potential just yet. Italy's rail network still needs major work, and as the worst conditions are in the country's south, Rome's current priority may be to work there first. Collaboration between the EU and non-member Switzerland may have unlocked huge amounts of funding and goodwill for continent-shaping projects like the tunnel, but engineers still need to grapple with a clutch of different states, many of whom are facing economic uncertainty. Still, while European rail's cleaner, faster future may not arrive the day the Gotthard Base Tunnel's ribbon is cut, at least it's on its way.

(Feargus O'Sullivan / The Atlantic CITYLAB, May 13, 2016, http://www.citylab.com/commute/2016/05/switzerland-is-opening-the-worlds-longest-ever-rail-tunnel-st-gotthard-base/482694/)

Florence's Arno river embankment collapses

The section of bank affected is very close to the historic Ponte Vecchio bridge

A section of the embankment of the River Arno in central Florence collapsed on Wednesday morning, sending part of the road and at least 20 parked cars into a newly formed ditch.

The collapse took place very close to the famous Ponte Vecchio, a medieval covered bridge over the Arno.

The hole is about 200m (650ft) in length and 7m (23ft) across.

Firefighters believe the chasm has been created by the failure of a large water pipe beneath the surface.

Florence's Mayor Dario Nardella tweeted (in Italian) that no-one had been harmed in the incident on Lungarno Torrigiani.

He appealed to motorists to remove their cars from the nearby area, and said the water supply to part of the city centre was cut off.

Regional paper Corriere Fiorentino reports that thousands of residents are without water.

The first sign of the problem came not long after midnight, when the police were called, the mayor told Italy's Ansa news agency.

The major collapse took place at 06:14 local time, Mr Nardella said.

BBC NEWS, 25 May 2016,
http://www.bbc.com/news/world-europe-36377407

ΕΝΔΙΑΦΕΡΟΝΤΑ - ΠΕΡΙΒΑΛΛΟΝ

Eternal Flame Falls

The **Eternal Flame Falls** is a small waterfall located in the Shale Creek Preserve, a section of Chestnut Ridge Park in Western New York. A small grotto at the waterfall's base emits natural gas, which can be lit to produce a small flame. This flame is visible nearly year round, although it can be extinguished and must occasionally be re-lit.

The Eternal Flame Falls were featured in the book *Secret Places* by Bruce Kershner.

Once considered an "obscure" attraction in the region, recent media attention and improvements to the access trail have led to an increased number of visitors in recent years.[2] The increased popularity of the falls has led to some negative impacts, such as an increase in litter, vandalism, pollution, and impacts on the surrounding terrain by tourists,[1] but also fueled a successful public protest against a plan to clear a nearby forested area to install a disc golf course in 2012.[3][4]

Composition and source of gas

Geologists from Indiana University Bloomington and Italy's National Institute of Geophysics and Volcanology studied Eternal Flame Falls in 2013 in an effort to better understand how natural gas emitted from naturally occurring hydrocarbon seeps contribute to greenhouse gases in the atmosphere. They found that the 'macro seep' at Eternal Flame Falls had higher concentrations of ethane and propane (about 35%) than other known natural gas seeps, which typically contain a greater proportion of methane.[5] They estimated that the seep at the falls emits approximately one kilogram (2.2 lb) of methane per day.[6]

The researchers also noted the presence of numerous other 'micro seeps' in the area of the falls. By comparing the gas emitted by these seeps with gas from wells in the area, they determined that the gasses originate from Rhinestreet Shale approximately 400 meters (1,300 ft) below the surface. Tectonic activity likely opened faults in the shale, allowing the gas to reach the surface.[5]

According to one geologist involved in the 2013 study, the seep's apparent source could provide evidence for a previously unknown geologic mechanism by which natural gas is produced within shale. Typically, shale must be hot (around 100 °C [212 °F]) for its carbon structures to break down and form smaller natural gas molecules. However, the shale from which Eternal Flame Falls draws its gas is much cooler, in addition to being younger and shallower than typical gas-bearing shale. This may indicate that additional, as yet undemonstrated, processes can contribute to the creation of natural gas in shale; one possibility is that a catalyst capable of breaking down shale in cooler conditions is present.[7]

References

1. *Conheady, Matt. "Eternal Flame Falls, Orchard Park – Waterfall Photos, Maps, Information". Nyfalls.com. Retrieved January 21, 2015.*

2. *Cernavskis, Andra (July 10, 2014). "Eternal Flame draws crowds to Orchard Park". The Buffalo News. Retrieved January 21, 2015.*

3. *"Eternal Flame Falls: Nature Burning Brightly". WGRZ.com. March 21, 2012. Retrieved January 21, 2015*

4. *Spencer, Naomi (January 26, 2012). "Discs cease flying near Eternal Flame Falls". Orchard Park Bee. Retrieved January 24, 2015.*

5. *"Geologists study mystery of 'eternal flames'". IU News Room: Indiana University. May 9, 2013. Retrieved January 21, 2015.*

6. *Etiopea, Giuseppe; Drobniakc, Agnieszka; Schimmelmannd, Arndt (May 2013). "Natural seepage of shale gas and the origin of 'eternal flames' in the Northern Appalachian Basin, USA". Marine and Petroleum Geology **43**:178–186. doi:10.1016/j.marpetgeo.2013.02.2009. Retrieved 21 January 2015.*

7. *Main, Douglas (May 10, 2013). "World's 'Most Beautiful' Eternal Flame Reveals New Gas Source". Livescience.com. Retrieved January 25, 2015.*

(https://en.wikipedia.org/wiki/Eternal_Flame_Falls)

ΕΝΔΙΑΦΕΡΟΝΤΑ – ΛΟΙΠΑ

Can 3D printing save history?
3D scans, 3D modelling and 3D printing to the rescue…

(Image Credit: Institute for Digital Archaeology)

360 degree photos and video are most associated with virtual reality, but 3D modelling is now being used to faithfully reconstruct – and even 3D-print – ancient monuments and artefacts. Palmyra in Syria is an UNESCO World Heritage Site, a 1,800-year-old Roman monument all but destroyed late last year by Daesh.

While the 250,000 people killed, 6.5 million displaced and 4.8 million refugees since 2011 (UN estimates) are the real tragedy of the Syrian conflict, the speedy resurrection of Palmyra's famous Arch of Triumph using 3D photos and 3D modelling techniques is being hailed as a defiant act. The message? If they knock it down, we have the technology to rebuild it – and quickly.

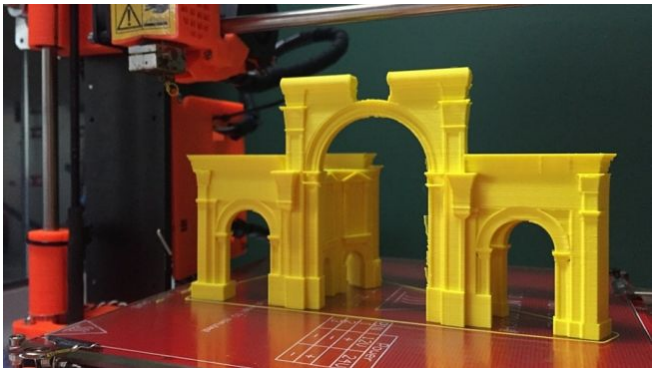

3D printings of the site from the New Palmyra Project's data (Image Credit: New Palmyra Project)

Pioneering project

Reconstructed using a 3D computer model created from photographs, the Harvard University-based Institute for Digital Archaeology (IDA) last week displayed in Trafalgar Square, London, a life-size replica of the Arch of Triumph. The replica will arrive at the now secure Palmyra site later this year.

Not only is it a pioneering project for a new generation of digital archaeologists, but it's all happened very quickly. So very quickly, in fact, that some worry that it's become a propaganda tool for the Assad regime. Others think it a defiant message to anyone disrespecting critical world heritage. Either way, there's no doubting that technology will play a huge role in resurrecting Palmyra and other world heritage sites.

Palmyra attracted around 150,000 tourists a year before the Syrian War (Image Credit: Wikimedia)

Eye in the sky

Given the anticipated vandalism of Daesh, 2014-15 saw something of a rush to 3D-scan world heritage sites in Syria. Digital archaeologist Bassel Khartabil started his New Palmyra Project, CyArk and the Lahore University of Management Sciences digitally documented heritage sites in Pakistan, and the IDA populated its open-source Million Images Database, capturing millions of 3D images of threatened objects.

After the capture of Palmyra, before and after satellite imagery from Urthe Cast was consulted by the UN to confirm the site's devastation. Urthe Cast's goal is to monitor all world heritage sites daily – close-up 3D scans are one thing, but the world's heritage sites need constant monitoring. From the skies above.

Something missing? Palmyra as UNESO photographed it last week (Image Credit: UNESCO/F. Bandarin)

Drones and 3D printing grids

A team from UNESCO has just visited Palmyra to assess the damage, armed with radar to scan beneath the monuments, and with drones to produce 2D aerial images of them from the air. Faithful reconstruction demands precision, so the entire site will again be mapped in 3D.

"A machine in one or two hours gives you a perfect reconstruction of an object … before it would take weeks and weeks," Francesco Bandarin, assistant director-general for culture at UNESCO, told the Wall Street Journal.

However, the main work has already been done. The IDA already had 360-degree images from Palmyra in the Million Image Database, and has therefore been able to accurately reconstruct the Arch of Triumph using proprietary cement-based 3D printing techniques. A 3D printing grid will be set up on the site itself to repair other sections.

The New Palmyra Project extensively photographed the site using 3D cameras (Image Credit: New Palmyra Project)

King Tut's tomb tech

The use of 3D scanning and 3D printers in archaeology is fast becoming decisive. In April 2016 international archaeologists in Egypt used infrared thermographyto map the walls of Tutankhamun's tomb in the Valley of the Kings, which might giveaway the location in a secret chamber of the long-sought resting place of Queen Nefertiti. Even the theory about there being a hidden room at all comes solely from forensic 3D laser scans by Factum Arte in 2009 that mapped the chamber in excruciating detail to produce high-resolution 3D scans.

British Egyptologist Nicholas Reeves used the 3D data to develop an intriguing hypothesis about Nefertiti, and Factum Arte itself then went ahead and built a 1:1 replica of Tutankhamun's tomb, which opened two years ago.

3D printing is also being used to revive vintage cars (Image Credit: KWSP)

Recreating lost artefacts

While the riches of Tutankhamun's tomb – pulled out of the ground in 1922 – are now safely (well, safe-ish) locked away in Cairo's Egyptian Museum, until recently a vintage Amilcar from just a few years later lay in tatters.

That was until engineering company KWSP from Brackley in Northamptonshire, UK, manufactured a one-off gearbox cover using only an old black and white photograph of the car. KWSP design engineers measured and scanned the existing gearbox and then created CAD data of the complete historic assembly in 1927, reverse-engineering the entire vehicle before 3D printing the components they needed.

"It has been a fascinating and hugely rewarding challenge to use the latest in digital fabrication to recreate a unique component, using modern manufacturing design techniques that interface with an assembly that was handmade in the 1920s," says Kieron Salter, managing director of KWSP.

"This is where advances in 3D printing really bring value, but it's not just about pressing a button and producing an object in three dimensions," he added, stating that the real added value is in the design validation and final manufacturing.

3D scans can also be used to recreate artefacts and 3D printing downloads in the virtual space (Image Credit: LGfL)

Virtual reconstruction

As well as digital reconstruction, 3D imagery of objects and artefacts can also be used extensively in the virtual space. The London Grid for Learning (LGfL) just won an award at BETT for its Maya: A Journey through the Maya World digital teaching resource, which uses augmented reality. It also makes available 3D printing files for some of the AR artefacts – a model of the Maya flute can be downloaded and recreated with a 3D printer.

Digital defiance

Although Palmyra is getting all the headlines, the Institute for Digital Archaeology is planning more 3D-printed replications throughout 2016 and 2017. "It is our hope that it will become a model for future similar endeavours," says the IDA's website. "While there are those who seek to encourage us to forget the past – to forget the shared history that unites us – we are dedicated to ensuring that the visual reminders that keep that history alive remain a part of the human experience."

Palmyra's famous Arch of Triumph may have gotten fast-tracked, but the list of world heritage sites destroyed or damaged by Daesh alone is extensive. Lives need rebuilding in Syria way more than Palmyra, of course, but with 3D modelling and printing techniques maturing fast, the age of defiant digital reconstruction is quickly taking shape – and the Universe of Things just got a whole lot more serious.

(Jamie Carter / World of tech, 6 May 2016, http://www.techradar.com/us/news/world-of-tech/can-3d-printing-save-history--1320111/1)

Για δυνατούς λύτες

Η μεγαλύτερη απόδειξη στην ιστορία των Μαθηματικών φτάνει τα 200 terabyte

Και τώρα βγάλτε μια κόλλα χαρτί. Ή μάλλον βγάλτε μερικά εκατομμύρια κόλλες.

Τρεις μαθηματικοί καμαρώνουν για τη μεγαλύτερη απόδειξη μαθηματικού προβλήματος, ένα τερατώδες αρχείο των 200 terabyte, περίπου όσο το σύνολο των ψηφιοποιημένων βιβλίων στη Βιβλιοθήκη του Κογκρέσου.

Όπως αναφέρει ο δικτυακός τόπος του περιοδικού Nature (http://www.nature.com/news/two-hundred-terabyte-maths-proof-is-largest-ever-1.19990), η άκρως μακροσκελής λύση αφορά το πρόβλημα της «μπούλειας πυθαγόρειας τριπλέτας», το οποίο βασανίζει τους μαθηματικούς εδώ και δεκαετίες.

Το πρόβλημα θέτει το ερώτημα του κατά πόσον είναι δυνατό να χρωματιστεί κάθε θετικός ακέραιος αριθμός κόκκινος ή μπλε, έτσι ώστε καμία τριάδα ακεραίων που ικανοποιεί την πυθαγόρεια εξίσωση $\alpha^2=\beta^2+\gamma^2$ να μην είναι ομοιόμορφα χρωματισμένη.

Για παράδειγμα, στην πυθαγόρεια τριπλέτα 3, 4 και 5, αν το τρία και το 5 είχαν χρωματιστεί μπλε, το 4 θα έπρεπε να είναι κόκκινο.

Η απάντηση στο μεγάλο πρόβλημα αναρτήθηκε στην υπηρεσία προδημοσίευσης arXiv από τον Ρόναλντ Γράαμ του Πανεπιστημίου της Καλιφόρνια στο Σιαν Ντιέγκο, τον Όλιβερ Κούλμαν του Πανεπιστημίου του Σουάνζι στη Βρετανία και τον Βίκτορ Μάρεκ του Πανεπιστημίου του Κεντάκι στο Λέξινγκτον.

Οι τρεις ερευνητές αποδεικνύουν ότι η απαίτηση του προβλήματος ικανοποιείται για τους ακέραιους αριθμούς από το 1 έως το 7.824 αλλά όχι πιο πάνω. Όταν κανείς φτάσει στο 7.825, είναι αδύνατο να περιέχουν και κόκκινο και μπλε όλες οι τριπλέτες που ικανοποιούν το πυθαγόρειο θεώρημα.

Για να λύσουν το πρόβλημα, οι ερευνητές χρειάστηκαν 2 μέρες επεξεργασίας σε 800 επεξεργαστές του υπερυπολογιστή Stampede του Πανεπιστημίου του Τέξας.

Αν και υπάρχουν περισσότεροι από 10^{2300} τρόποι να χρωματίσει κανείς τους ακέραιους μέχρι το 7.825, οι τρεις μαθηματικοί εκμεταλλεύτηκαν συμμετρίες των αριθμών, καθώς και διάφορες τεχνικές της θεωρίας των αριθμών, για να περιορίσουν τις πιθανότητες που έπρεπε να εξετάσει ο υπερυπολογιστής στο ένα τρισεκατομμύριο.

Στην επόμενη φάση, η λύση επιβεβαιώθηκε με τη βοήθεια διαφορετικού λογισμικού.

Οι μαθηματικές αποδείξεις που προκύπτουν από υπολογιστές, και είναι πρακτικά αδύνατο να επιβεβαιωθούν από ανθρώπους, γίνονται όλο και συχνότερες τα τελευταία χρόνια.

Όπως όμως επισημαίνει ο Όλιβερ Κούλμαν της ερευνητικής ομάδας, η απόδειξη στο πρόβλημα δεν προσφέρει καμία εξήγηση γιατί ο χρωματισμός των τριπλετών είναι αδύνατος πέρα από το 7.825, ούτε εξετάζει το εάν ο συγκεκριμένος αριθμός έχει κάποια ιδιαίτερη σημασία.

Και αυτό θέτει εν αμφιβόλλω το κατά πόσον η απόδειξη είναι πραγματικά μαθηματικά -τουλάχιστον αν δεχθεί κανείς ότι στόχος των μαθηματικών είναι να προσφέρουν κατανόηση και γνώση και όχι να συσσωρεύουν αχανείς όγκους δεδομένων.

Αυτό, σχολιάζει το Nature, κατέστη προφανές στην περίπτωση του προηγούμενου κατόχου του ρεκόρ μεγαλύτερης απόδειξης, ένα τέρας των 13 gigabyte που δημοσιεύτηκε το 2014.

Ένα χρόνο αργότερα, μαθηματικός του Πανεπιστημίου της Καλιφόρνια στο Λος Άντζελες εξέτασε το ίδιο πρόβλημα με τον παραδοσιακό τρόπο και προσέφερε έτσι μια πιο «ουσιαστική» λύση.

(Βαγγέλης Πρατικάκης / Newsroom ΔΟΛ, 26 Μαϊ. 2016, http://news.in.gr/science-technology/article/?aid=1500080369)

A bridge too far? 11 spectacular new bridges that break the mold

The most spectacular bridges in the world

Garden Bridge by Thomas Heatherwick, in progress (London, United Kingdom)

Danjiang Bridge by Zaha Hadid Architects, in progress (Taipei, Taiwan)

Cirkelbroen by Olafur Eliasson, 2015 (Compenhagen, Denmark)

Lucky Knot Bridge by NEXT Architects, in progress (Changsha, China)

Puente Laguna Garzón by Rafael Viñoly Architects, 2015 (Garzón, Uruguay)

Sölvesborg Bridge by Ljusarchitektur 2013 (Sölvesborg, Sweden)

Sarajevo Bridge by BCQ Architectura Barcelona, in progress (Barcelona, Spain)

Helix Bridge by Cox Architecture, 2011 (Marina Bay, Singapore)

Zhangjiangjie Bridge by Haim Dotan, in progress (Zhangjiangjie City, China)

Køge North Station by COBE, in progress (Køge, Denmark)

Nine Elms Bridge by Bystrup, in progress (London, United Kingdom)

(CNN STYLE, May 25, 2016, http://edition.cnn.com/2016/04/27/architecture/spectacular-new-bridges-that-break-the-mold)

The most anticipated buildings of 2016

Zayed National Museum, Abu Dhabi

World Trade Center Transportation Hub (New York, United States)

Tao Zhu Yin Yuan Tower (Taipei, Taiwan)

Tate Modern extension (London, United Kingdom)

OMA's Taipei Performing Arts Center (Taipei, Taiwan)

Latin American Art Museum (Miami, Florida, United States)

National Museum of African American History and Culture (Washington DC, United States)

Ping An Financial Center (Shenzhen, China)

(CNN STYLE, May 25, 2016, http://edition.cnn.com/2016/04/27/architecture/spectacular-new-bridges-that-break-the-mold)

Η πιο ωραία γέφυρα βρίσκεται στην Ήπειρο!

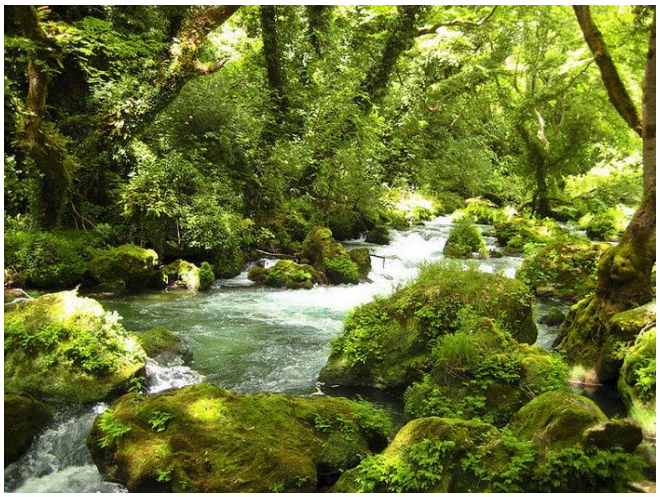

Ο Θύαμις ή Θύαμης ή Καλαμάς είναι ο μεγαλύτερος ποταμός της Ηπείρου και ο έβδομος μεγαλύτερος στην Ελλάδα. Θύαμις είναι το αρχαίο όνομά του, ενώ Καλαμάς αποκαλούνταν στο παρελθόν ο μεγαλύτερος παραπόταμός του. Με το πέρασμα του χρόνου οι δύο ονομασίες ταυτίστηκαν.

Το μήκος του είναι 115 χιλιόμετρα. Οι πηγές του βρίσκονται στο όρος Δούσκο, κοντά στα σύνορα του νομού Ιωαννίνων με την Αλβανία και εκβάλλει στο Ιόνιο πέλαγος, βόρεια της Ηγουμενίτσας, σχηματίζοντας Δέλτα.

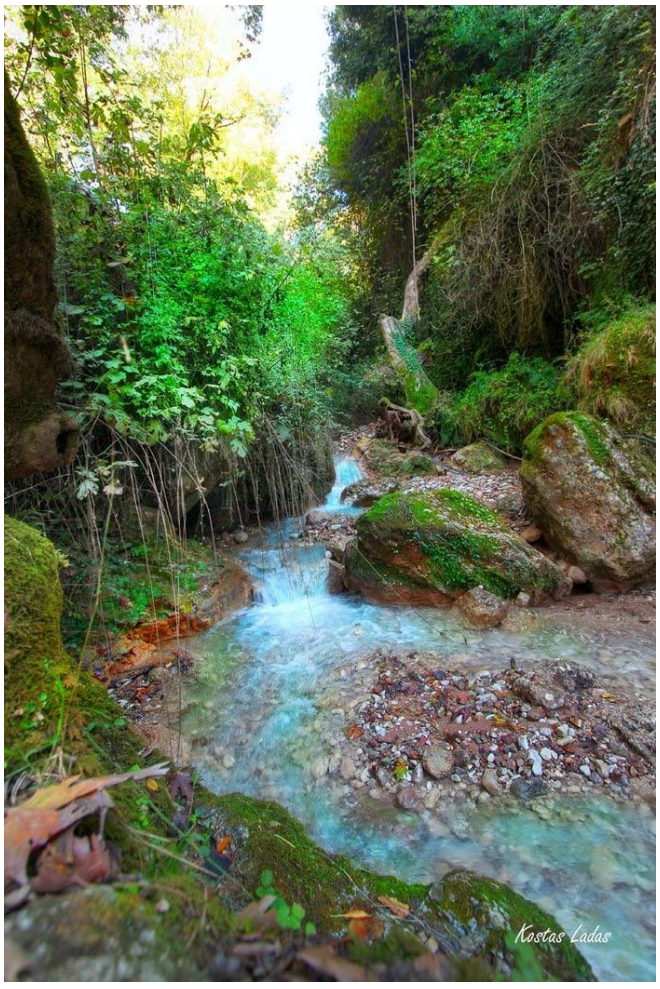

Κατά τη διαδρομή του ο ποταμός σχηματίζει σε πολλά σημεία καταρράκτες. Ο εντυπωσιακότερος από αυτούς έδωσε το όνομά του στο χωριό Καταρράκτης.

Επίσης κοντά στο χωριό Λίθινο, ο Θύαμις περνά μέσα από έναν τεράστιο διαβρωμένο βράχο, ο οποίος έχει πάρει το σχήμα τοξωτής γέφυρας. Της Θεογέφυρας.

Θεογέφυρο το αποκαλούσαν ανέκαθεν οι κάτοικοι της περιοχής. Αλλά και οι ιστορικοί έτσι το μνημονεύουν. Είναι δημιούργημα των ορμητικών νερών του ποταμού.

Έχει μήκος 45 μέτρα και πλάτος 3-4 μέτρα και βρίσκεται 20 περίπου μέτρα πιο ψηλά από τα νερά του ποταμού.

Το σχήμα του όμοιο με αυτό που το ανθρώπινο χέρι έχει δώσει στα διάφορα πέτρινα γεφύρια. Τοξωτό. Με την διαφορά ότι η φύση, που πήρε την θέση του ανθρώπινου παράγοντα στην προκειμένη περίπτωση, δεν ήταν τόσο λεπτομερειακή. Τόσο τελειομανής.

Περιορίστηκε στο να δώσει ένα βασικό σχήμα στο γεφύρι και απέφυγε τις λεπτομέρειες

Η διαδρομή του Θύαμη, μετά την πεδιάδα της Βελλάς, συνεχίζεται μέσα από απότομους βράχους και γκρεμούς.

Ειδικότερα μετά το χωριό Καταρράκτης η μορφολογία του εδάφους είναι τέτοια, που υποχρέωνε, χρόνια τώρα, τα νερά του Καλαμά να κονταροχτυπιούνται με τους βράχους. Αργά αλλά υπομονετικά σ' αυτή την ιδιόμορφη μονομαχία τα νερά ήταν αυτά που άλλαξαν τη μορφή του τοπίου.

Οι βράχοι σιγά-σιγά νικήθηκαν. Υποχώρησαν. Η διάβρωση του εδάφους από τα νερά ήταν τέτοια στο πέρασμα του χρόνου, που οι χαράδρες μεγάλωσαν. Το τοπίο έγινε ακόμη πιο εντυπωσιακό ακόμη πιο όμορφο.

Συνηθίζεται κάθε τι μεγάλο, αξιοθαύμαστο ή και δύσκολα ερμηνευόμενο, να αγκαλιάζεται από παραδόσεις και θρύλους. Έτσι και για το Θεογέφυρο.

Λένε ότι μια γυναίκα λεχώνα από το Λίθινο μια μέρα πήγε στο Μοναστήρι για ν᾽ ανάψει τα καντήλια του, αφήνοντας πίσω το παιδί της να κοιμάται. Το πέρασμα του ποταμού πρώτα γινόταν με μια λιάσα. Με μια πρόχειρη ξύλινη γέφυρα.

Καθώς έφθασε στο μοναστήρι άρχισε να πέφτει δυνατή βροχή. Το ποτάμι θέριεψε. Τα νερά του ανέβηκαν πολύ και παρέσυραν την ξύλινη γέφυρα. Στο γύρισμά της η λεχώνα γυναίκα βλέπει την γέφυρα να λείπει και γεμάτη αγωνία για το πως θα περάσει απέναντι σκύβει, γονατίζει και προσεύχεται «…Θεέ μου τι θα κάνω τώρα που είμαι λεχώνα και θα πρέπει να βυζάξω το παιδί μου. Θα ξυπνήσει και θα κλαίει…» είπε στην προσευχή της.

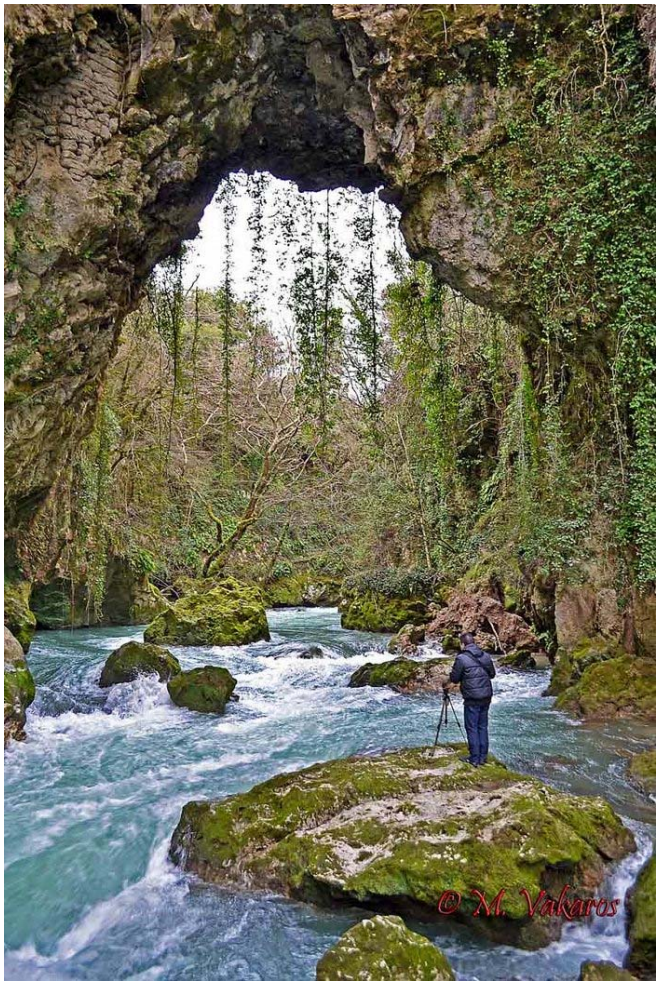

Τότε με μιας τα νερά του ποταμού υποχώρησαν και στο σημείο που ήταν η ξύλινη γέφυρα, χάθηκαν. Είχαν χωνέψει κάτω από μια μεγάλη πέτρα για να βγουν και πάλι στην επιφάνεια λίγα μέτρα πιο κάτω. Η λεχώνα μόλις διαπίστωσε ότι μπορεί να περάσει απέναντι έτρεξε στο σπίτι της και τάϊσε το παιδί της, που στο μεταξύ μόλις είχε ξυπνήσει.

Αφού το τάισε τότε συνειδητοποίησε τι ακριβώς έγινε στο ποτάμι. Τρέχει χτυπάει την καμπάνα του χωριού φωνάζοντας «…Ελάτε χωριανοί έγινε θαύμα!! Ελάτε χωριανοί έγινε θαύμα!! Ο Θεός χάλασε την ξύλινη γέφυρα και έφτιαξε μια δική του…»

Μαζεύτηκαν οι χωριανοί και πήγαν στο σημείο της διάβασης, όπου διαπίστωσαν πραγματικά το ποτάμι να περνάει κάτω από έναν βράχο ο οποίος σχημάτιζε ένα φυσικό γεφύρι. Έτσι λοιπόν η παράδοση λέει ότι σχηματίστηκε το γεφύρι.

Ο Θεός άκουσε την προσευχή της γυναίκας και δημιούργησε ένα γεφύρι για να περάσει αυτή απέναντι να ταΐσει το μικρό της αγγελούδι. Για τον λόγο αυτό οι κάτοικοι του χωριού έβγαλαν το γεφύρι Θεογέφυρο, ονομασία η οποία είναι γνωστή ως τα σήμερα.

(30 Μαΐου 2016, http://www.pentapostagma.gr/2016/05)

ΝΕΕΣ ΕΚΔΟΣΕΙΣ ΣΤΙΣ ΓΕΩΤΕΧΝΙΚΕΣ ΕΠΙΣΤΗΜΕΣ

TWENTY YEARS OF FRC TUNNEL SEGMENTS PRACTICE: LESSONS LEARNT AND PROPOSED DESIGN PRINCIPLES

ITA Working Group 2

The construction of underground infrastructures for transport purposes (roads, railways, and metro), for mountain, sea straits or rivers crossing, for water transportation (clean or sewage water), and for utilities, including multi-purpose tunnels has a key role in the development of modern society. In this context, the use of mechanised tunnelling faces continuously increasing challenges in terms of diameter, depth, machine power, adaptability to different geological context. Consequently, the conception of the lining - usually made of precast segments - has to evolve accordingly in terms of mechanized behaviour, bearing capacity, crack control and water-tightness.

In the last two decades, the use of Fibre Reinforced Concrete (FRC) progressed and was adopted in several tunnel projects. Among the benefits related to the inclusion of fibre reinforcement in the cementitious composites, the most important is the noticeable increase of the post-cracking tensile residual properties. In addition, the fibre reinforcement facilitates production process of the lining segments. The enhancement of the general structural behaviour together with the improvement of the industrialized production of precast tunnel segments are probably the two main key-factors of the continuously growth in using FRC in precast tunnel linings.

The aim of this report is to provide advances in the design of FRC tunnel lining in accordance with the objectives of the International Tunnelling Association (ITA) prescribed in Section II of the Statutes of the ITA (ITA, 1976). Standards and recommendations related to the design of general FRC elements are already available, but they do not provide details on specific requirements and loading conditions applicable in the case of tunnel lining segments. The scope of the report is hence to take advantage of twenty years of FRC practice in precast tunnel lining - including research and feedback from real cases – to provide additional design principles which complete the existing standards and recommendations for the specific case of tunnel lining.

This document was conceptually agreed during the meeting of ITA Working Group 2 (WG2) in Budapest, 2009. The first early draft document was presented in Vancouver, 2010. After several discussions and meetings within WG2 the current version was completed, it was reviewed by the WG2 members, and it went through the formal approval process of ITA.

http://www.ita-aites.org/es/publications/wg-publications/download/1496_028de5fc7a39634cf5c08bf16eb622b7

(ITA Working Group 2, 2016)

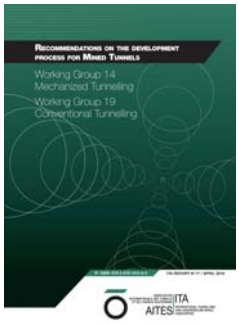

RECOMMENDATIONS ON THE DEVELOPMENT PROCESS FOR MINED TUNNELS

ITA Working Group 14

ITA's working groups on mechanized (WG 14) and on conventional tunnelling (WG 19) elaborated several documents regarding the specific tunnelling methods [1], [2], [8]. In many projects the ground conditions allow either conventional or mechanized tunnelling methods. Therefore, many Owner's organisations have to find an answer on the question which would be the most appropriate tunnelling method for their project.

Both working groups agreed during the WTC 2010 in Vancouver that recommendations on this topic shall be a joint work of both working groups. The answer on the question of the most appropriate tunnelling method depends on many factors for each individual project, not only on the ground conditions but also on many other factors as discussed herein this report. It also depends significantly on the knowledge gained during the project development and on other projects in the area. The complexity of the topic does not allow a simple approach.

The present document intends to highlight the influence of the main project requirements and the factors affecting the selection of the tunnelling method depending on the different project phases. This document does not include typical technical data, such as advance rates, penetrations rates depending on ground conditions, etc. Such aspects shall be treated in a future ITA-Report.

Each project is unique and requires independent project-specific assessment. However, these recommendations represent guidelines and suggestions for the project development with respect to the selection of the tunnelling method in general. The recommendations were developed on the "design – bid – build" procurement model. If other models, such as e.g. the "design – build" are chosen, the general approach will be the same, but with a different allocation of the responsibilities.

The present report does not treat this topic in detail which shall be analysed in a future document.

Also the list of typical documents is only a first collection of some examples. This list shall be developed in a next report of ITA.

These recommendations are intended to be used by Owner's representatives, tunnelling engineers (Design Engineers and Site Supervision), Contractors and Subcontractors.

http://www.ita-aites.org/es/publications/wg-publications/download/1489_74e9622b6fa111bbb9654af0d528fd06

(ITA Working Group 14, 2016)

ITATECH GUIDANCE FOR PRECAST FIBRE REINFORCED CONCRETE SEGMENTS - VOL 1 DESIGN ASPECTS

ITAtech AG PFRCS

This document has been written to assist tunnel designers, contractors and owners in understanding the benefits of and limitations in the use of fibre reinforcement for precast concrete segments for tunnel linings, installed using tunnel boring machines. Guidance is also provided on specifications and testing.

Fibres can be used as reinforcement in precast concrete segmental tunnel linings, either, most commonly, as "fibre only" (as 'Primary' reinforcement) or in combination with conventional (bar) reinforcement - a "combined solution" (as 'Secondary' reinforcement). The state of the art is defined by a large number of reference projects, where fibre reinforced concrete (FRC) segments have been used successfully. Projects using FRC segments report the following benefits of its use:

- Excellent durability;
- Damage due to handling and installation is minimized;
- Performance in the relevant Ultimate and Service Limit States (ULS and SLS) can be reliably demonstrated;
- Reduced damage of segments;
- Overall manufacturing costs are lower than for conventionally reinforced concrete.
- A lower carbon footprint

However, their application in this field has been stifled due to the limited, or even absent, regulatory framework covering this type of product. With the publication of standards specifically dealing with fibre properties, and international design guidelines such as the Model Code 2010, edited by fib, this obstacle has been overcome.

Many research studies and full scale tests on the behaviour of fibre reinforced concrete have been carried out in recent years in various countries. They have greatly contributed to a better characterization of FRC, thereby providing a better understanding of the behaviour of this material and allowing projects to set specific minimum performance requirements.

The aim of this document is to present the common understanding of designers, manufacturers and users of fibre reinforced concrete segments of what constitutes good practice in this field of engineering. This is the first edition of what is intended to be a "live document". ITAtech welcomes all feedback on this document and has plans to keep this document up to date as well as publishing guidance on production aspects of FRC.

http://www.ita-aites.org/es/wg-committees/committees/itatech/publications/download/1495_1ae2aacb16ee523cb37fabac09609fc6

(ITAtech Publications, 2016)

VIBRATION CONTROL IN URBAN DRILL & BLAST TUNNELLING

ITAtech AG Excavation

Blasting is an integral part of the excavation process in underground construction and civil engineering. Due to the high energy content of explosives it is an inexpensive and highly effective method for rock breaking. As explosives have continually been developing due to a high level of research, they have also become remarkably safer. However, it would be careless to ignore the negative side-effects of blasting operations. Due to urbanization, blasting operations are executed more often in populous areas. For this reason it is important to perform the blasting works so that the possible effects on the environment and people nearby are minimized. One of the inevitable negative side-effects of excavation with blasting is blasting-induced vibrations.

The aim of this paper is to discuss the general aspects of blast vibrations and it should give an overview of the blast vibration regulations and legislations in Europe. Furthermore, this paper should also outline modern methods which can be used to efficiently reduce blast vibrations. The first method which is discussed, is improving the delay design by using non-electric detonators. With these detonators, it is possible to set up an efficient system of detonators with a large number of delay times. The paper also treats the importance of the drilling accuracy and choosing the right explosive type. The last method which is shown is the vibration isolation of sensitive equipment. This method is easy to implement and very useful in urban drill and blast tunneling.

http://www.ita-aites.org/es/wg-committees/committees/itatech/publications/download/1491_4b98a8b40255f7a0a1d623c864fdc92b

(ITAtech Publications, 2016)

MUIR WOOD LECTURE 2016

GROUND SUPPORT FOR CONSTRUCTABILITY OF DEEP UNDERGROUND EXCAVATIONS

Peter Kaiser

For the economic and safe construction of deep tunnels, a contractor has to be presented with efficient and effective ground control measures, i.e., support classes that can be rapidly installed and are effective in managing stress-fractured ground. For this purpose, it is necessary to properly anticipate the rock mass behaviour and then provide flexible but reliable means for the support of a shell of stress-damaged ground around the excavation such that a tunnelling project can proceed without unnecessary delays. Stress-driven rock mass failure in brittle rock in the form of gradual ravelling or sudden strain bursting may often slow the tunnelling progress. Both failure processes impose difficult and hazardous conditions for tunnel con-

struction whether the tunnel is advanced by TBM or drilling and blasting.

Robust engineering integrating empirical experience, engineering analysis and sound construction methods provide the key to successful tunnelling and timely project completion. Designs that respect the complexity and variability of the ground, consider the practicality and efficiency of construction, and ensure the effectiveness of ground control measures, lead to fewer project interruptions and, consequently, fewer claims or cost overruns. Robust engineering in highly stressed, brittle failing rock means to design for rock mass degradation and to ensure that all construction tools work well with broken rock.

Some challenges to overcome for economic constructability are engineering design aspects that matter for the selection of the most appropriate excavation technique and the most efficient and effective support systems. This article discusses both fundamental and practical means to better understand and properly document (e.g., in tender documents) the anticipated rock mass and excavation behaviour; better qualify relevant rock mass characteristics and their variability; adopt representative models and inputs to capture the actual rock mass behaviour; and account for practical constraints during construction (i.e., by matching a design to a chosen construction technique). These elements of excavation design are discussed and the impact of naturally variable conditions is reviewed. Guidance is provided for the quantification of anticipated rock mass behaviour near excavations and for the selection of design inputs to arrive at ground control measures that provide both safe and efficient construction. It is discussed how stress-fractured ground is prone to ravelling and how it imposes large deformations due to rock mass bulking. It is concluded that deformation-based support selection principles are most suitable for conditions with stress-fractured ground. Guidance is also provided to arrive at support systems that are suitable for highly stressed tunnels in brittle rock for civil construction and mining operations.

The primary conclusions highlight the need for improvements in better anticipating the rock mass behaviour at the tender stage and the need to design ground control measures from a perspective of practicality rather than theoretical analysis.

Specifically, with respect to excavation stability assessment, it is necessary to anticipate brittle failure processes and to properly describe the implications of shallow rock mass damage and bulking of stress-fractured ground (e.g., stand-up time reductions). With respect to support selection, conventional support design approaches, based on standard rock mass rating systems, are severely limited in conditions where stress-driven failure processes dominate. They do not provide effective support systems for stress-fractured ground, because they do not account for mining-induced stresses, stress changes and related deformations. For tunnelling and mining at depth, it is necessary to select support systems that are effective in controlling the bulking of broken rock and able to yield when strained by deformations imposed by the stress-fractured ground. This can be achieved by following the deformation-based approach described in this article. Since rock mass bulking can impose excessive deformations that cannot be estimated by standard numerical models, it is necessary to separately estimate the deformation demand when bulking dominates (e.g., in late stage mining).

With respect to constructability, it is concluded that conditions of brittle failure must be anticipated early and thus well described in a quantitative manner in tender documents. This should include design inputs relevant for estimating stress-fracturing, for anticipating the extent of rock mass degradation and its impact on stand-up time. Most importantly, flexible and effective support systems (classes) must be provided to manage rapidly changing ground conditions and prevent related delays.

http://www.ita-aites.org/es/publications/muir-wood-lecture/download/1494_016e3026669fb6331bcb2af5dd011772

(ITA, 2016)

ΗΛΕΚΤΡΟΝΙΚΑ ΠΕΡΙΟΔΙΚΑ

[The British Tunnelling Society Conference and Exhibition, October 11th - 12th 2016]

www.geoengineer.org

Κυκλοφόρησε το Τεύχος #134 του **Newsletter του Geo-engineer.org** (Μαΐου 2016) με πολλές χρήσιμες πληροφορίες για όλα τα θέματα της γεωμηχανικής. Υπενθυμίζεται ότι το Newsletter εκδίδεται από τον συνάδελφο και μέλος της ΕΕΕΕΓΜ Δημήτρη Ζέκκο (secretariat@geoengineer.org).

The ITA@NEWS #60 – May 2016
www.ita-aites.org

- Message from Tarcisio CELESTINO, ITA President
- Successful week in San Francisco for the World Tunnel Congress 2016
- ITA Tunnelling Awards deadline extended to June 13th
- WTC 2017 - Call for abstracts
- WTC 2016-itacus session press release
- Photos of WTC 2016 are available
- Twenty years of FRC Tunnel Segments Practice
- Recommendations on the development process for mined tunnels
- ITAtech Guidance for Precast Fibre Reinforced Concrete Segments - Vol 1 Design Aspects
- Vibration Control in Urban Drill & Blast Tunnelling
- Muir Wood lecture 2016
- TBM Applications II, Bergen, Norway from 6th to 7th June 2016
- IABR 2016 - Urban Underground Day, 23rd June 2016, Rotterdam, The Netherlands
- 52nd ISOCARP Congress, Durban, South Africa, 12-16 September 2016
- 8th Nordic Grouting Symposium, 26-27 September 2016, Oslo, Norway

ΕΚΤΕΛΕΣΤΙΚΗ ΕΠΙΤΡΟΠΗ ΕΕΕΕΓΜ (2015 – 2018)

Πρόεδρος	:	Γεώργιος ΓΚΑΖΕΤΑΣ, Δρ. Πολιτικός Μηχανικός, Καθηγητής Ε.Μ.Π. president@hssmge.gr, gazetas@ath.forthnet.gr
Α' Αντιπρόεδρος	:	Παναγιώτης ΒΕΤΤΑΣ, Πολιτικός Μηχανικός, ΟΜΙΛΟΣ ΤΕΧΝΙΚΩΝ ΜΕΛΕΤΩΝ Α.Ε. otmate@otenet.gr
Β' Αντιπρόεδρος	:	Μιχάλης ΠΑΧΑΚΗΣ, Πολιτικός Μηχανικός mpax46@otenet.gr
Γενικός Γραμματέας	:	Μιχάλης ΜΠΑΡΔΑΝΗΣ, Πολιτικός Μηχανικός, ΕΔΑΦΟΣ ΣΥΜΒΟΥΛΟΙ ΜΗΧΑΝΙΚΟΙ Α.Ε. mbardanis@edafos.gr, lab@edafos.gr
Ταμίας	:	Γιώργος ΝΤΟΥΛΗΣ, Πολιτικός Μηχανικός, ΕΔΑΦΟΜΗΧΑΝΙΚΗ Α.Ε.- ΓΕΩΤΕΧΝΙΚΕΣ ΜΕΛΕΤΕΣ Α.Ε. gdoulis@edafomichaniki.gr
Έφορος	:	Γιώργος ΜΠΕΛΟΚΑΣ, Δρ. Πολιτικός Μηχανικός, Επίκουρος Καθηγητής ΤΕΙ Αθήνας gbelokas@teiath.gr, gbelokas@gmail.com
Μέλη	:	Ανδρέας ΑΝΑΓΝΩΣΤΟΠΟΥΛΟΣ, Δρ. Πολιτικός Μηχανικός, Ομότιμος Καθηγητής ΕΜΠ aanagn@central.ntua.grn
		Βάλια ΞΕΝΑΚΗ, Δρ. Πολιτικός Μηχανικός, ΕΔΑΦΟΜΗΧΑΝΙΚΗ Α.Ε. vxenaki@edafomichaniki.gr
		Μαρίνα ΠΑΝΤΑΖΙΔΟΥ, Δρ. Πολιτικός Μηχανικός, Αναπληρώτρια Καθηγήτρια Ε.Μ.Π. mpanta@central.ntua.gr
Αναπληρωματικό Μέλος	:	Κωνσταντίνος ΙΩΑΝΝΙΔΗΣ, Πολιτικός Μηχανικός, ΕΔΑΦΟΜΗΧΑΝΙΚΗ Α.Ε. kioannidis@edafomichaniki.gr
Εκδότης	:	Χρήστος ΤΣΑΤΣΑΝΙΦΟΣ, Δρ. Πολιτικός Μηχανικός, ΠΑΝΓΑΙΑ ΣΥΜΒΟΥΛΟΙ ΜΗΧΑΝΙΚΟΙ Ε.Π.Ε. editor@hssmge.gr, ctsatsanifos@pangaea.gr

ΕΕΕΕΓΜ
Τομέας Γεωτεχνικής
ΣΧΟΛΗ ΠΟΛΙΤΙΚΩΝ ΜΗΧΑΝΙΚΩΝ
ΕΘΝΙΚΟΥ ΜΕΤΣΟΒΙΟΥ ΠΟΛΥΤΕΧΝΕΙΟΥ
Πολυτεχνειούπολη Ζωγράφου
15780 ΖΩΓΡΑΦΟΥ

Τηλ. 210.7723434
Τοτ. 210.7723428
Ηλ-Δι. secretariat@hssmge.gr ,
geotech@central.ntua.gr
Ιστοσελίδα www.hssmge.org (υπό κατασκευή)

«ΤΑ ΝΕΑ ΤΗΣ ΕΕΕΕΓΜ» Εκδότης: Χρήστος Τσατσανίφος, τηλ. 210.6929484, τοτ. 210.6928137, ηλ-δι. ctsatsanifos@pangaea.gr, editor@hssmge.gr, info@pangaea.gr

«ΤΑ ΝΕΑ ΤΗΣ ΕΕΕΕΓΜ» «αναρτώνται» και στην ιστοσελίδα www.hssmge.gr